Dynamics of smooth muscle contraction

Dynamics of smooth muscle contraction

De dynamische eigenschappen van de contractie van glad
spierweefsel

Proefschrift

ter verkrijging van de graad van doctor
aan de Erasmus Universiteit Rotterdam
op gezag van de rector magnificus
Prof. dr P.W.C. Akkermans M.A.
en volgens besluit van het college voor promoties.

De openbare verdediging zal plaatsvinden op
woensdag 25 juni 1997 om 13:45 uur

door

Gommert Abraham van Koeveringe
geboren te 's-Gravenpolder

Promotie commissie

Promotor: Prof. Dr F.H. Schröder

Overige leden: Dr ir. R. van Mastrigt (tevens co-promotor)
Prof. Dr P.R. Saxena
Prof. Dr R.M. Heethaar
Dr P. Schiereck

Voor Melanie
Voor mijn ouders

Contents

CHAPTER 1

General Introduction,
Aim and Structure of the thesis

Scanning electron microscopy image of smooth muscle tissue the spindle shaped cells can be identified clearly.
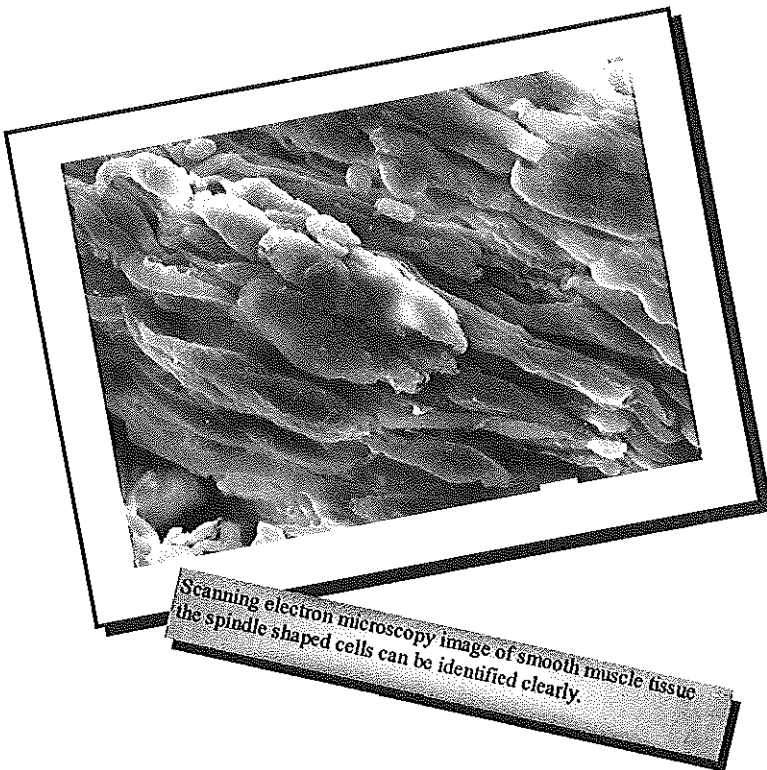
Fortiter in re, suaviter in modo: strong in essence, smooth in manner

Smooth muscle can economically maintain tonus for a long time and in many organs, its purpose is to maintain organ dimensions. It is however relatively slow and also inefficient as far as mechanical work is concerned.

Smooth muscle is found in the majority of organs in the human body. It is characterized by an abundant functional diversity associated with many regulatory systems in combination with, most likely, a common intracellular contractile apparatus. The regulatory systems involve different neurotransmitters, hormones, ions, metabolites, and responses mediated by other associated cells and nerves. In the urinary bladder a special kind of smooth muscle has evolved in which the maintenance of tonus is less important than the generation of mechanical work necessary to evacuate urine. In the major part of its cycle, the filling phase, the muscle is in the relaxed state, and it only develops force for a relatively short period during micturition. In this way the function of it closely resembles that of skeletal muscle.

Smooth muscle and striated, i.e., skeletal, muscle are differentiated on the basis of their microscopic appearance. A similar force generating system, the sliding filament cross-bridge mechanism is recognized in both muscle types. However, the many different regulatory properties seen in smooth muscle are not found in skeletal muscle. In the smooth muscle cell, cross-bridge interaction is proportionally regulated by the level of intracellular calcium, whereas in skeletal muscle it is just switched on and off (21). Smooth muscle cells in hollow organs contract and maintain tonus in a coordinated fashion and are controlled groupwise, while skeletal muscle cells are recruited individually, each with a separate nerve ending. Smooth muscle is relatively efficient in maintaining force for a long time during which virtually no work is done, while skeletal muscle is basically designed to convert energy to mechanical work with a high power output. The relatively fast force development compared to other types of smooth muscle makes the dynamics of the contractile apparatus of urinary bladder smooth muscle an interesting field of research. In addition, the regulatory systems of smooth muscle have to be understood in order to explain pathology and to design new drugs to eliminate subversive behaviour. One way to investigate the regulatory system is to monitor the target system, i.e., the contractile apparatus, in different regulation modes. In this study a detailed monitoring of the dynamics of the target system was used in order to investigate both the regulatory system and its target.

Smooth muscle in the urinary system

In tubular organs like the ureter, epididymis, and ductus deferens, smooth muscle is used to propel fluids by peristalsis. Smooth muscle is also found in urine collecting tissue such as the renal calyces and pyelum and probably maintains a tonus there. In organs with an excretory function, i.e., seminal vesicles and prostate, smooth muscle is used to expel the excretory products. Recently it has been shown that an enlargement of the prostate becomes significant only when a considerable smooth muscle tonus coexists. In the urinary bladder, smooth muscle's major function is neither continuous propulsion nor maintenance of tonus but short acting active evacuation of urine.

The anatomy of the bladder

The bladder can be divided into two components: The bladder body, the part situated above the ureteral orifices, and the base, consisting of the posterior trigone, deep detrusor and the anterior bladder wall.

In the wall of the urinary bladder three layers can be identified. The innermost mucosal layer consists of three layers of transitional cells that form both an active and a passive protective barrier for the bladder wall against the hypertonic urine. Next a smooth muscle layer can be identified, which consists of relatively large diameter bundles of smooth muscle that form a complex meshwork. On the outside an adventitial layer of connective tissue covers the bladder. This layer is in some regions covered with peritoneum. (8,25)

The muscle bundles or myofibrils in the body of the detrusor crisscross through the muscle wall without a clear hierarchic organization. Longitudinally oriented muscle bundles tend to predominate the inner and outer aspect of the detrusor muscle coat. These longitudinal fibers are closely interrelated with the capsule of the prostate or the anterior vaginal wall. On the dorsal side, the fibers have a close relation to the anterior aspect of the rectum. Within the bladder wall, an extensive exchange of fibers between adjacent muscle bundles can be identified. The detrusor thus consists of constantly branching and reuniting smooth muscle bundles. Single smooth muscle cells are surrounded by a dense basal lamina, except at some junctional regions. These junctional regions are responsible for the spread of a stimulus through the tissue. A junction type frequently seen in detrusor smooth muscle is the "tight junction", which comprises a region with a length of 1 µm and a cell-cell distance of 10-20 nm. In addition some "intermediate junctions" and "peg and socket junctions" can be distinguished. "Gap junctions", a form of tight junctions with a direct cytoplasmic connection (gap) are frequently seen in other kinds of smooth muscle but seem absent from detrusor smooth muscle (8).

The innervation of bladder muscle

The detrusor muscle is innervated by parasympathetic and sympathetic nerve fibers. Parasympathetic innervation originates via the nervi erigentes from the second to the fourth sacral segment. The sympathetic fibers are derived from the 9th to the 12th thoracic and the 1st and second lumbar segment via the plexus hypogastricus. Parasympathetic fibers are mostly cholinergic while sympathetic fibers mainly comprise nor-adrenergic fibers. Throughout the whole bladder wall small autonomic ganglia, with mostly cholinergic fibers, can be found. The smooth muscle in the muscle coat of the bladder is abundantly interlaced by mainly cholinergic nerve fibers. Nerve terminals lie within 20 nm from the surface of the muscle cells. In the dome of the bladder a very sparse noradrenergic nerve supply can be found. In some other species than humans a non-adrenergic non-cholinergic nerve supply has been shown. For example, in the pig bladder adenosine triphosphate (ATP) has been identified as a neurotransmitter (5). In humans vasoactive intestinal polypeptide (VIP) has been identified as an inhibitory neurotransmitter, which causes relaxation. The more caudal regions of the urinary bladder contain a relatively increasing number of nor-adrenergic fibers. Here a clear sex difference can be identified. A male bladder neck has an abundant nor-adrenergic innervation and is only sparsely cholinergically innervated (9). These sympathetic nerves extend into prostate gland and seminal vesicles. From a physiological point of view, a sympathetically evoked contraction in this region prevents retrograde semen flow during ejaculation. In contrast, nor-adrenergic nerves are not widely represented in the female bladder neck, so that nerve supply in this region is still predominantly cholinergic. (8,20)

Passive and active mechanical properties of the detrusor wall

The urinary bladder has two distinct functions: a collection function and an evacuation function. In the collecting phase the bladder fills at a rate in the order of 1 ml/min towards a volume of several hundred milliliters without, in the normal situation, a significant increase in intravesical pressure. Unstimulated, non-contracting bladder muscle behaves like a passive visco-elastic material. One can see that stretch, when applied quickly, induces an initial rise in tension which decays when the rate of the lengthening is reduced. This process is called stress-relaxation (32). In addition, several inhibitory neuronal mechanisms have been identified, which might explain part of the described relaxation effect. (10,23)

In the emptying phase, the muscle is stimulated to contract and an active force is generated which is superimposed on the passive force. This force depends on the speed of shortening and on the length of the muscle, like in other smooth and striated muscles. Active force decreases with increasing speed of shortening as a result of energy constraints. As in skeletal muscle, the force

generated by smooth muscle increases with increasing muscle length to a maximum. This length dependence is in skeletal muscle as a consequence of the changes in overlap between the filaments explained by the number of cross-bridges that can be made between the contractile proteins. The length range over which smooth muscle can operate is considerably larger than the range for skeletal muscle so that it is unlikely that the length dependence of force development in smooth muscle can be explained on a similar basis.

The physiology and pharmacology of detrusor contraction

In any muscle type, shortening or force is generated by a cyclic interaction of two kinds of proteins, myosin, organized in thick filaments and actin, the thin filaments to which the thick filaments attach bonds c.q. cross-bridges with small heads. A complex series of events precedes force development in smooth muscle, the so called excitation-contraction coupling. In-vivo, the detrusor dome is stimulated mainly via cholinergic nerves, which release acetylcholine. This increases the intracellular calcium concentration by calcium influx from the extracellular space, or by release from intracellular calcium stores. Intracellularly, calcium binds to calmodulin. This calcium-calmodulin complex then binds to myosin-light-chain kinase (MLCK), which phosphorylates the myosin light chain. The phosporylation of myosin increases its affinity to the thin filaments and allows actin to activate a myosin magnesium-ATPase, that provides the energy for cross-bridge formation. The attachment of cross- bridges is followed by an energy (ATP) consuming process of detachment. In cross-bridge cycling, attachment and detachment are repeated successively. When the myosin light chain remains phosphorylated and only attachment and, ATP consuming, detachment occur, a relatively fast cycling results. However, if energy conditions are less optimal, a slower cycling can occur in which every cycle comprises phosphorylation and dephosphorylation. These slowly cycling cross-bridges are called "latch-bridges" (7). Latch-bridges maintain tonus at a very low energy level. Since bladder contraction is a relatively fast process for smooth muscle, latch-bridges are not thought to play an important role in the evacuation phase. However, these bridges might have a function in the muscle tonus after fast filling in the collecting phase, before stress relaxation occurs. (18)

The time course of isometric force development

In addition to just measurement of the maximum amplitude of isometric force, valuable information on the dynamics of smooth muscle contraction can be obtained by determination of the time constant of force development. Muscle contraction is a physiological activation process to a saturation level. Such a process can often be described by a mono-exponential function. The time constant of an exponential function quantifies the rate at which maximum

contraction is reached. A time constant represents the time elapsed until 63% of saturation level is reached. The time constant is thus indicative of the rate of force development and can be used to identify rate limiting processes in the excitation-contraction or pharmaco-mechanical coupling. Several methods can be used to determine time constants. One of these methods is phase plot analysis. (3,19,27,29) Using this method a plot is made of the time-derivative of force dF/dt as a function of the force. Mono-exponential force development results in a straight line in this plot, the slope of which is the negative reciprocal of the time constant. Another method to determine the time constant is by fitting a mono-exponential function to the force time-plot, using a computerized procedure.

Contraction velocity in smooth muscle

When a muscle is allowed to shorten, its contraction velocity is an important denominator in the dynamics of smooth muscle contraction. The velocity of shortening decreases with increasing force. A hyperbolic force-velocity relationship was first described by Hill in 1938 (16). The contraction velocity at zero force; called the maximum shortening velocity differs in different kinds of tissue. For example maximum shortening velocity in smooth muscle is approximately 0.3 strip lengths/s (this study), in skeletal muscle 1.45 strip lengths/s and in cardiac muscle 0.61 strip lengths/s (6). Generally, the maximum shortening velocity is believed to be a mechanical index of cross-bridge cycling rate. This maximum shortening velocity can be determined by either "quick release" techniques (15) or the "stop test". In order to obtain a complete force-velocity relation either the muscle contraction velocity has to be measured at different force values c.q. afterloads or the generated force can be measured at different shortening velocities. In the frequently used quick release technique the muscle strip is subjected to a series of preset afterloads during maximal stimulation at L_0 (the muscle length at which maximum force is developed). After a preset time interval the velocity of shortening is measured. A disadvantage of this technique is that measurementsat different afterloads, necessary to determine one maximum shortening velocity value, take place at different lengths of the muscle. A length dependence of the maximum shortening velocity can thus not be determined. Another disadvantage is that the quick release technique does not discriminate between active and passive contributions to force development. Especially in urinary bladder tissue passive forces can increase to very high levels, well beyond the actively generated force, at longer lengths.

In the stop test the force at a preset length is measured after linear shortening to this length at different rates. Using this technique, measurements can be done easily with and without stimulation so that passive forces can be subtracted from active forces. In this way, maximum shortening velocity can be

determined at higher passive forces associated with longer lengths and at higher velocities. The stop test can be applied clinically when urine flow is interrupted suddenly, while intra vesical pressure is measured (10).

Aim of the thesis

The aim of this thesis is to study excitation-contraction coupling and pharmaco-mechanical coupling in the smooth muscle of the urinary bladder. As a tool, the time course of isometric force development is analyzed in terms of time constants and related to the maximum shortening velocity, a parameter indicating the rate of cross-bridge cycling. In addition, a new excitatory stimulus with a fast pathway to the contractile units, the ultra-violet light flash, is explored. Most measurements were done in pig urinary bladder, which is the best animal model from a urological point of view. As a verification for the applicability to the human situation and to develop a method to detect basic pathological detrusor changes, time constants and maximum shortening velocity were determined in small cold cup biopsies of human bladder.

Structure of the thesis

Isometric force development in smooth muscle results from a complex series of regulatory processes. In chapter 2 different stimulatory pathways in pig urinary bladder smooth muscle strips were selected using electrical and pharmacological stimuli in combination with pathway blocking agents. A model describing excitatory pathways and interactions was developed. Time constants of force development could be associated with different pathways and provided additional information on the time course. It was found that influx of extracellular calcium limited the rate of force development especially when triggered by receptor stimulation.

In a subsequent study the influence of urethral obstruction, which is often caused by pathologic enlargement of the prostate, on the rate and amplitude of force development by the detrusor was studied. Obstruction of the urinary bladder is a clinical syndrome, which is commonly diagnosed in urological practice (2). Morphological changes such as muscle hypertrophy resulting in trabeculation can partly be distinguished by cystoscopy. Hypertrophied muscle shows distinct functional changes in vitro (1) In urodynamic tests a number of in-vivo functional changes can be identified. Bladders show an increased pressure at unaffected or reduced flow rates. In a number of cases, unstable contractions can be detected in the collecting phase (4). Some bladders show a decreased compliance i.e. a gradual increase in pressure at normal filling rates. In Chapter 3 an animal model is presented for bladder outlet obstruction in guinea-pigs which was developed at Johns Hopkins University in Baltimore. This model served to produce obstruction induced bladder dysfunction, which was signified by pathological urodynamic patterns also seen in humans after urethral obstruction. Chapter 4 describes a study performed on this model in which changes in force development by the detrusor muscle were investigated in vitro.

In order to verify that the rate of isometric force development of the detrusor muscle is limited by the influx of extracellular calcium as found in chapter 2, a method was used to manipulate the intracellular calcium concentration. This was done by loading "caged calcium" into the muscle cells (Gurney et al. 1987; Tsien & Zucker, 1986), which can be released by a high intensity ultra-violet (UV) light flash. The high costs of the commonly used UV lasers (Lea et al, 1990), to evoke such a flash are commonly beyond the budget of basic muscle research projects. Therefore, a new UV flash instrument was developed, based on a commercially available photo-flash unit. Chapter 5 describes how this unit was tested by measuring the in-vitro free calcium concentration after exposure of "caged calcium" to UV light. A physiological

change in free calcium concentration could be evoked by photolysis of caged calcium using the described flash unit.

Application of an ultraviolet, UV, light flash to smooth muscle loaded with "caged calcium" resulted in a contraction. However, control fibers, which were not loaded with "caged calcium", did also show a contraction upon exposure to UV light. Further investigation of this effect is described in Chapter 6. Amplitude and rate of force development were determined in response to electrical field and UV flash stimulation in the presence or absence of either ryanodine(24), which inhibits release of intracellular calcium, or tetrodotoxin, which eradicates nerve activity, or atropine, which inhibits cholinergic nerve activity. It was concluded that the newly discovered UV stimulation method had a fast, at least partly nerve mediated, pathway to the contractile units mediated by calcium from intracellular stores.

The cross-bridge cycling rate is the ultimate rate limiting factor in muscle contraction. If other rate limiting factors are eliminated, it determines the rate of force development under isometric conditions. Maximum shortening velocity, the mechanical index of the cross-bridge cycling rate can be determined from a force-velocity relation. From a theoretical point of view, the pre-stretched length of the muscle should not have an effect on the maximum shortening velocity, as this is extrapolated to zero force and thus independent of the number of attached cross-bridges. In smooth muscle several modulators of cross-bridge cycling have been described (14,22) . Using the stop test method in chapter 7 it was possible to investigate the muscle length dependence of the force-velocity relation. The maximum shortening velocity was shown to increase with increasing stretched muscle length. The effect could be due to an up-regulation of cross bridge cycling or a changed orientation or contents of intracellular contractile proteins.

In the literature, there is no consensus on the origin of the mechanism that limits the time constant of isometric force development. The time constant is frequently related to the maximum shortening velocity and the series elasticity. Series elasticity is the elastic component in the muscle tissue which is located in series with the contractile element. Previous research, described in chapter 2, indicated that stretching of the series elasticity by the cycling cross-bridges would lead to force development at a very high rate, that is never measured under physiological circumstances. It was hypothesized that the normal rate of force development depends on a slower mechanism such as the influx of extracellular calcium. In chapter 8, the time constant of isometric force development and maximum shortening velocity were directly compared to determine the factors that influence the value of the time constant. Additionally, time constants before and shortly after an imposed muscle shortening were compared. This comparison gained more insight in functional changes of the muscle that occur after shortening, i.e., shortening induced deactivation, which

was earlier described by Groen (11) and Gunst et al. (12) .

In order to be able to investigate a possible relation of maximum shortening velocity and pathological bladder conditions in the near future, small cold cup biopsies were used   to determine maximum shortening velocity in the human detrusor. In chapter 9 the temperature dependence of the force-velocity relation was studied in these biopsies, that were obtained during a trans-urethral operation. Muscle mechanics experiments in skeletal muscle are generally done at room temperature while smooth muscle experiments have to be done at 37°C as the muscle tends to be very slow at room temperature. Therefore, temperature dependence of the force-velocity relation in smooth muscle is an interesting study object. It was shown to be possible to measure several force-velocity relations under different circumstances, in this case temperatures, in one biopsy. Additionally, maximum shortening velocity and time constants in human urinary bladder tissue could be compared to the pig model, which was amply used in this thesis.

References

1. Arner, A., Malmquist, U. and Uvelius, B. (1990) Metabolism and force in hypertrophic smooth muscle from rat urinary bladder. *Am.J.Physiol* 258 (Cell Physiol. 27): C923-C932.
2. Blaivas J.G. (1988) Pathophysiology and differential diagnosis of benign prostatic hypertrophy. *Urology*, 32(6 Suppl): 5-11.
3. Boom, H.K.B., Dernier van der Gon, J.J., Nieuwenhuijs, J.H.M., and Schiereck, P. (1973) Cardiac contractility: actin-myosin interaction as measured from the left ventricular pressure curve. *Eur. J. Cardiol.* 1/2: 217-224.
4. Bosch, R. (1990) Instability of the bladder: Pathophysiology Unknown? A synopsis of clinical points of interest. *Neurourol. Urodyn.* 9: 563-565.
5. Brading, A.F., Mostwin, J.L., Sibley, G.N.A. and Speakman, N.J. (1986) The role of smooth muscle and its possible involvement in diseases of the lower urinary tract. *Clin. Sci. Lond.* 70: 7-13.
6. Brenner, B. (1986) The necessity of using two parameters to describe isotonic shortening velocity of muscle tissue: the effect of various interventions upon initial shortening velocity and curvature. *Basic Res. Cardiol.* 81: 54-69.
7. Dillon, P.F., Aksoy, M.O., Driska, S.P. and Murphy, R.A. (1981) Myosin Phosphorylation and the Cross-Bridge Cycle in Arterial Smooth Muscle. *Science.* 211: 495-497.
8. Dixon, J.S. and Gosling, J.A. (1994) The anatomy of the bladder, urethra and pelvic floor. In: Mundy, A R, Stephenson, T P, Wein, A J (eds) Urodynamics; principles, practice and application. Churchill Livingstone, Edinburgh, UK, p 3-14.
9. Gosling, J.A. (1979) The structure of the bladder and urethra in relation to function. *Urol. Clin. North Am.* 6: 31-38.
10. Griffiths, D.J., Van Mastrigt, R., Van Duyl, W.A. and Coolsaet, B.L.R.A. (1979) Active mechanical properties of the smooth muscle of the urinary bladder. *Med. Biol. Eng. Comput.* 17: 281-219.

11. **Groen, J.** Functional modelling of voiding. Thesis: Erasmus University Rotterdam, The Netherlands. April 17, 1996.

12. **Gunst, S.J., Wu, M.F. and Smith, D.D.** (1993) Contraction history modulates isotonic shortening velocity in smooth muscle. *Am. J. Physiol.* 265: C467-C476.

13. **Gurney, A.M., R.Y. Tsien and H.A. Lester.** (1987) Activation of a potassium current by rapid photochemically generated step increases of intracellular calcium in rat sympathetic neurons. *Proc.Natl.Acad.Sci.USA.* 84: 3496-3500.

14. **Haeberle, J.R. and Hemric, M.E.** (1994) A model for the coregulation of smooth muscle actomyosin by caldesmon, calponin, tropomyosin, and the myosin regulatory light chain. *Can. J. of Physiol. and Pharmacol.* 72: 1400-1409.

15. **Hellstrand, P. and Johansson, B.** (1979) Analysis of the length response to a force step in smooth muscle from rabbit urinary bladder. *Acta Physiol. Scand.* 106: 221-238.

16. **Hill, A.V.** (1938) The heat of shortening and the dynamic constants of muscle. *Proc. Roy. Soc. London B.* 126: 136-195.

17. **Lea, T.J., M.J. Fenton, J.D. Potter and C.C. Ashley.** (1990) Rapid activation by photolysis of nitr-5 in skinned fibres of striated adductor muscle from the scallop. *Biochim.Biophys.Acta.* 1034: 186-194.

18. **Levin, R.M., Wein, A.J. and Longhurst, P.A.** (1994) Neuropharmacology of the lower urinary tract. In: Mundy, A R, Stephenson, T P, Wein, A J (eds) Urodynamics; principles, practice and application. Churchill Livingstone, Edinburgh, UK, p 29-42.

19. **Meiss, R.A.** (1975) Graded activation in rabbit mesotubarium smooth muscle. *Am. J. Physiol.* 229: 455-465.

20. **Mundy, A.R. and Thomas, P.J.** (1994) Clinical physiology of the bladder, urethra and pelvic floor. In: Mundy, A R, Stephenson, T P, Wein, A J (eds) Urodynamics; principles, practice and application. Churchill Livingstone, Edinburgh, UK, p 15-28.

21. **Murphy, R.A.** (1989) Special topic: contraction in smooth muscle cells. Annu. Rev. Physiol. 51: 275-283.

22. **Peiper, U. and Dee, J.** (1994) Smooth muscle contraction kinetics at different calcium concentrations. *Canadian Journal of Physiology and Pharmacology.* 72: 1338-1344.

23. **Steers, W.D.** (1992) Physiology of the urinary bladder. In: Walsh, P C, Retik, A B, Stamey,T A, Vaughan, E D (eds) Campbell's Urology, 6 th edition. W.B. Saunders Company, Phyladelphia, p 142-176.

24. **Sutko, J.L. and Kenyon, J.L.** (1990) Actions of Ryanodine. *J. Gen. Physiol.* 96, 439-441.

25. **Tanagho, E.A.** (1992) Anatomy of the lower urinary tract. In: Walsh, P C, Retik, A B, Stamey, T A, Vaughan, E D (eds) Campbell's Urology, 6 th edition. W.B. Saunders Company, Phyladelphia, p 40-69.

26. **Tsien, R.Y. and R.S. Zucker.** (1986) Control of cytoplasmic calcium with photolabile tetracarboxilate 2-nitrobenzhydrol chelators. *Biophys.J.* 50: 843-853.

27. **Van Mastrigt, R.** (1988) The length dependence of the series elasticity of pig bladder smooth muscle. *J. Muscle Res. Cell Motil.* 9: 525-532.

28. **Van Mastrigt, R.** (1991) The force recovery following repeated quick releases applied to pig urinary bladder smooth muscle. *J. Muscle Res. Cell Motil.* 12: 45-52.

29. **Van Mastrigt, R. and Glerum, J.J.** (1985) Electrical stimulation of smooth muscle strips from the urinary bladder of the pig. *J. of Biomed. Eng.* 7: 2-8.

30. **Van Mastrigt, R. and Griffiths, D.J.** (1979) Contractility of the urinary bladder. *Urol. Int.* 34: 410-420.

31. **Van Mastrigt, R. and Tauecchio, E.A.** (1982) Series-elastic properties of strips of smooth muscle from pig urinary bladder. *Med. Biol. Eng. Comput.* 20: 585-594.

32. **Van Mastrigt, R., Coolsaet, B.L.R.A. and Van Duyl, W.A.** (1978) Passive properties of the urinary bladder in the collection phase. *Med. Biol. Eng. Comput.* 16:471-482.

CHAPTER 2

Excitatory pathways in smooth muscle investigated by phase-plot analysis of isometric force development
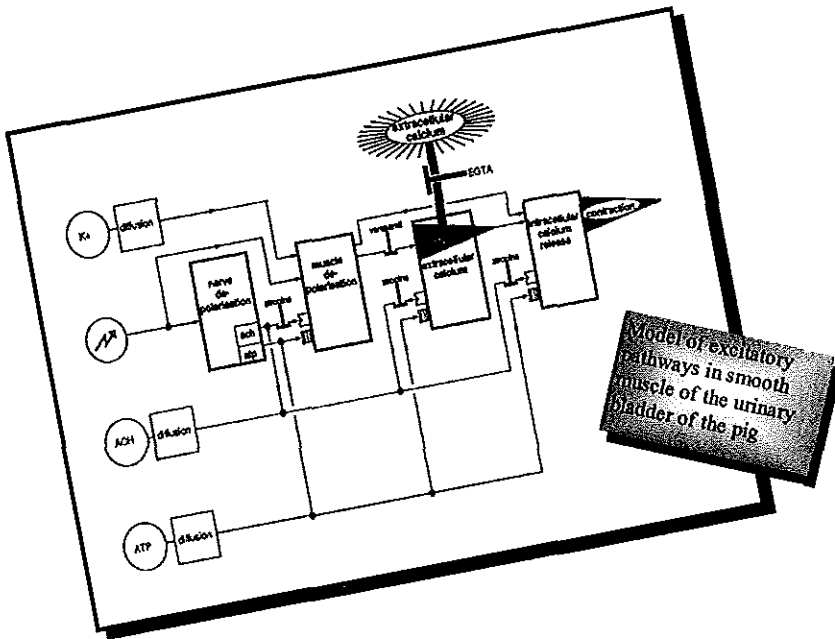
G.A. van Koeveringe and R. van Mastrigt.

Summary

Excitatory pathways in the smooth muscle of the pig urinary bladder were investigated using phase-plot analysis of isometric contractions. The phase plots, plots of the rate of change of the force as a function of the force itself, were dominated by a straight line described by the horizontal intercept (F_{iso}) and the vertical intercept (U). The quotient F_{iso}/U is a time constant that characterizes the rate-limiting step in isometric force development in the muscle. Bladder strips of 1 mm diameter were activated by electrical field stimuli, acetylcholine, potassium, and ATP in combination with selective pathway inhibitors such as verapamil, atropine, or a calcium-free solution containing ethylene glycol-bis(8-aminoethyl ether)-N,N,N',N'-tetra-acetic acid. When pathways that depended significantly on depolarization or intracellular calcium release were selected, the time constant was significantly smaller, indicating a faster process. The results indicated that the rate-limiting step in force development was determined by the influx of extracellular calcium.

Introduction

Isometric force development in smooth muscle results from a complex series of events. With phase-plot analysis this process can be characterized by one time constant (4, 15, 18, 20, 22). This time constant has been shown to be independent of both the external calcium concentration and the size of the strip but dependent on the length of the interstimulus interval (22). Such dependence may result from a change in calcium sensitivity of the regulatory-contractile apparatus (17), suggesting that this parameter characterizes intracellular processes. In the present study different stimulatory pathways in pig urinary bladder smooth muscle strips were selected using electrical and pharmacological stimuli in combination with pathway blocking agents. In similar studies on other smooth muscle preparations pathway interactions have been deduced on the basis of the maximum isometric force developed (2, 6, 9, 11, 14). In the present study the time constants that could be associated with the different pathways provided aditional information. Together with information derived from other studies (1-3, 5-8, 14, 17, 18), this led to the development of a complete diagram describing excitatory pathways and interactions for pig urinary bladder smooth muscle.

Materials and Methods

Experiments were performed on pig urinary bladders obtained from the local slaughterhouse ~15 min after slaughter. Strips of 2 x 2 cm were cut from the anterolateral wall of the bladder and transported to the laboratory in oxygenated Krebs solution. The mucosa and the submucosal fat layer were removed, and muscle strips of 1 mm diameter and 10 mm length were excised. To facilitate diffusion the thin fascia layer covering the muscle fiber was opened and for the greater part removed. Three such smooth muscle strips each from a different bladder were suspended in one organ bath, which contained 15 ml of Krebs solution (13) equilibrated with 95% O_2-5% CO_2. Each strip was attached at one end to a glass rod, fixed to the bottom of the organ bath, and at the other end to a FT03 force transducer (compliance 0.002 m/N) with 0.7 metric silk thread. All strips were prestretched to a tension of 0.01 N. The contents of the organ bath could be drained within 1 s and filled within 5 s from a heated and aerated solution storage container.

Strips were stimulated electrically by applying alternating pulses of 7.5 V with a 100-Hz repetition frequency and 5-ms duration to two parallel platinum electrodes, one on each side of the set of three strips. Pharmacological stimulation was performed by replacing the contents of the organ bath with an isosmolar solution containing 123 mM potassium chloride, 0.01 mM acetylcholine, or 3 mM ATP.

In two series of three bladder strips, all four stimuli were tested. Electrical and pharmacological stimuli were applied in random order, each tested stimulus being preceded by an extra electrical stimulus in normal Krebs solution to standardize prestimulus conditions. A rest interval of 5 min followed electrical stimulation and an interval of 10 min followed pharmacological stimulation before the next stimulus was applied.

After all stimuli were tested, the contents of the organ bath were replaced by a calcium-free solution containing 2 mM ethylene glycol-bis(8-aminoethyl ether)-*N,N,N',N'*-tetraacetic acid (EGTA) (referred to as EGTA treatment). After a diffusion period of 1 min, the last applied stimulus in normal Krebs solution was tested with EGTA treatment. Next the calcium-free EGTA solution was washed out, and after 10 min the next stimulus was applied. Because verapamil and atropine were difficult to wash out, in 16 series of 3 strips only one type of stimulus was investigated in each series in the presence of these agents. In 8 of these 16 a Krebs solution containing 0.05 mM verapamil (referred to as verapamil treatment) and in the other 8 a solution containing 0.01 mM atropine (referred to as atropine treatment) replaced the contents of the organ bath after the testing of all stimuli in normal Krebs solution. After a diffusion period of 1 min, the last applied electrical or pharmacological stimulus was repeated in the presence of either atropine or verapamil treatment.

All isometric contractions were sampled at a rate of 10 Hz with a PDP 11 type computer and stored for further analysis. Plots of the rate of change in force as a function of force, i.e., phase plots, were made (4, 20). For the greater part such phase plots of isometric smooth muscle contractions can be characterized by a straight line (15, 20, 22) where F is the measured force, F_{iso} is the maximum

$$\frac{dF}{dt} = \frac{1}{C} (F_{iso} - F) \qquad \text{Eq.1}$$

extrapolated force, t is time, and C is the time constant for isometric force development. The intercept of the straight line with the vertical axis, i.e., dF/dt at $F = 0$, is called U, which equals F_{iso}/C.

The solution to *Eq. 1* describes the time course of isometric force development.

$$F = F_{iso} [1 - e^{-(t/C)}] \qquad \text{Eq.2}$$

C represents the limiting rate constant in the excitation-contraction coupling process.

Artifacts due to fluid movements could be recognized as irregular spikes, usually in the first part of the phase plot, and such parts were excluded from further processing. All values determined for F_{iso}, U, and C in one strip were normalized by dividing by the corresponding parameter value of the electrically stimulated contraction preceding the first pharmacological stimulus. The normalized values of F_{iso}, U, and C were averaged for each stimulus-treatment
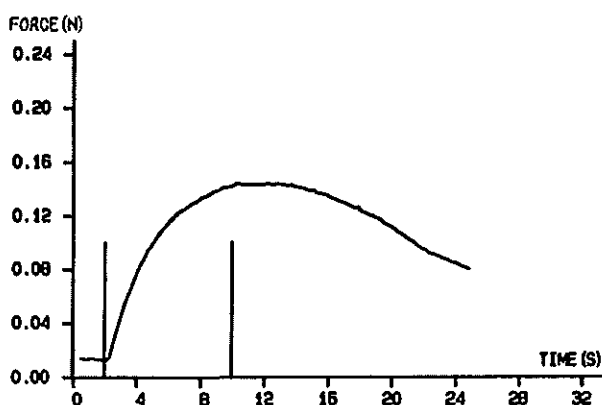

Figure 1. Force-time plot of an electrically stimulated isometric contraction from a strip of pig urinary bladder smooth muscle.

combination. The Mann-Whitney U test was used to determine the significance of the differences in the averaged normalized parameters. To compare different stimuli during a treatment, relative values for F_{iso} were calculated by dividing the parameters values during a treatment by the corresponding values in normal Krebs solution. Variance analysis was carried out to study the influence of the applied treatment, stimulus, serial number (18 series of 3 strips), and strip number (3 strips in 1 organ bath) on the parameters F_{iso}, U, and C.

Results

Figure 1 shows an example of the force development during an electrically stimulated isometric contraction, and Fig.2 shows the phase plot calculated from these data.

Table 1 shows the means ± SE of the unnormalized parameter values for F_{iso}, U, and C. Only the values of the standard electrically stimulated contraction measured in each of the 54 strips in normal Krebs solution were taken into account. This standard electrically stimulated contraction was the contraction preceding the first pharmacological stimulus and the contraction that served as the standard in the normalization procedure as described in METHODS AND MATERIALS.

In Figs. 3-5 the first four bars show respectively the average normalized values of F_{iso}, U, and C (means ± SE) for electrically stimulated contractions in
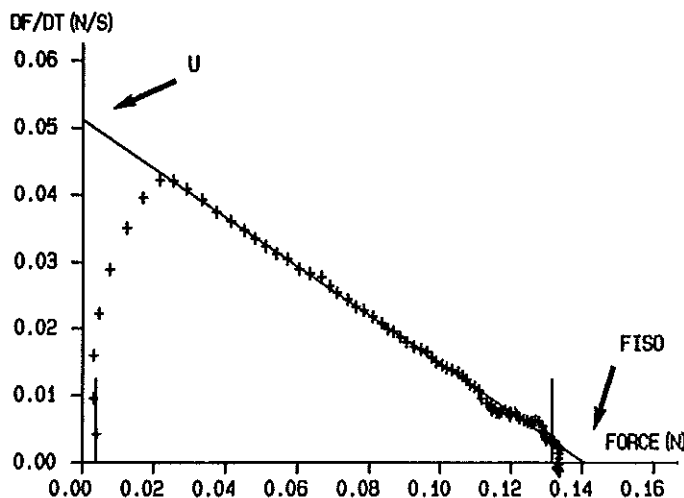

Figure 2. Phase plot, a plot of rate of change of force (dF/dt) as a function of the force itself, derived from force-time plot shown in Fig. 1. The straight line dominating the phase plot is characterized by parameters F_{iso} (maximum extrapolated force) and U. Time constant F_{iso}/U is called C.

normal Krebs solution, in calcium-free solution containing EGTA (labelled E), in normal Krebs solution containing verapamil (labelled V), and in normal Krebs solution containing atropine (labelled A). The second group of four bars shows the average normalized values of F_{iso}, U, or C for contractions stimulated by potassium chloride, the third group for contractions stimulated by acetylcholine, and the fourth group for contractions stimulated by ATP.

A statistical comparison of the first bars in each group ($n = 54$) in Figs. 3-5, i.e., the significance of the differences between the average normalized values or F_{iso}, U, and C for the different stimuli in normal Krebs solution, yielded the following results. In normal Krebs solution all three parameters were significantly different for all stimuli ($P \leq 0.001$), except for F_{iso} values for electrical and acetylcholine stimulation.

The significances of the differences between the bars within the groups in Figs. 3-5, i.e., the differences between the average normalized values F_{iso}, U, and C of contractions evoked by the same stimulus in (normal) Krebs solution or

Table 1.

Unnormalized values for parameters F_{iso}, U, and C.

Parameter	Mean ± SE
F_{iso}, N	0.047 ± 0.003
U, N/s	0.016 ± 0.001
C, s	3.080 ± 0.144

F_{iso}, maximum extrapolated force; U, intercept of straight line with vertical axis; C, time constant for isometric force development. Only the values of the standard electrically stimulated contraction measured in each of the 54 strips in normal Krebs solution were included.
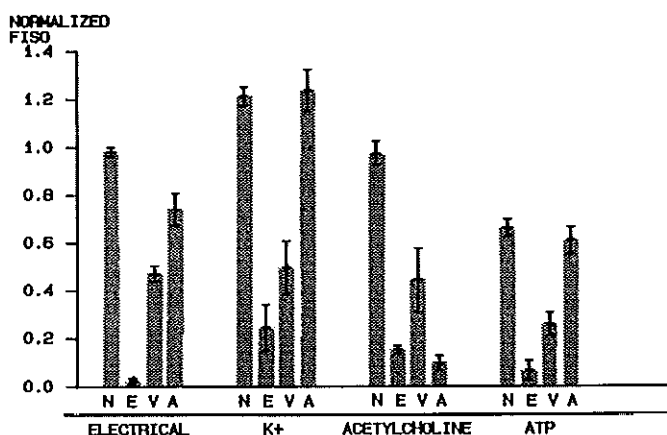

Figure 3. Average normalized values for F_{iso} (horizontal intercept in Fig.2) for electrically, potassium-, acetylcholine-, or ATP-stimulated contractions in normal Krebs solution (N), a calcium-free solution containing EGTA (E), verapamil (V), or atropine (A), Brackets, ±SE.
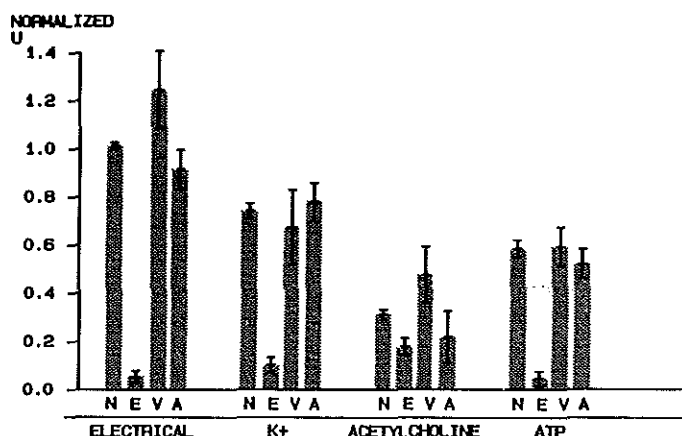
NORMALIZED
U

Figure 4. Average normalized values for *U* (vertical intercept in Fig.2) for electrically, potassium-, acetylcholine-, or ATP-stimulated contractions in normal Krebs solution (N), a calcium-free solution containing EGTA (E), verapamil (V), or atropine (A), Brackets, ±SE.

during the application of the different treatments, are shown in Table 2. For all stimuli in the different treatments the F_{iso} values were smaller ($P \leq 0.002$) than the corresponding values in normal Krebs solution except those for potassium and ATP stimuli in atropine. The *U* values for all stimuli in EGTA treatment were smaller ($P < 0.03$), but the values in verapamil or atropine treatment were not significantly different from the corresponding values in normal Krebs except for the electrical stimulus in atropine. The *C* values for all stimuli in verapamil treatment, for acetylcholine and ATP stimuli in EGTA treatment, and for the electrical and acetylcholine stimuli in atropine treatment were smaller ($P < 0.03$)

NORMALIZED
C

Figure 5. Average normalized values for *C* (time constant, negative reciprocal value of *C* describes slope of straight line in Fig.2) for electrically, potassium-, acetylcholine-, or ATP-stimulated contractions in normal Krebs solution (N), a calcium-free solution containing EGTA (E), verapamil (V), or atropine (A), Brackets, ±SE.
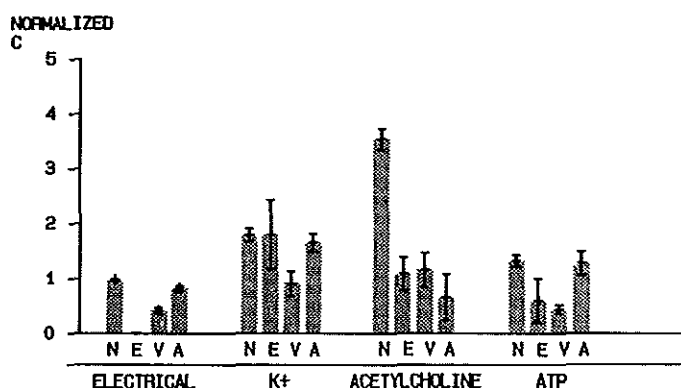
than the corresponding values in normal Krebs.

In Fig. 6 these differences for F_{iso} are expressed in relative values (means $\pm$ SE). In Fig. 6 the first group of four bars shows the effect of a calcium-free EGTA solution, the second group the effect of verapamil solution, and the third group the effect of atropine solution on the electrically stimulated contraction (bar 1, Elec) and the contractions evoked by potassium chloride (bar 2, K^+), acetylcholine (bar 3, ACh), and ATP (bar 4, ATP).

A comparison of the significances of the differences between the values of F_{iso} for contractions evoked by the different stimuli for each treatment, i.e., the differences between the different bars (for which $n = 6$) in each group of four in Fig. 6, yielded the following results. The relative F_{iso} values in EGTA and verapamil treatments were not significantly different for any stimulus applied, except for electrical and ATP stimuli in verapamil treatment ($P < 0.05$) and for electrical and acetylcholine stimuli in EGTA treatment ($P < 0.01$). During atropine treatment a difference was seen in F_{iso} values for all compared stimuli except potassium and ATP stimuli.

Table 2. Significances of differences in normalized values of F_{iso}, U, and C for different stimuli between different treatments

<div align="center">Treatments Compared</div>

Parameter	Stimulus	Normal-EGTA	Normal-verapamil	Normal-atropine	EGTA-verapamil
F_{iso}	Elec	0.0001	0.0001	0.0006	0.0037
	K^+	0.0001	0.0002	0.6397	0.1093
	ACh	0.0001	0.0029	0.0001	0.0104
	ATP	0.0001	0.0003	0.8245	0.0091
U	Elec	0.0001	0.1855	0.0470	0.0037
	K^+	0.0001	0.3491	0.6135	0.0039
	ACh	0.0301	0.1530	0.1602	0.0547
	ATP	0.0001	0.7301	0.8437	0.0033
C	Elec	0.1774	0.0001	0.0116	0.5218
	K^+	0.7487	0.0031	0.9019	0.2623
	ACh	0.0003	0.0002	0.0003	0.6310
	ATP	0.0459	0.0004	0.7864	0.3333

Two-tailed probability, corrected for ties, resulting from a Mann-Whitney U test; $n = 6$. Elec, electrical stimulus; K^+, potassium stimulus; ACh, acetylcholine stimulus; ATP, ATP stimulus

Finally, the variance analysis of the parameters F_{iso}, U, and C with respect to the 3 treatments, the 4 stimuli, the 18 serial numbers, and the 3 strips per series showed that treatment, stimulus, and serial number all forms significant sources of variance. The strip number did not contribute to a significant degree to the variance in these parameters.

Discussion

The complex interaction of excitatory stimuli and blocking agents in the sequence of events leading from stimulation to contraction cannot be described completely by the observation of changes in maximum developed force alone. Analysis of phase plots of isometric contractions provides additional information on the dynamics of the development of force in such a contraction in terms of the
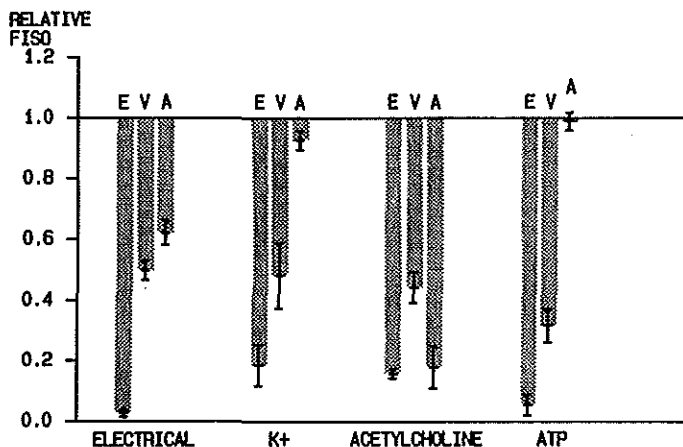
Figure 6. Relative values for F_{iso} (F_{iso} values in presence of a treatment divided by F_{iso} values in normal Krebs) for electrically (Elec), potassium (K^+)-, acetylcholine (ACh)-, or ATP-stimulated contractions in EGTA, verapamil or atropine treatment.

parameters F_{iso}, U, and C, which define the straight line that dominates the phase plot (Fig.2). This straight line can be understood in terms of a simple model that ascribes the development of force to the recruitment of units that are changed from a noncontractile to a contractile state (22). In this model F_{iso} or the extrapolated maximum isometric force represents the maximum number of activated units after an infinitely long stimulation. The parameter U represents the chance that noncontractile units change to the contractile state. U therefore provides information on the prestimulus conditions. F_{iso} and U together define C ($=F_{iso}/U$), which forms the rate constant that limits the rate of force development during a contraction. The smaller the C value the faster is the isometric force

development. The mean value of the time constant C in this preparation of pig bladder smooth muscle equals ~3s (see Table 1). In some instances it has been suggested that the time course of isometric contraction development in smooth muscle is determined by the contractile element lengthening the series elastic element of the muscle.

In the APPENDIX it is demonstrated that this mechanism is associated with a time constant in the order of 0.16 s for this type of muscle. This indicates that the stretching of the series elastic element is a much faster process, taking place in the early (nonexponential) part of the phase plot, which has a duration of ~1s.

The strips were prestretched to 0.01 N of initial tension. At this passive tension, the strip was considerably shorter than L_{max}, the length at which maximum force can be generated. For this kind of smooth muscle tissue the passive tension at L_{max} is approximately half the tension that the tissue can actively generate (see Fig.6 in Ref. 19). In this muscle it is not possible to perform reproducible measurements at L_{max} because the high passive tension at L_{max} causes a continuous passive lengthening that interferes with the active measurements (9).

The variance analysis, carried out to establish the reproducibility of the parameters, shows that the applied treatment and stimulus, the two sources of variance of major interest, contribute significantly of the variance in all three parameters. The variance associated with the strip number was not significant compared with the residual variance in contrast to the variance associated with serial number, indicating that the three strips in each series were more comparable than the strips in different series. Inasmuch as all strips were obtained from different bladders, this effect can only be ascribed to minute differences in composition or pH of the metabolic fluids possibly due to toxic cell debris .

The results obtained by analysis of the presented data in terms of F_{iso}, U and C and those of other studies in this field (1-3, 8, 14, 17, 18) were summarized in the block diagram shown in Fig. 7. This diagram shows the effective pathways and interactions in the excitation-contraction and pharmacokinetic coupling in pig detrusor smooth muscle. The following considerations led to this diagram. From all stimuli applied in normal Krebs solution, potassium resulted in the highest F_{iso} values (Fig.3). Because the potassium-induced contraction remained unaffected by atropine (Figs. 3-5), potassium was assumed to mainly cause a direct cell depolarization, which plays a central role in reaching a strong isometric contraction. The U value associated with potassium stimulation was not the highest and was considerably smaller than that for electrical stimulation (Fig.4), resulting in a higher C value (Fig. 5) or a slower force development. This effect was ascribed to the diffusion process necessary to transport the depolarizing agent to cellular level.

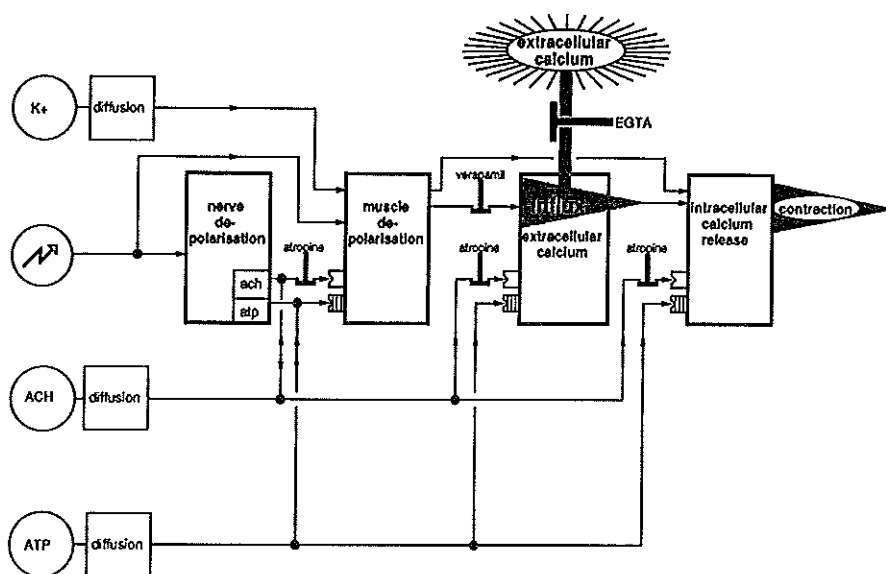Stimulation with acetylcholine in normal solution led to slightly smaller,

Figure 7. Summarizing diagram of excitatory pathways describing sequence of events that lead from stimulation to mechanical force development in smooth muscle of urinary bladder of the pig. This smooth muscle tissue can be activated by electrical field stimulation, which depending on pulse duration causes either nerve or muscle depolarization. It can also be activated by pharmacological stimuli such as high potassium, causing depolarization of muscle cell membrane, acetylcholine, causing receptor-operated muscle depolarization and receptor-operated influx of extracellular and release of intracellular calcium. ATP performs similar operations via an ATP receptor. Time delay caused by diffusion of pharmacological agents is denoted by square labeled diffusion. As an example, sequence of events leading from electrical stimulation to development of force is as follows. Electrical stimulus activates nerves (1st block), thus causing muscle depolarization either by releasing acetylcholine (which can be blocked by atropine) or by ATP. Muscle depolarization (2nd block) operates calcium channels, which can be blocked by verapamil, causing an influx of extracellular calcium (3rd block). This process can be prevented by binding extracellular calcium using EGTA. Raised intracellular calcium concentration or muscle depolarization itself causes a release of intracellularly stored calcium (4th block), and calcium activates intracellular contractile apparatus. K^+, potassium stimulus; spark sign (arrow), electrical field stimulus; ACh, acetylcholine stimulus; ATP, ATP stimulus; tap signs (z), sites of action of pathway inhibitors.

but nevertheless comparable, values for F_{iso} (Fig. 3) but even lower values for U (Fig. 4), resulting in even higher C values (Fig.5). Inasmuch as acetylcholine exerts its effect for a substantial part via receptor-operated calcium influx (2,3), this seems to be a rate-limiting step. If the smaller C values for potassium- and ATP-stimulated contractions are considered, this process of receptor-operated calcium influx was even slower than the diffusion of the agent to the cell membrane, which must also play a role in this type of contraction. ATP gave rise

to a higher U and smaller C value than acetylcholine (Figs. 4 and 5). If receptor-operated calcium influx indeed forms the rate-limiting step for acetylcholine-stimulated contractions, this effect might be explained by assuming either that ATP gives rise to added depolarization or that the ATP receptor is provided with a faster pathway to the contractile units (5, 8, 18). Further evidence that ATP gives rise to added depolarization is provided by the observation that the C value for potassium, which exerts its effect mainly via depolarization, is also smaller. Despite the diffusion factor, the C value of an ATP-stimulated contraction was quite similar to the C value of an electrically stimulated contraction, again providing evidence for such a fast pathway to the contractile units. Generally, both acetylcholine and ATP are thought to give rise to receptor-operated cell depolarization as well as receptor-operated calcium influx and receptor-operated intracellular calcium release (Fig.7).

During EGTA treatment the value of F_{iso} for electrical and ATP stimuli was reduced to <10% of its value in normal Krebs, indicating a substantial dependence on external calcium. The larger F_{iso} values for acetylcholine and potassium stimuli in EGTA treatment indicate that contractions evoked by these stimuli are less dependent on external calcium but alternatively release intracellularly stored calcium. For an acetylcholine stimulus this release is probably initiated by muscarinic receptor stimulation (3,16). During potassium stimulus a possible intracellular calcium release, resulting in a high F_{iso} value during EGTA treatment (Fig.3), could be due to cholinergic nerve stimulation, but the atropine resistance of the potassium-stimulated contraction (Fig. 3) militates against this hypothesis, favouring the alternative hypothesis of a depolarization-operated intracellular calcium release. This mechanism also has been suggested for arterial smooth muscle (17).

Verapamil reduced the value for F_{iso} to approximately half its value in normal Krebs (Fig. 3). The F_{iso} value for ATP was reduced even further (Fig. 3). A statistically significant difference was found between the reductions of the relative F_{iso} values resulting from electrical stimulation compared with ATP stimulation during verapamil treatment, indicating that verapamil affects the ATP-stimulated contraction more than the electrically induced contraction.

Atropine reduced F_{iso} for acetylcholine-stimulated contractions to 80% and for electrically stimulated contractions to ~40% (Fig. 3) of pretreatment values, indicating that the electrically stimulated contraction is ~40% cholinergic mediated. A similar effect has been shown by previous studies on human detrusor (12).

After Verapamil treatment the U values for all stimuli were not significantly different (Table 2) from the U values in normal Krebs solution, whereas with EGTA treatment U values were significantly reduced, indicating a smaller chance for units to change to the contractile state due to a lack of external calcium. Verapamil does not alter the external calcium concentration and did not consistently reduce U values, indicating the calcium is not available in sufficient

amounts or is not fast enough to allow units to become contractile to the same degree as before treatment (see the lower F_{iso} and the lower C value in verapamil treatment compared with values in normal Krebs, Figs. 3 and 5, Table 2). Also favouring this hypothesis is the fact that U after atropine treatment remained unaffected; i.e. atropine does not affect extracellular calcium concentration. In this manner the dependence of U on the length of the interstimulus interval, which has been reported previously (22), can be explained by a change in calcium sensitivity resulting from a gradual increase in the amount of calcium bound to the intracellular stores during the interstimulus interval.

For all stimuli during verapamil and EGTA treatment, except for electrical and potassium stimuli in EGTA, a significantly smaller C value was found (Fig.5, Table 2), indicating that a shorter time was needed to reach the maximum isometric force. It was therefore concluded that intracellular calcium release is a faster process than extracellular calcium influx.

For contractions evoked by acetylcholine and electrical stimuli during atropine treatment the C values were significantly reduced compared with the values in normal solution (Fig. 5, Table 2). This indicates that the rate-limiting step in the contraction development is blocked by atropine, which is a muscarinic receptor blocker.

Although the present data could not provide evidence that verapamil blocked depolarization-operated calcium channels more potently than receptor-operated channels (1-3), the remaining calcium dependence of contractions evoked in verapamil treatment could be explained either by assuming that certain depolarization-operated calcium channels were blocked completely and others were left unaffected or by assuming that channels were blocked partially. If the effects of calcium-free EGTA solution and verapamil on the differently stimulated contraction are compared, a clear difference in the values for F_{iso} and U could be observed for all stimuli. For all stimuli except potassium, the values for F_{iso} of contractions evoked during EGTA treatment were significantly smaller than those during verapamil treatment (see Table 2). This indicates that the calcium channels that can be blocked by verapamil are not the only sources of the external calcium necessary for contraction.

It is concluded that the diagram shown in Fig. 7 summarizes the effective pathways for isometric force development in pig urinary bladder smooth muscle. Phase-plot analysis provided a way to identify the rate-limiting pathways in the excitation-contraction and pharmacomechanical coupling process for the various stimuli applied. A hierarchy in rate limitation was shown. Under normal circumstances the rate-limiting step in isometric force development in this kind of smooth muscle is the influx of extracellular calcium. Both muscle depolarization and intracellular calcium release are faster processes even when triggered by receptor stimulation

Appendix

If the time course of isometric contraction development of a muscle strip were determined by the contractile element stretching the series elasticity, the associated time constant could be estimated as follows.

Suppose the muscle can be modeled as a contractile element with a length l_1 and a linear force-velocity characteristic

$$F = F_{iso} - F_{iso}/L_{max}.(dl_1/dt) \qquad\qquad \text{Eq.3}$$

(where v_{max} is the maximum contraction velocity), in series with a linear series elasticity E with length l_2

$$F = E.l_2 \qquad\qquad \text{Eq.4}$$

Adding the derivatives of the lengths l_1 and l_2 of both elements gives

$$F = F_{iso} + F_{iso}/(L_{max}.E)(dF/dt) \qquad\qquad \text{Eq.5}$$

The solution of *Eq.5* is a monoexponential function

$$F = F_{iso} [1 - \exp(-t/\tau)] \qquad\qquad \text{Eq.6}$$

with a time constant

$$\tau = F_{iso}/(E.L_{max}) \qquad\qquad \text{Eq.7}$$

This time constant can be normalized so that it consists of two dimensionless groups

$$\tau = (F_{iso}/E.l)[1/(L_{max}/l)] \qquad\qquad \text{Eq.8}$$

By use of *Eq. 4*, the first group can be rewritten as

$$F_{iso}/E.l = E.l_2 (F_{iso})/E.l = l_2(F_{iso})/l \qquad\qquad \text{Eq.9}$$

Here $l_2 (F_{iso})$ means the length of the series elastic element at F_{iso}. This length divided by the total length of the muscle strip is known from quick release studies on the same preparations (19)

$$l_2 (F_{iso})/l = 0.04 \qquad\qquad \text{Eq.10}$$

The second dimensionless group *Eq. 8* is also known for this preparation (21)

$$L_{max}/l = 0.25 \qquad\qquad Eq.11$$

Combining of *Eqs. 8-11* gives

$$\tau = 0.16 \text{ s}$$

References

1. Andersson, K.E., M. Fovaeus, E. Morgan, and G. McLorie. (1986) Comparative effects of five different calcium channel blockers on the atropine resistant contraction in electrically stimulated rabbit urinary bladder. *Neurourol. Urodyn.* 5: 579-586.
2. Baba, K., M. Kawanishi, T. Satake, and T. Tomita. (1985) Effects of verapamil on the contractions of guinea-pig tracheal muscle induced by Ca, Sr and Ba. *Br. J. Pharmacol.* 84: 203-211.
3. Bolton, T. (1979) Mechanisms of action of transmitters and other substances on smooth muscle. *Physiol. Rev.* 5•: 606-718.
4. Boom, H.K.B., J.J. Dernier van der Gon, J.H.M. Nieuwenhuijs, and P. Schiereck. (1973) Cardiac contractility: actin-myosin interaction as measured from the left ventricular pressure curve. *Eur.J.Cardiol.* 1/2: 217-224.
5. Brading, A.F., J.L. Mostwin, G.N.A. Sibley, and M.J. Speakman. (1986) The role of smooth muscle and its possible involvement in disease of the lower urinary tract. *Clin.Sci.Lond.* 70: 7-13.
6. Brading, A.F., and P. Sneddon. (1980) Evidence for multiple sources of calcium for activation of the contractile mechanism of guineapig taenia coli on stimulation with carbachol. *Br.J.Pharmacol.* 70: 229-240.
7. Casteels, R., and L. Raeymaekers. (1979) The action of acetylcholine and catecholamines on an intracellular calcium store in the smooth muscle cells of the guinea pig taenia coli. *J.Physiol.Lond.* 294: 51-68.
8. Fujii, K. (1988) Evidence for adenosine triphosphate as an excitatory transmitter in guinea-pig, rabbit and pig urinary bladder. *J.Physiol.Lond.* 404: 39-52.
9. Griffiths, D.J., R. van Mastrigt, W.A. van Duyl, and B.L.R.A. Coolsaet. (1979) Active mechanical properties of the smooth muscle of the urinary bladder. *Med.Biol.Eng.Comput.* 17: 281-290.
10. Itoh, T., H. Kuriyama, and H. Suzuki. (1981) Excitation-contraction coupling in smooth muscle cells of the guinea-pig mesenteric artery. *J.Physiol.Lond.* 321: 513-535.
11. Itoh, T., H. Ueno, and H. Kuriyama. (1985) Calcium-induced calcium release mechanism in vascular smooth muscles-assessments based on contractions evoked in intact ans saponin-treated skinned muscles. *Experientia Basel* 41: 989-996.
12. Kinder, R.B., and A.R. Mundy. (1985) Atropine blockade of nerve-mediated stimulation of the human detrusor. *Br.J.Urol.* 57: 418-421.
13. Krebs. H.A. (1932) Untersuchungen über die Harnstoffbildung im Tierkorper. *Hoppe Seylers Z. Physiol. Chem.* 210: 33-67.
14. Marthan, R., J.P. Savineau, and J. Mironneau. (1987) Acetylcholine-induced contraction in human isolated bronchial smooth muscle: role of an intracellular calcium store. *Respir.Physiol.* 67: 127-135.
15. Meiss, R.A. (1975) Graded activation in rabbit mesotubarium smooth muscle. *Am.J.Physiol.* 229: 455-465.
16. Mostwin, J.L. (1985) Receptor operated intracellular calcium stores in the smooth

muscle of the guinea-pig bladder. *J.Urol.* 133: 900-905.

17. **Somlyo, A.P., and B. Himpens.** (1989) Cell calcium and its regulation in smooth muscle. *FASEB J.* 3: 2266-2276.

18. **Van Koeveringe, G.A., and R. van Mastrigt.** (1988) Excitation contraction coupling in the urinary bladder of the pig. *J.Muscle Res.Cell Motil.* 9: 467.

19. **Van Mastrigt, R.** (1988) The length dependence of the series elasticity of pig bladder smooth muscle. *J.Muscle Res. Cell Motil.* 9: 525-532.

20. **Van Mastrigt, R., and J.J. Glerum.** (1985) Electrical stimulation of smooth muscle strips from the urinary bladder of the pig. *J. Biomed. Eng.* 7: 2-8.

21. **Van Mastrigt, R., and J.J. Glerum.** (1985) In vitro comparison of isometric and stop-test contractility parameters for the urinary bladder. *Urol. Res.* 13: 11-17.

22. **Van Mastrigt, R., J.W.B. Koopal, J. Hak, and J. van de Wetering.** (1986) Modeling the contractility of urinary bladder smooth muscle using isometric contractions. *Am.J.Physiol.* 251 (Regulatory Integrative Comp.Physiol. 20):R978-RR983.

.

CHAPTER 3

The Guinea pig as a model of gradual urethral obstruction

Jacek L. Mostwin, Omer M. A. Karim, Gommert A. van Koeveringe
and Eva L. Brooks (Johns Hopkins University, Baltimore, U.S.A.)

Summary

We developed a new model of partial urethral obstruction using the guinea pig. We placed jeweler's jump rings loosely around the proximal urethra of immature guinea pigs and allowed the obstruction to develop gradually as the animal grew. After 4 or 8 weeks of obstruction, we studied the filling and emptying characteristics of the bladder during continuous repetitive cycling under urethane anesthesia. Following this examination, bladders were removed and weighed. Wet weight was compared to urodynamic findings. We identified four abnormal urodynamic patterns: high pressure voiding, instability, poor compliance and decompensation. All obstructed bladders showed weight gain associated with muscle hypertrophy, but the degree of weight gain was different for each of the various urodynamic categories. High pressure voiding was associated with the least weight gain, whereas instability and decompensation showed the most weight gain. The results are consistent with a thesis that partial urethral outlet obstruction in the guinea pig gives rise to several distinct forms of abnormal voiding characterized by high pressure in the early stages, and progressing to more advanced forms of dysfunction characterized by instability and decompensation in the later stages.

Introduction

Following initial clinical observations that men with bladder obstruction due to benign prostatic hyperplasia show signs of unstable bladder contractions during the filling phase of cystometry (1,2), attempts were made to produce bladder instability in animal models by obstructing the urethra in order to produce sources of tissue for pharmacological and other investigations of the unstable bladder. Several animal models have been developed using the pig (3), rat (4), rabbit (5,6), and cat (7). The pig model which has given rise to the thesis that bladder instability is associated with a postjunctional type of denervation supersensitivity. (8) The guinea pig has not previously been considered as an animal model for the study of the effect of urethral obstruction on the bladder. We selected this animal for several reasons: it is small, inexpensive and easily housed. No special operating room facilities are required. Much is already known about the basic pharmacologic properties of the guinea pig bladder smooth muscle (9), and more is known about the electrical properties of the guina pig bladder smooth muscle than any other mammalian bladder, making this a theoretically attractive model for the eventual investigation of changes in electrical properties arising after urethral obstruction. (10,11,12) In a preliminary report (13) we found that placement of jeweler's jump rings around the urethra of

the immature (250-300 gm) guinea pig resulted in bladder muscle hypertrophy and abnormal voiding as the animal grew, without otherwise interfering with animal growth. The operation was well tolerated, 33 of 34 animals survived and gained weight. Urodynamic investigation after 4 or 8 weeks of 16 obstructed animals showed four distinctly different voiding patterns when compared to 7 normal and 6 sham operated controls: we described these as high pressure, instability, poor compliance and decompensation. We wished to repeat this study using only one ring size, describing more completely the storage and emptying characteristics of the hypertrophied bladder which develops following obstruction, and relating this, if possible, to the degree of hypertrophy.

Methods and Materials
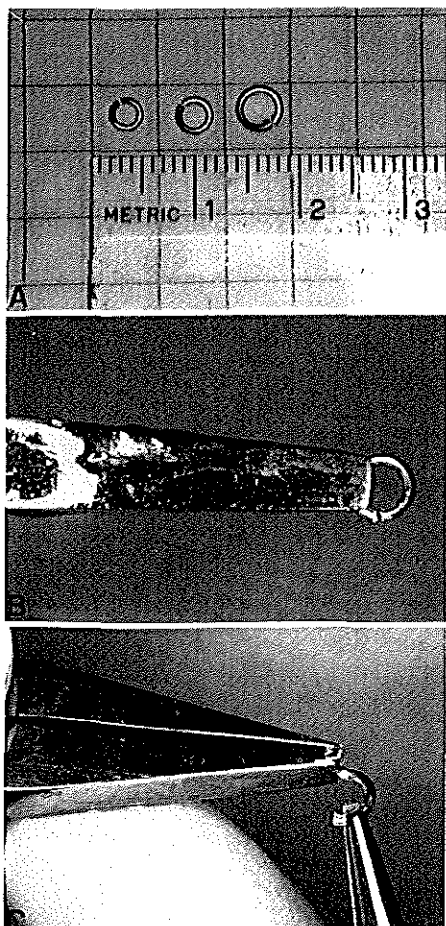
In order to eliminate as much unnecessary variability in the method of obstruction as possible, we selected jeweler's jump rings, simple silver twist open rings of standard industrial diameter and gauge, as the method of occlusion. This technique has not been decribed before, except for our preliminary report (13). Rings were available from a local jewelry repair shop and could be obtained in many different sizes from standard jewelry supply catalogues (Figure 1a). When twisted open and twisted closed again, these rings retained their precise shape without becoming deformed, thus minimizing potential variability due to size and deformity of the occluding material (Figure 1b,c).

Our goal was to produce gradual rather than acute obstruction, to create a model which would most closely represent naturally occurring obstruction such as that which occurs in the presence of benign prostatic

Figure 1. a) Jeweler's jump rings obtained from a local jewelry supply store, b) Ring held in flat-tipped forceps, c)ring twisted open by additional narrow-nosed pliers.

hyperplasia or posterior urethral valves. We therefore placed rings loosely about the urethrae of immature guinea pigs weighing 250-300 gms and allowed the obstruction to develop gradually as the animal grew to a more mature weight of 600-800 gm.

Operative procedure

Twenty immature male albino guinea pigs (Hartley strain) weighing 250-300 gm underwent partial urethral obstruction as follows: after anesthesia with intraperitoneal sodium pentobarbital (40mg/kg), the peritoneal cavity was entered through a low vertical midline abdominal incision and the bladder identified. The bladder was drained of urine by syringe and a monofilament
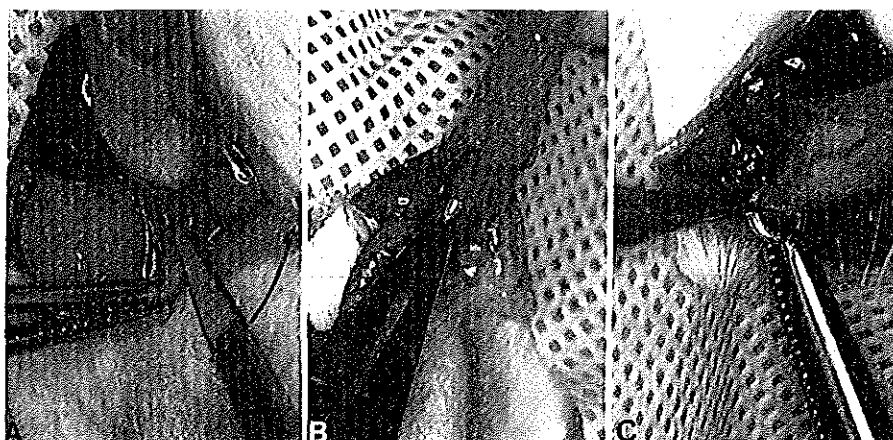

Figure 2. Operative technique: a)connective tissue anterior to bladder neck indicated by closed scissor tips, b) open ring placed around the exposed proximal urethra, c)ring closed.

nylon suture placed through the bladder for traction. The delicate connective tissue anterior to the bladder neck was identified and opened with scissors (Figure 2a). The loose areolar tissue beneath this layer was separated carefully without cutting to avoid injury to small blood vessels in this space. These vessels are friable, bleed easily, and may possibly contribute to excessive perivesical fibrosis during healing. In this manner the bladder neck and proximal urethra were exposed. Without further dissection, a silver jeweler's jump ring (2.2 mm internal diameter) was twisted open and passed around the proximal urethra without damaging the web of connective tissue forming the lateral vesical pedicle containng blood vessels and nerves to the bladder (Figure 2b). The open end of the ring easily pierced this delicate tissue with minimal trauma. The ring was twisted closed (Figure 2c) and the abdominal incision closed in two layers with absorbable suture. The operation was performed under
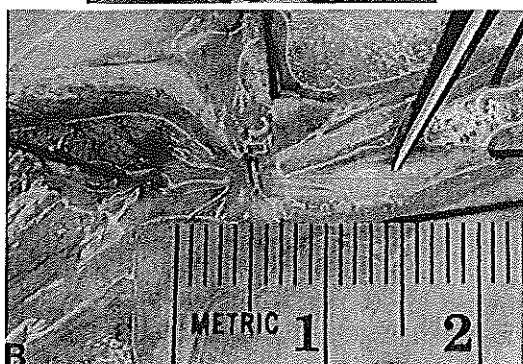
Figure 3. Location of ring following bladder removal: a)posterior aspect, the ring is located midway between ureters and ejaculatory ducts. b)sagittal section, ureteral orifice (left) is identified by black pin, ejaculatory duct opening into urethra (right) is identified by closed forceps tips, the ring is located midway between them in the approximate position of the bladder neck.

sterile conditions, usually in 10 minutes or less.

Urodynamic procedure

Four or eight weeks following initial obstruction, animals were anesthetized with intraperitoneal urethane (1gm/kg) (14). After 30-45 min the distended bladder could be felt through the abdominal wall. If not, a 25 gauge needle could be used to locate the bladder and fill it with 2-3 ml 0.9% saline by syringe until it was palpable. Two 24 gauge 1.6 cm pediatric angiocatheters were inserted percutaneously into the bladder. One was connected to a continuous infusion pump (Harvard Bioscience), the other to a pressure transducer amplified and displayed onto moving tracer paper (initially Life-Tech, and later Harvard Bioscience and Gould). The signal was also digitized and stored on magnetic disc for subsequent analysis (IBM XT, Data Acquisition A/D convertor 2801, CODAS Waveform scroller). The urethra was neither instrumented nor catheterized. The bladder was filled at a continuous rate of 0.82 ml/min with 0.9% NaCl at 20°C. The animal was observed for signs of voiding or leakage of solution per urethram. The volume voided was collected in a graduated pipette connected to pressure transducer for recording of voided volume. At least 10 voiding cycles were observed in each animal. We examined the following urodynamic parameters in the voiding cycles of all animals: resting bladder pressure (RBP), the intravesical pressure at the beginning of each new voiding cycle; end-filling pressure (EFP), the maximum pressure measured before active bladder contraction was seen;

Table 1: Urodynamic categories of 9 normal and 17 obstructed guinea pigs.

			4 wks	8 wks	Total
1	Normal	NML			9
2	High pressure	HIP	1	5	6
3	Unstable	UNS	4	1	5
4	Low compliance	LWC	1	1	2
5	Decompensated	DEC	2	2	4

peak voiding pressure (PVP); compliance (CMP), the ratio of the infused volume per cycle to EFP-RBP; residual urine (PVR); voided volume (VV); and bladder capacity (CAP). The entire procedure usually took about 90-120 minutes. At the end of this procedure, the animal was sacrificed with CO_2 inhalation, the bladder and urinary tract examined grossly, and the bladder removed by dividing at the bladder neck. The bladders were separated from associated structures, excessive fat and connective tissue, blotted once on each side to absorb surface moisture, then weighed on an electronic scale. Bladder weight and urodynamic parameters were tabulated and compared to normals by Dunnet's method for multiple comparisons (one-tailed).

Results

Twenty animals were obstructed with identical 2.2 mm i.d. silver jeweler's jump rings. There were 9 unoperated controls. All animals survived and gained weight at a rate similar to that of unoperated control animals. At either 4 or 8 weeks, cystometry was successfully performed on 17 of 20 obstructed animals and 9 normal control animals. The animals were then sacrificed and the bladders removed.

Figure 4.
Hematoxylin and eosin preparation of normal (left) and obstructed (right) bladder muscle. Both examined under identical magnification (x 575). Normal to obstructed weight ratio approximately 2:1, normal to obstructed nuclear ratio, approximately 2:1.
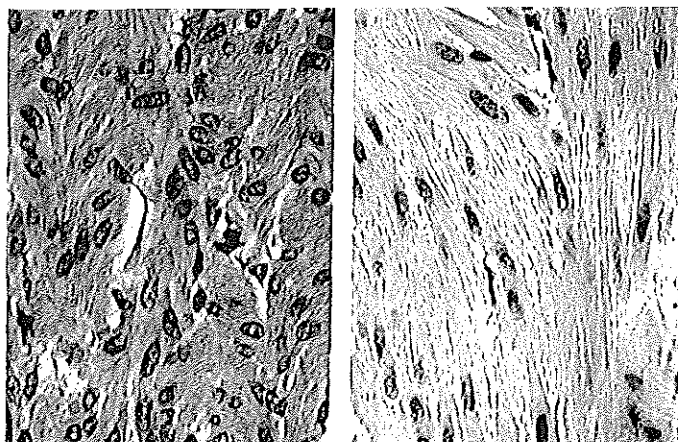
Table 2: Urodynamic parameters for 9 normal and 17 obstructed guinea pigs listed in Table 1. (Mean values; S.E.M. below in parentheses)

	WT(g)	RBP	EFP	PVP	CMP	PVR	VV	CAP
NML		1.06	3.08	28.73	1.32	0.39	2.77	3.16
	(0.05)	(0.39)	(0.53)	(2.66)	(0.19)	(0.15)	(0.26)	(0.30)
LWC	0.76	2.38*	7.23	25.30	0.08*	2.11	0.90**	3.01
	(0.05)	(0.03)	(1.18)	(1.37)	(0.01)	(1.34)	(0.19)	(1.15)
HIP	0.85	4.27	8.15	66.32	0.26	2.59	1.52	4.11
	(0.07)	(0.47)	(0.52)	(6.16)	(0.06)	(0.53)	(0.18)	(0.46)
UNS	1.171	3.46	8.13	31.81	0.26	2.48	1.72	4.20
	(0.15)	(1.05)	(1.32)	(1.96)	(0.07)	(0.71)	(0.34)	(0.53)
DEC	1.471	17.601	22.6	28.53	0.35	6.06	0.22*	6.28
	(0.11)	(1.81)	(1.30)	(1.92)	(0.16)	(2.46)	(0.04)	(2.45)

* = $p < 0.05$
** = $p < 0.01$

WT	Wet weight of bladder (gm)
RBP	Resting bladder pressure (cm H2O)
EFP	End filling pressure (cm H2O)
PVP	Peak voiding pressure (cm H2O)
CMP	Compliance (infused volume per cycle/(EFP-RBP); ml/cmH2O)
PVR	Residual urine (ml)
VV	Volume voided (ml)
CAP	Bladder capacity (ml)

NML	Normal controls
HIP	High pressure
UNS	Unstable
LWC	Low compliance
DEC	Decompensated

Table 3: Effect of obstruction on urodynamic parameters expressed as percentage of normal

	WT(g)	RBP	EFP	PVP	CMP	PVR	VV	CAP
NML	100.0	100.0	100.0	100.0	100.0	100.0	100.0	100.0
HIP	157.4	402.6	264.7	230.8*	19.5	660.7	54.9	130.0
UNS	216.7*	326.6	264.1	110.7	20.0	632.4	62.0	132.7
LWC	141.3	224.5	234.9	88.0	6.2*	538.3	32.*	95.6
DEC	272.2*	1660**	734**	99.3	26.6	1545	8.0*	198.6

* = $p < 0.05$ ** = $p < 0.01$

a. NORMAL

b. HIGH PRESSURE

c. UNSTABLE

d. LOW COMPLIANCE
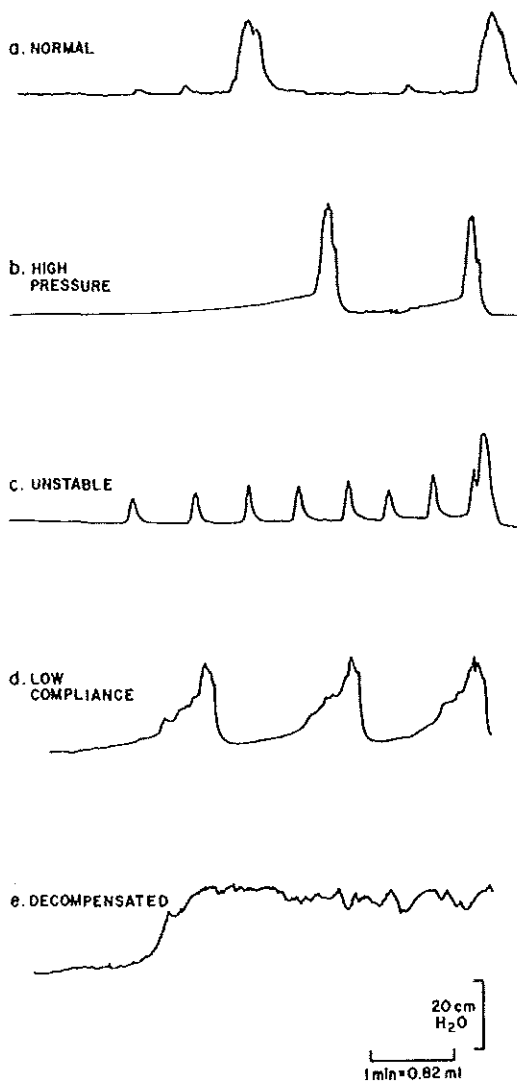
e. DECOMPENSATED

20 cm H₂O

1 min = 0.82 ml

Figure 5. Representative urodynamic tracings: a)normal, b)high pressure, c)unstable, d)poor compliance, e)decompensation. All drawn to scale shown in lower right hand corner for ease of comparison.

Postmortem examination indicated that the ring had remained closed and in place, without migration, erosion or abscess formation. Scarring was minimal. The ring was usually found in a position midway between the ejaculatory ducts and the ureteral orifices, corresponding closely to the location of a median bar contracture (Mercier's bar) which might be seen in a human patient with benign prostatic hyperplasia (Figure 3a,b). Bladders which were increased in weight showed histological features of hypertrophy, manifested by an increase in the ratio of cytoplasm to number of nuclei (Figure 4. Trabeculation of the sort seen in human bladders with advanced obstruction was not seen. No animal showed ureteral dilatation or hydronephrosis.

Urodynamic Patterns

The urodynamic tracings were examined independently of weight changes or gross appearance of the bladder. We separated the animals into five groups based on the appearance of their filling and voiding patterns. The groups were: Normal, High pressure, Unstable, Low compliance, Decompensated. The number of animals in each group is shown in Table 1. The mean absolute values of the urodynamic parameters along with standard errors of the mean for each group are listed in Table 2. The value of each variable has been compared to the corresponding

variable in the normal group by t-test and the statistical significance of the difference is indicated where present. In Table 3, the urodynamic parameters are expressed as percentages of normal, and statistically significant differences from the normal have been indicated. Figure 5(a-e) shows representative tracings from each of the five urodynamic categories which are more fully described below:

Normal (Figure 5a)

Cystometrograms of normal animals showed stable and compliant filling, with an occasional small amplitude pre-contraction. As indicated in Table I, the average capacity was 3.16 ml (0.30), the voiding pressure 28.73 cm H_2O (2.66), and the post-void residual 0.39 ml (0.15). The filling portion was flat and the compliance was calculated to be 1.32 ml/cmH_2O (0.19).

High pressure (Figure 5b)

These cystometrograms showed markedly higher (> twofold) voiding pressure than normal or any of the other other categories in which instability, compliance change or decompensation dominated. There was only one dominant contraction at capacity, as opposed to bladders showing multiple large-amplitude contractions which we classified separately and labelled as "unstable" (Figure 5c). There was no significant difference in the capacity or the end-filling pressure of the high pressure voiders when compared to the low compliance and unstable groups, but the high pressure group showed less of an increase in weight compared to normal than did the unstable or any other group.

Instability (Figure 5c)

This pattern was termed "unstable" because it resembled the cystometrograms of human patients with clinically unstable bladders which show multiple unstable contractions on filling cystometry. We adapted the ICS definition of instability (15) to our animal model: low amplitude contractions which achieved one-third of normal voiding pressure were considered unstable. Since normal PVP was 28.7 cmH_2O, we considered contractions >10 cmH_2O to represent an unstable contraction. Unstable bladders showed greater weight gain than high pressure bladders, but the peak voiding pressure and capacity were not much higher than normal. The end-filling pressure was similar to high pressure and low compliance bladders and the compliance was not different than the high pressure bladders. The characteristics of both unstable and high pressure voiders are listed in Tables 2 and 3. Except for the difference in weight gain and the peak voiding pressure which was the distinguishing feature of this group, urodynamic features of the two groups, specifically, end filling pressure, compliance, voided volume, post-void residual and capacity, were quite similar.

Low compliance (Figure 5d)

These bladders showed high end-filling pressures but also generated sufficient active contraction at capacity to at least partially empty the bladder and result in a voiding cycle. The peak voiding pressure was similar to the control value and only slightly less than the unstable group. The bladder weight was increased 1.41 times that of control, the least of any of the four abnormal groups, but statistical significance was not achieved, owing to the small number of animals in the group (n=2). The capacity was only slightly reduced to 95% of the control value.

Decompensation (Figure 5e)

This description was reserved for those bladders which showed no evidence of active contraction. They filled to a high end-filling pressure, then overflowed passively at capacity with a large post-void residual volume. This group showed the most weight gain, 2.72 times greater than control. Interestingly, the pressure at which passive leakage occurred was almost identical to the peak voiding pressure of normal bladders, similar to the peak voiding pressure of unstable animals, and much less than the elevated peak voiding pressures of the high pressure voiders.

Discussion

Our results indicate that similar degrees of urethral obstruction in the guinea pig produce varying degrees of bladder muscle hypertrophy and voiding abnormalities which may resemble patterns found in humans with lower urinary tract outflow obstruction. We found that both the operation and the subsequent urodynamic studies could be easily performed. Almost all animals survived following surgery and gained weight. No animal developed hydroureteronephrosis. No animal died of a surgical complication. No animal died of acute urinary retention.

The use of the jeweler's jump ring, not previously described, may offer a universally applicable method for the experimental production of partial reproducible obstruction of tubular muscular structures such as blood vessels, vas deferens, ureter, intestinal segment or portion of the tracheobronchial tree. Previous investigations of animal models of urethral obstruction have focussed on instability alone. We identified four patterns of abnormal bladder cycling, only one of which appeared to resemble human instability and which we decided to classify as such. Each of the four patterns was associated with a different degree of increase in bladder weight, suggesting a possible chronological order in the progression from one kind of abnormality to another. High pressure voiding was associated with the least bladder hypertrophy, instability and

decompensation were associated with the most hypertrophy.

Our results are most consistent with a thesis that partial urethral outlet obstruction in the guinea pig gives rise to several distinct forms of abnormal voiding characterized by high pressure and a lesser degree of bladder weight increase in the early stages, progressing to more advanced forms of dysfunction characterized by instability and decompensation with a greater degree of bladder weight increase in the later stages. Examination of the data in Table 1 could, however, suggest an alternative thesis. We found that more of the unstable bladders were present in the group of animals studied four weeks after obstruction, and more high pressure voiders were found in the group after eight weeks of obstruction. How does one reconcile this observation with the differences in weight gain? One would have to assume that bladder weight does not increase steadily in response to obstruction, but rather, that the bladder hypertrophies to a given "set point" in any given animal, determined by the exact degree of obstruction and the physical or genetic limitations of tissue plasticity. In such a likelihood, each of the four abnormalities would represents one of four possible types of resonse, each being independent of the other. Further studies using this model may provide clarification.

Before applying the results of studies such as this to humans with infravesical obstruction, certain differences should be considered. We cannot, for example, on the basis of these studies, determine whether or not some of the high pressure voiding patterns which developed in guinea pigs represented "unstable" bladder contractions in the sense that the term is applied to humans. In humans, instability represents a bladder contraction elicited during the filling phase of cystometry which cannot be inhibited (15). A human patient may or may not be aware of such a developing unstable contraction, depending on the integrity of sensory mechanisms. Whereas such a single contraction occurring at the end of filling, whether high pressure or not, would be considered "unstable" in a human if it could not be inhibited, we might compare it to either the normal or the high pressure patterns in our guinea pigs, depending on the degree of pressure achieved during voiding. With respect to our experimental animals, we have used the term "instability" much more narrowly than it is used in the clinical sense when dealing with humans, limiting it to a series of low amplitude contractions which precede but do not result in effective emptying of the bladder. It can be said, however, that the various patterns seen in this study, i.e., high pressure voiding, instability (as we have defined it in our guinea pigs), poor compliance and decompensation are all seen in humans with bladder outflow obstruction.

We have found the guinea pig to be a useful model for studying the effect of partial urethral obstruction on the mammalian bladder. The use of jeweler's jump rings offers a fairly precise and theoretically controllable and reproducible method for producing obstruction. Placing the ring loosely around the urethra of immature animals may offer the advantage of allowing the obstruction to

develop gradually as the animal grows and minimizes the risk of postoperative death due to acute obstruction and tissue changes due to acute overdistention. Since muscle from guinea pig bladder has been used previously for successful electrophysiological study, the model potentially offers a source of obstructed tissue for such investigations and should complement existing animal models.

References

1. Hinman F, ed. (1983) Benign Prostatic Hypertrophy. New York, Springer-Verlag.
2. Turner-Warwick R. (1984) Bladder outflow obstruction in the male. in: Mundy AR, Stephenson TP, Wein AJ, eds. Urodynamics: principles, practice and applications. Edinburgh, Churchill-Livingstone, pp.183-204.
3. Sibley GN. (1987) The physiological response of the detrusor muscle to experimental bladder outflow obstruction in the pig. *Br J Urol.* 70:332-336.
4. Mattiasson A, Uvelius B (1982) Changes in contractile properties in hypertrophic rat urinary bladder. *J Urol.* 128:1340-1342.
5. Brent L, Stephens FD (1975) The response of smooth muscle cells in the rabbit urinary bladder to outflow obstruction. *Invest Urol.* 12:494-502.
6. Levin RM, High J, Wein AJ (1984) The effect of short term obstruction on urinary bladder function in the rabbit. *J Urol.* 132:789-791.
7. Levin RM, Kato K, Ruggieri M, McGuire EJ, Elbadawi A, Wein AJ (1989): The physiological effect of outlet obstruction on the cat. *J Urol.* 141:335A.
8. Speakman MJ, Brading AF, Gilpin CJ, Dixon JS (1987): Bladder outflow obstruction a cause of denervation supersensitivity. *J Urol.* 138:1461-1466.
9. Brading AF (1987): Physiology of bladder smooth muscle. In: Torrens M, Morrison JFB (eds) The Physiology of the Lower Urinary Tract. London, Springer-Verlag, 161-191.
10. Brading AF, Mostwin JL (1989): Electrical and mechanical responses of guinea pig bladder muscle to nerve stimulation. *Br J Pharmacol.* 98:1083-1090.
11. Mostwin JL (1986): The action potential of guinea pig bladder smooth muscle. *J Urol.* 135:1299-1303.
12. Mostwin JL (1988): Electrical membrane events underlying contraction of guinea pig bladder muscle. *Neurourol Urodyn.* 6:429-437.
13. Mostwin JL, Brooks EL (1989): A new guinea pig model of urethral obstruction. *J Urol.* 141:334A.
14. Peterson JS, Hanson RC, Noronha-Blob L (1989): In vivo cystometrogram studies in urethane-anesthetized and conscious guinea pigs. *J Pharmacol Met.* 21:231-241.
15. Bates P, Bradley WE, Glen E, Griffiths D, Melchior H, Rowan D, Sterling A, Zinner N, Hald T: (1979) The standardization of terminology of lower urinary tract function. *J Urol.* 121: 551-554.

CHAPTER 4

Effect of partial urethral obstruction on force development of the Guinea pig bladder

Normal urinary bladder muscle cells

Obstructed urinary bladder muscle cells
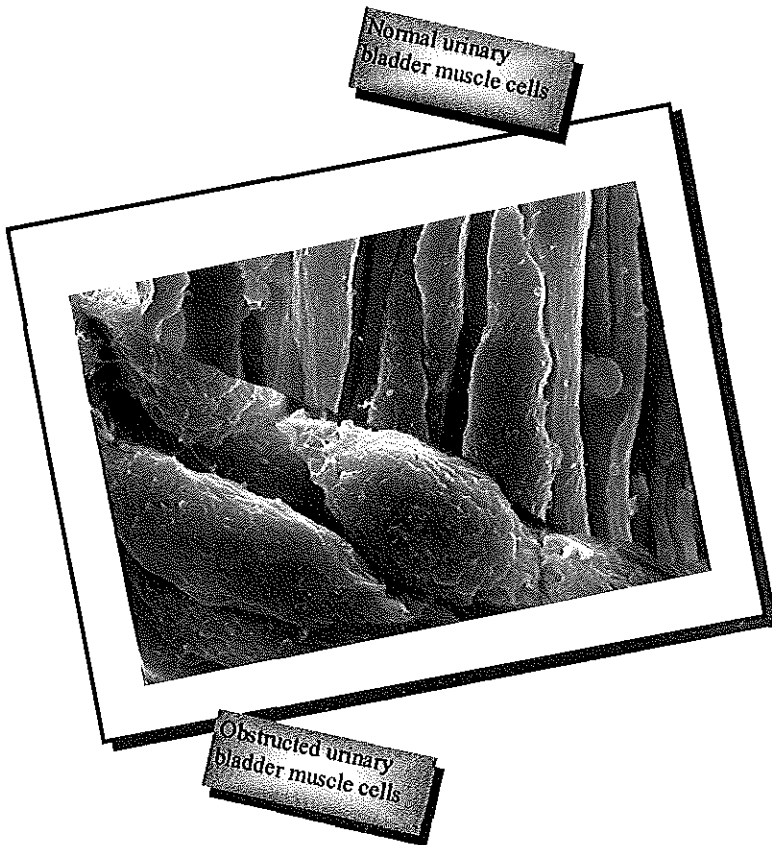
Gommert A. van Koeveringe, Jacek L.Mostwin (Johns Hopkins University Baltimore, U.S.A.), Ron van Mastrigt and Bram J.van Koeveringe

Summary

We created gradual partial urethral obstruction in 20 guinea pigs using silver jeweller's jump rings. After 4 or 8 weeks obstruction all animals underwent cystometry and were assigned to one of five urodynamic categories: Normal, high pressure voiding, unstable, low compliance or decompensated. After sacrifice, the contractile responses of bladder strips to electrical field stimulation of intramural nerves, direct electrical muscle stimulation, 0.1 mM carbachol and high K^+ solution were sampled by computer for phase plot analysis. Following 8 weeks obstruction, the value of the phase plot parameter F_{iso}, indicative of the number of contractile muscle units, was reduced to 60% of the control response to nerve stimulation ($p<0.05$) and to 77% of the control response to carbachol stimulation ($p<0.05$). Parameter C, the slope of the phase plot (indicative of unit recruitment during force development) was unchanged for all forms of stimulation. Although in the latter case not statistically significant, obstruction affected responses to nerve and muscle stimulation similarly suggesting that muscle change may possibly be a common denominator of dysfunction. In view of the reduction in F_{iso} and the increase in bladder weight, instability may represent a more advanced form of dysfunction due to obstruction than high pressure voiding.

Introduction

A model for urethral obstruction in male albino Guinea pigs was developed at Johns Hopkins University , Baltimore (10,11). The aim of this study was to investigate the changes in functional properties of the detrusor muscle tissue after a period of partial urethral obstruction. Changes in bladder contractility, whether or not combined with instability have been demonstrated by numerous clinical observations in man suffering from enlargement of the prostate (2,4). The Guinea pig model served to investigate both in vivo urodynamic properties and the in vitro detrusor muscle contractility. In organ bath studies detrusor muscle contractility had been investigated previously at the Erasmus University Rotterdam, The Netherlands by means of phase plot analysis (14,15). This method describes muscle force development by means of two parameter values, one of these representing a time constant (13). In order to relate in vitro to in vivo changes, we studied changes in phase plot parameter values after different time periods or in different categories of post-obstructive urodynamic dysfunction. Many previous studies on in vitro smooth muscle contractility concentrated on maximum developed force or pressure only (3,8,9). Besides the maximum generated force, this study also investigated the time dimension in the

force development.

Materials and Methods

Operation

Partial urethral obstruction was created in 20 immature albino guinea pigs (Hartley strain) weighing 250 -350 gm using jeweler's jump rings (2.2 mm i.d.) according to the method we have previously described (11). After anesthesia with intraperitoneal sodium pentobarbital (40mg/kg), the peritoneal cavity was entered through a low vertical midline abdominal incision and the bladder was identified. It was drained of urine by syringe and a monofilament nylon suture was placed through the bladder for traction. The delicate connective tissue anterior to the bladder neck was identified and opened with scissors. The loose areolar tissue beneath this layer was separated carefully without cutting to avoid injury to small blood vessels in this space. These vessels are friable, bleed easily, and may possibly contribute to excessive perivesical fibrosis during healing. In this manner the bladder neck and proximal urethra were exposed. Without further dissection, a silver jeweler's jump ring (2.2 mm internal diameter) was twisted open and passed around the proximal urethra without damaging the web of connective tissue forming the lateral vesical pedicle containing blood vessels and nerves to the bladder. The open end of the ring easily pierced this delicate tissue with minimal trauma. The ring was twisted closed and consequetively the abdominal incision was closed in two layers with absorbable suture. The operation was performed under sterile conditions, usually in 10 minutes or less. In this manner 10 animals were obstructed for a period of 4 weeks, 10 for 8 weeks and 10 served as controls.

Urodynamic investigation

All animals underwent cystometry under urethane anesthesia according to the method we have described previously (6,11). Four or eight weeks following initial obstruction, the animals were anaesthetized with intraperitoneal urethane (1gm/kg). After 30-45 min the distended bladder could be felt through the abdominal wall. If not, a 25 gauge needle was used to locate the bladder and fill it with 2-3 ml 0.9% saline by syringe until it was palpable. Two 24 gauge 1.6 cm pediatric angiocatheters were inserted percutaneously into the bladder. One was connected to a continuous infusion pump (Harvard Bioscience), the other to a pressure transducer amplified and displayed onto moving tracer paper (initially LifeTech, and later Harvard Bioscience and Gould). The signal was also digitized and stored on magnetic disc for subsequent analysis (IBM XT, Data Translation 2801 A/D convertor, CODAS Waveform scroller). The urethra was

neither instrumented nor catheterized. The bladder was filled at a continuous rate of 0.82 ml/min with 0.9% NaCl at 20°C.

The animal was observed for signs of voiding or leakage of solution per urethram. The volume voided was collected in a graduated pipette connected to a pressure transducer for recording of voided volume. At least 10 voiding cycles were observed in each animal. We examined the following urodynamic parameters in the voiding cycles of all animals: resting bladder pressure (RBP), the intravesical pressure at the beginning of each new voiding cycle; end filling pressure (EFP), the maximum pressure measured before active bladder contraction was seen; peak voiding pressure (PVP); compliance (CMP), the ratio of the infused volume per cycle to EFP-RBP; residual urine (PVR); voided volume (VV); and bladder capacity (CAP). After examination of the cystometric tracings, animals were assigned to one of five urodynamic categories, based on the appearance of the tracing. The five categories: "normal", "high pressure voiding", "unstable", "low compliance" and "decompensated" are further defined in the RESULTS section.

At the end of this procedure, the animal was sacrificed with CO_2 inhalation, the bladder and urinary tract were examined grossly, and the bladder was removed by dividing at the bladder neck. The bladders were separated from associated structures, excessive fat and connective tissue, blotted once on each side to absorb surface moisture, then weighed on an electronic scale. Bladder weight and urodynamic parameters were tabulated and compared to normals by nonpaired t-test.

Examination of in vitro contraction

Smooth muscle bundles were identified in the muscularis of the urinary bladder of each animal. From these bundles six 0.5 mm x 8 ($\pm$ 1) mm strips (wet weight was determined following experiment) were cut longitudinally. Special care was taken so that strips had similar lengths. Each of the 6 strips was suspended at 0.5 gm tension in an organ bath (vol 0.2 ml) modified for isometric tension recording and electrical stimulation by paired platinum ring electrodes. The strips were perfused continuously in one direction at a constant rate with a modified Krebs solution containing (mM): NaCl 120; KCl 5.9; $NaHCO_3$ 15.4; $MgCl_2$ 1.2; NaH_2PO_4 1.0; $CaCl_2$ 2.5; glucose 11, equilibrated with 97% O_2 / 3% CO_2, pH 7.4 at 36°C. Following equilibration for 1 hr, all six tissue strips were simultaneously exposed to the following stimuli, separated by additional equilibration periods of 10 minutes:

1. field stimulation of intramural nerves (0.050 ms, 50 V, 128 Hz trains for 5 s)
2. direct electrical muscle stimulation (5.0 msec, 5 V, 128 Hz for 5 s)
3. carbachol 10 mM (12 s) dissolved in Krebs solution
4. Potassium rich solution, KCL replaced NaCl, so that the potassium

concentration totalled 142 mM in Krebs solution (60 s)
Following the in vitro contractility studies, each strip was removed, blotted once and weighed.

Calculation of force development parameters

The isometric tension transducers were connected to an analog/digital converter. Waveforms from each of the six strips were sampled per computer in Baltimore at 10Hz and stored as electronic files. These files were sent by electronic telecommunication (BITNET, the early Internet) to Rotterdam for phase plot analysis. The phase plot curves and parameters were sent back to Baltimore as electronic files. The average of the six strips from each animal was calculated and correlated with bladder weight and urodynamic category. Statistical significance was tested using Student's t- test (STATGRAPHICS).

Phase plot analysis (Figure 1)

Phase plot analysis was performed by calculating instantaneous dF/dt(t) (time derivative of force F: the rate of force development) and displaying dF/dt(F) (time derivative of force dF/dt plotted against the force F itself) (13,14).
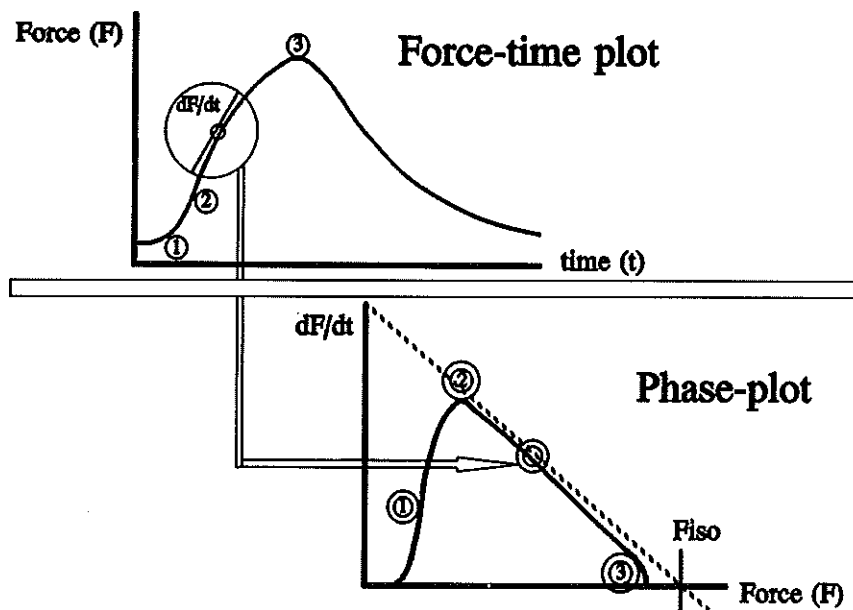

Figure 1: Phase plot, a plot of the rate of change of force (dF/dt) as a function of the force (F) was derived from the force-time plot as indicated. The numbers 1, 2 and 3 in the phase plot correspond to points 1, 2 and 3 in the force-time plot, from which they were calculated. The straight line portion of the phase-plot curve can be extrapolated to the F axis to yield the parameter Fiso; the negative reciprocal value of the slope is parameter C.

The straight line portion of this curve was extrapolated to the dF/dt and F intercepts yielding two parameters of force development:

F_{iso}: The value of F at dF/dt=O, the extrapolated theoretical maximum isometric force which the tissue can generate in response to a stimulus. F_{iso} indicates the maximum number of contractile muscle units

C: the limiting rate constant of excitation-contraction coupling. It indicates the recruitment rate of contracting units and is the negative reciprocal value of the slope of the fitted straight line.

The values of the force development parameters F_{iso} and C were calculated for every strip, 6 strips were obtained from each animal. To correct for differences in cross-sectional area, measured forces are generally expressed in terms of stress, i.e. force normalized by cross-sectional area. As in our case all strips in all series were similar in length, F_{iso} values could be normalized by dividing by strip weight. C was independent of specimen weight and was not adjusted. For each animal an average parameter value for the 6 strips was calculated per stimulus. Consequetively, a mean F_{iso} and C was calculated for one stimulus either in a 4 or 8 weeks obstructed group or in one of the five urodynamic categories or in the control group.

Results

All animals underwent successful partial surgical obstruction of the urethra and gained weight at rates similar to controls. Histological data on a limited number of strips showed that these consisted of purely muscle tissue with a few small connective tissue sheaths.

Changes in contractility parameters after 4 and 8 weeks obstruction

The average phase plot parameter values calculated for 4 and 8 weeks obstructed muscle strips are presented in tabular form in Table 1. In Figure 2 and 3, the values are displayed in histograms. It can be seen that following 8 weeks of obstruction, the value of phase plot parameter F_{iso} (indicative of the maximum number of contractile muscle units) in response to field stimulation specific for nerves was reduced to 60 % (p<0.05) and in response to carbachol was reduced to 77 % (p=0.2) of the control response. Values for the parameter C, the slope of the phase plot (indicative of unit recruitment during force development) were unchanged for all forms of stimulation. The parameter F_{iso} for direct muscle stimulation was reduced to 68% of the control response, but this result was not significant (p=0.10).

Relationship of changes in contractility and urodynamic parameters

The urodynamic study was successfully performed on 17/20 animals and

Table 1: Force development parameters in normal and obstructed bladder muscle in response to electrical and pharmacological stimulation[†].

	No obstruction (N=10)	4 wks obstruction (N=10)	8 wks obstruction N=10)
stimulus	Fiso (mN/mg)	Fiso (mN/mg)	Fiso (mN/mg)
nerve (field)	6.50 ± 0.69	4.06 ± 0.69 *	3.87 ± 1.00 *
muscle (direct)	5.85 ± 0.50	4.52 ± 0.59	3.93 ± 1.01
carbachol	5.96 ± 0.75	7.00 ± 0.37	4.68 ± 0.75
high-potassium	9.24 ± 0.85	7.67 ± 0.48	6.23 ± 1.43
stimulus	C (sec)	C (sec)	C (sec)
nerve (field)	0.74 ± 0.04	0.85 ± 0.09	0.86 ± 0.07
muscle (direct)	0.74 ± 0.04	0.93 ± 0.15	1.07 ± 0.14
carbachol	5.12 ± 0.70	10.26 ± 1.88	6.86 ± 0.83
high-potassium	13.73 ± 1.13	16.91 ± 1.24	12.95 ± 1.62

[†] Values reported are for F_{iso} (normalized by weight; see Materials and Methods) and for C (unnormalized). Values are mean ± SEM for electrically (nerve and muscle specific), carbachol, and potassium stimulated contractions in normal control and in 4 and 8 weeks obstructed bladders. * $p \leq 0.05$.

9/10 controls. These results have been previously presented in detail (6) and form the basis of a separate report (11).

Normal animals showed stable and compliant cystometry curves, with an occasional small amplitude precontraction. Average weight of normal bladders was 0.54 ± 0.005 g (N=9).

Four urodynamic abnormalities were identified in the obstructed animals:

1. High pressure: a markedly higher (> twofold) voiding pressure than in the normal or any in of the other categories in which instability, compliance change or decompensation dominated. Average bladder weight in this group was 0.85 ± 0.07 g (N=6).

2. Unstable: resembled the cystometrograms of human patients with clinically unstable bladders which show multiple unstable contractions superimposed on the filling cystometry. Bladder weight was 1.17 ± 0.15 g (N=5).

3. Low compliance: showed high endfilling pressures but also generated sufficient active contraction at capacity to at least partially empty the bladder so that a voiding cycle resulted. Bladder weight was 0.76 ± 0.05 g (N=2).

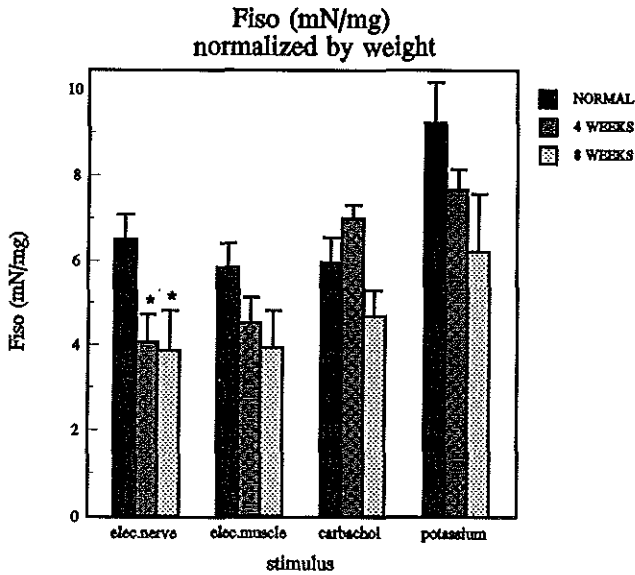4. Decompensated: showed no evidence of an active contraction,

Figure 2: Mean ± SEM for F_{iso}, normalized by weight (all strips in all series had a similar length, see Methods), for electrically (elec.; nerve and muscle specific), carbachol and potassium stimulated contractions in normal control and in 4 and 8 weeks obstructed bladders. * A significant reduction compared to the normal controls is shown in response to nerve stimulation after 4 ($p<0.05$) and 8 ($p\leq0.05$) weeks obstruction.
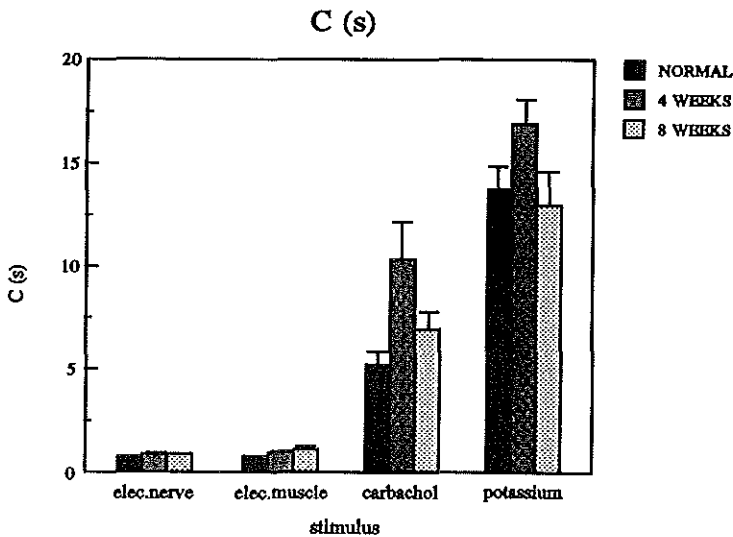

Figure 3: The recruitment rate of contractile units (parameter C) in Guinea pig bladder muscle. Mean, and the standard error of the mean, for electrically (nerve and muscle specific), carbachol and potassium stimulated contractions in normal control and in 4 and 8 weeks obstructed bladders.

Table 2: Average bladder weight and force development parameters of normal and obstructed bladders in response to electrical and pharmacological stimuli according to category of urodynamic dysfunction[†].

	Normal	High pressure	Unstable	Low Compliance	Decompensated
	N=9	N=5	N=6	N=2	N=4
Average bladder weight (g)	0.54 ± 0.01	0.85 ± 0.07	1.17 ± 0.15	0.76 ± 0.05	1.47 ± 0.11
Stimulus	Fiso (mN/mg)	Fiso (mN/mg)	Fiso (mN/mg)	Fiso (mN/mg)	Fiso (mN/mg)
nerve (field)	6.55 ± 0.77	5.83 ± 1.49	2.97 ± 0.56 **	3.28 ± 0.48	2.31 ± 0.72 **
muscle (direct)	5.71 ± 0.53	6.15 ± 1.83	3.03 ± 0.41 **	3.08 ± 0.26	3.22 ± 0.87 *
carbachol	6.01 ± 0.83	5.82 ± 1.22	6.17 ± 0.80	5.50 ± 1.40	5.43 ± 1.28
high-potassium	8.92 ± 0.88	8.50 ± 2.42	5.98 ± 0.85 *	5.64 ± 0.35	5.89 ± 1.21
Stimulus	C (s)	C (s)	C (s)	C (s)	C (s)
nerve (field)	0.73 ± 0.05	0.81 ± 0.04	0.90 ± 0.14	0.56 ± 0.06	1.01 ± 0.11
muscle (direct)	0.74 ± 0.03	0.86 ± 0.08	0.86 ± 0.12	0.63 ± 0.16	1.76 ± 0.63 *
carbachol	4.92 ± 0.74	6.81 ± 1.23	11.67 ± 1.96	11.52 ± 2.71	7.26 ± 2.65
high-potassium	13.01 ± 1.00	16.08 ± 1.38	14.95 ± 2.86	12.98 ± 0.70	13.33 ± 2.29

[†] Values reported are for F_{iso} (normalized by weight; see Materials and Methods) and for C (unnormalized). Values are mean ± SEM for electrically (nerve and muscle specific), carbachol, and potassium stimulated contractions in normal control, high pressure, unstable, low compliance and decompensated categories of obstruction. * $p<0.05$; ** $p<0.01$.

filled to a high endfilling pressure, then overflowed passively at capacity with a large postvoid residual volume. Bladder weight was 1.47 ± 0.11 g (N=4).

The force development parameters in response to four stimuli (field stimulation of nerves, direct muscle stimulation, carbachol and high potassium) for all animals in each of the four urodynamic categories and in the control group are displayed in Table 2. The values are displayed in histograms in Figures 4 and 5. A significant reduction in F_{iso} value was found in response to direct nerve stimulation in unstable and in decompensated bladders to 35% ($p<0.01$) and to 45% ($p<0.01$) of the control response. In response to direct muscle stimulation the F_{iso} value was reduced to 56% ($p<0.05$) of the control response in the decompensated group and to 53% ($p<0.05$) of the control response in the unstable group. In response to carbachol no reduction of F_{iso} could be shown in either of these two groups. In response to high-potassium stimulus F_{iso} showed a reduction in the unstable group to 67% ($p<0.05$) of the control response. In C values also in the different categories of in vivo urodynamic dysfunction no
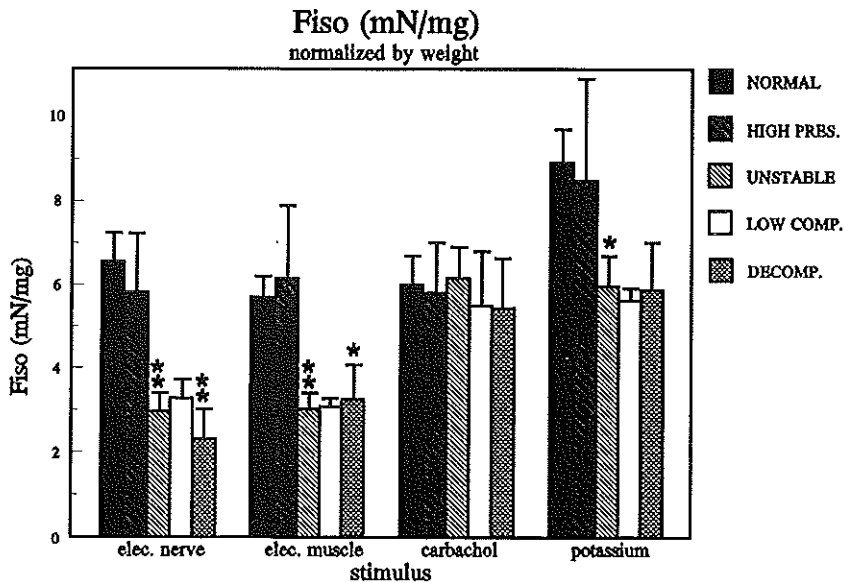
Figure 4: Mean ± SEM for Fiso, normalized by weight (all strips in all series had a similar length, see Materials and Methods), for electrically (elec.; nerve and muscle specific), carbachol and potassium stimulated contractions in normal control, the high pressure (PRES.), the unstable , the low compliance (COMP.) and the decompensated (DECOMP.) categories of obstruction. In the unstable group a significant reduction compared to the normal controls is shown in response to nerve (**p<0.01), muscle (**p<0.01) and potassium (*p<0.05) stimulation. In the decompensated group the reduction was significant in response to nerve (**p<0.01) and muscle (*p<0.05) stimulation.

significant change was seen when compared with the normal controls, except for the C values of direct muscle stimuli in the decompensated group.

Our results did not show a gradual increase of changes either urodynamic parameters or in muscle contractility parameters between 4 and 8 weeks of obstruction.

Discussion

In this study, in vivo and in vitro bladder function was studied after a prolonged time of urethral obstruction in a Guinea pig model. More specifically, parameters of in vitro isometric force development were related to four, in vivo identified patterns (11) of abnormal bladder function secondary to the obstruction.

When bladder weight alone was observed, the weight increased when advancing from normal- via high pressure voiding- and unstable- to decompensated bladders. This observation suggests that a decreasing in vivo

bladder function and an increase in bladder weight were associated. Previous research on bladder smooth muscle has shown that it is not possible to perform reproducible measurements at L_{max} (5). Active measurements were performed well below L_{max} because, a continuous passive lengthening at L_{max} interferes with these measurements. Therefore, muscle strips were prestretched to a constant tension of 5 mN. In order to quantify bladderfunction in vitro, the time course of force development in these muscle strips was analysed.

Obstructed guinea pig bladder showed a significant reduction in the force development parameter associated with the number of contracting muscle units upon ideal stimulation (F_{iso}, Fig 2). The parameter C, indicative of the recruitment rate of contractile units during a contraction, did not show a significant change (Fig 3). Figure 6 illustrates the resulting parallel downward shift in the straight line part of the phase plot as it occurred with obstruction.
In the above definition of F_{iso} and C, "muscle unit" can refer to either a cell or a contractile structure within a cell (e.g. crossbridges).

Previous research (7,9) has not shown a decrease in DNA concentration in obstructed bladder muscle tissue so that a decrease in F_{iso} cannot be explained by a decay in the number of cells per gram of tissue. This favours the alternative hypothesis of " muscle unit" meaning an intracellular contractile structure.

No gradual change in in vitro force development parameters in response to obstruction could be demonstrated in the sense that the changes observed after 4 and 8 weeks of obstruction were not significantly different. This suggests that bladders did not all follow a sequence of changes at the same pace. This
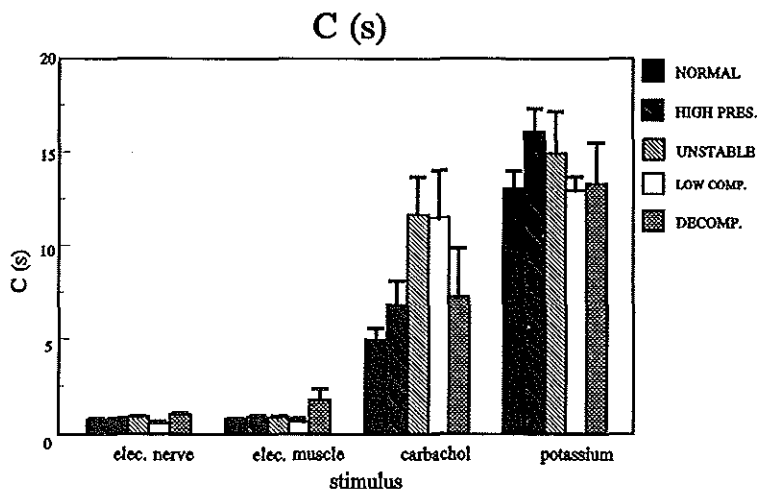

Figure 5: The recruitment rate of contractile units (parameter C) in Guinea pig bladder muscle. Mean ± SEM for electrically (elec.; nerve and muscle specific), carbachol and potassium stimulated contractions in normal control, the high pressure (PRES.), the unstable, the low compliance (COMP.) and the decompensated (DECOMP.) categories of obstruction.

phenomenon can be explained by either a different responsiveness of the bladder in different animals or spontaneous differences in the degree of obstruction in the animals.

In Figure 4 it seems that the force development parameter F_{iso} shows two distinctly different values. Normal bladders and bladders with high pressure voiding showed high F_{iso} values. Unstable and decompensated bladders showed F_{iso} values on a lower level. As bladders with high pressure voiding alone showed neither significant changes in the force development parameters nor in
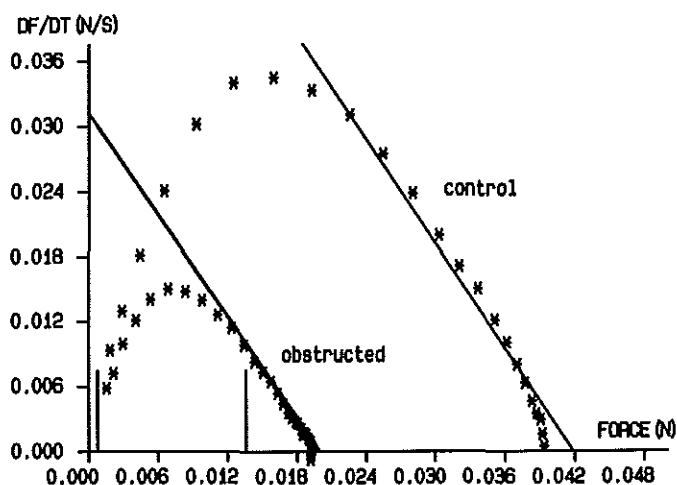

Figure 6: Phase plots [dF/dt (F)] derived from bladder strip contractions of a control animal and of an obstructed animal. These plots typically illustrate the parallel shift in the straight line part occurring with obstruction.

bladder weight, high pressure voiding is likely to be the least severe grade of dysfunction. High pressure voiding may just be due to a lower flow rate and thus representing an initial physiological response to obstruction. The unstable bladders however showed a significant reduction in the values of the force development parameter F_{iso} in association with a significant bladder weight gain. This indicates that instability represents a more advanced form of response to obstruction. The decompensated bladders showed significant changes in parameter values of F_{iso}, similar to changes seen in the unstable group, especially in response to field stimulation of nerves and to direct muscle stimulation.

The force development parameters showed occasionally variable responses, such as F_{iso} in response to carbachol and C in response to direct muscle stimulation. No obvious explanation could be given for this effect.

The decompensated bladders weighed significantly more than bladders in any other category, which suggests that decompensation is the final step in the decreasing bladder function. Due to a small sample size (N=2) no conclusions could be drawn for the low compliance category, however the reduction of F_{iso} in

this group suggests that this form of dysfunction has characteristics similar to those of instability or decompensation, although the relatively low bladder weight militates against this hypothesis.

The decline in F_{iso} with increasing bladder weight suggests several possible explanations. An increase in the amount of connective tissue might result in a relative decrease of the number of contractile muscle units (crossbridges) per gram of bladder tissue. As a consequence the DNA concentration per gram of tissue would decrease, which is contradicted by previous studies on obstructed bladder tissue (7,9), thus impairing the likeliness of this explanation. A reduction in F_{iso} might also be explained by the hypothesis that fewer units can be stimulated to the treshold where contraction occurs i.e. obstruction affecting the conversion of chemical into mechanical energy. Another hypothesis would be that the average muscle cell size increases, without a consequent increase in the number of contractile units per cell, leaving a smaller number of contractile units (crossbridges) per gram of tissue. This effect can be assigned to a previously described lower actin and myosin content of obstructed muscle tissue (12). Analogous to the findings of Arner et al. (1): An increase in cell size might also cause a different orientation of crossbridges so that less force is generated in the direction in which force is measured. Considerably more data will be needed in order to fully explain the decrease in F_{iso} associated with bladder weight gain.

In Figure 2 and in Figure 4, nerve stimulation did, besides a slightly better statistical significance, not seem to be more affected by obstruction than direct muscle stimulation. The latter is a more direct form of stimulation as opposed to nerve stimulation, so that this could indicate that the here described effects of obstruction are mostly determined by muscle change alone.

In pig bladders the value of the parameter C has been shown to be related to an intracellular process (13) i.e. the influx of extracellular calcium. As C showed similar values when the bladder was obstructed in this study, this process was apparently not affected by obstruction. Changes in presumably faster contractile processes such as crossbridge attachment and cycling could not be detected because the slower influx of extracellular calcium is the rate limiting step.

It is concluded that the parameter that characterizes maximal in vitro force development is impaired in obstructed guinea pigs with unstable and decompensated bladders and not in animals characterized by high pressure voiding alone. On the basis of increased bladderweight the former dysfunctions can be interpreted as more advanced stages. There was no change in the rate of isometric force development in vitro in the obstructed animals. Generally, bladder dysfunction and impaired in vitro force development are associated, and appear to be greater (more advanced) as bladder weight increases.

References

1. **Arner, A., Malmquist, U and Uvelius, B.** (1990): Metabolism and force in hypertrophic smooth muscle from rat urinary bladder. *Am.J.Physiol.*258 (Cell Physiol. 27): C923-C932.
2. **Blaivas J. G.** (1988): Pathophysiology and differential diagnosis of benign prostatic hypertrophy. *Urology,* 32(6 Suppl):5-11.
3. **Brading, A.F. and Sibley, G.N.A.** (1983): A superfusion apparatus to study field stimulation of smooth muscle from mammalian urinary bladder. *J. Physiol.,* 334:1112P.
4. **Coolsaet, B. and Blok, C.** (1986): Detrusor properties related to prostatism. *Neurourol. Urodynam.* 5: 435-447.
5. **Griffiths, D.J., Van Mastrigt, R., Van Duyl, W.A. and Coolsaet, B.L.R.A.** (1979): Active mechanical properties of the smooth muscle of the urinary bladder. *Med. & Biol. Eng. & Comput.,* 17:281-290.
6. **Karim, O.M.A., Van Koeveringe, G.A. and Mostwin, J.L.** (1990): Development of abnormal voiding patterns following partial urethral obstruction of the guinea pig urethra. *J. Urol.,*143:355A.
7. **Lindner, P, Mattiasson, A, Persson, L. and Uvelius, B.** (1988): Reversability of detrusor hypertrophy and hyperplasia after removal of infravesical outflow obstruction in the rat. *J. Urol.,* 140: 642-646.
8. **Malkowicz, S.B., Wein, A.J., Elbadawi, A., Van Arsdalen, K., Ruggieri and M.R., Levin, R.M.** (1986): Acute biochemical and functional alterations in the partially obstructed urinary bladder. *J. Urol.,* 136: 1324-1329.
9. **Mattiasson, A. and Uvelius, B.** (1982): Changes in contractile properties in hypertrophic rat urinary bladder. *J. Urol.,* 128: 1340-1342.
10. **Mostwin, J.L. and Brooks, E.L.** (1989): A new guinea pig model of urethral obstruction. *J. Urol.,* 141:334A.
11. **Mostwin, J.L., Karim, O.M.A., Van Koeveringe, G.A. and Brooks, E.L.** (1991): The guinea pig as a model of gradual urethral obstruction. *J. Urol.,* 145:854-858.
12. **Uvelius, B. et al.** (1989): Contractile and cytoskeletal proteins in detrusor muscle from obstructed rat and human bladder. *Neurourol. Urodyn.* 8: 396-398.
13. **Van Koeveringe, G.A. and Van Mastrigt, R.** (1991): Excitatory pathways in smooth muscle investigated by phaseplot analysis of isometric force development. *Am.J.Physiol.* 261 (Regulatory Integrative Comp. Physiol. 30): R138-144.
14. **Van Mastrigt R, Koopal, J.W.B., Hak, J. and Van de Wetering, J.** (1986): Modeling the contractility of urinary bladder smooth muscle using isometric contractions. *Am. J. Physiol.,* 251:R978-983.
15. **Van Mastrigt, R. and Glerum J.J.** (1985): Electrical stimulation of smooth muscle strips from the urinary bladder of the pig. *J. Biomed. Eng.* 7: 2-8.

"

CHAPTER 5

Photolysis of caged calcium using a low-cost flash unit: efficacy analysis with a calcium selective electrode
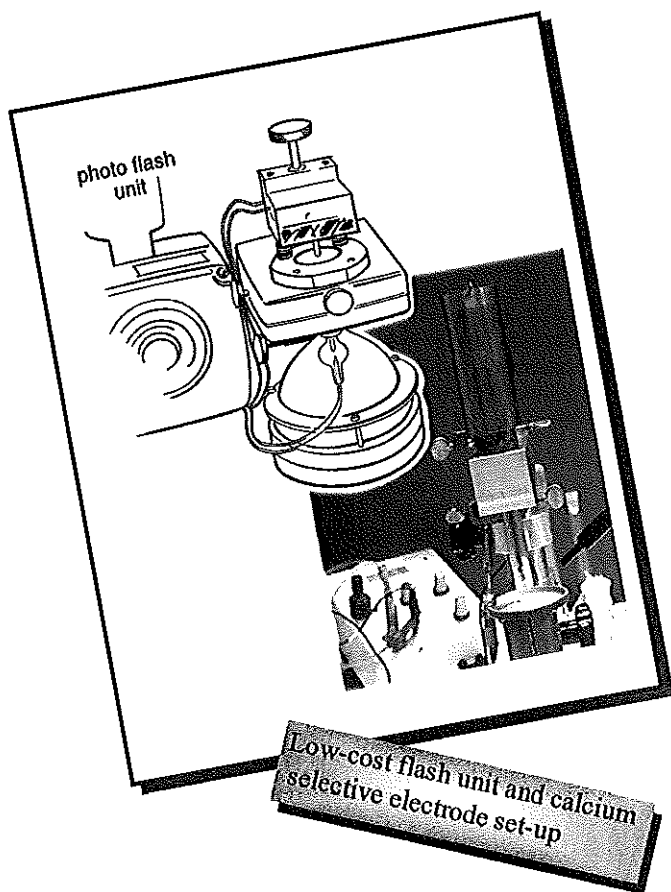
G. A. van Koeveringe and R. van Mastrigt

Abstract

Photolysis of caged calcium (Nitr5, Calbiochem®) can be used to study calcium dependent processes such as excitation-contraction coupling and muscular mechanics. Expensive high energy light sources are routinely used for UV light exposure; this study describes an alternative low cost Xenon flash unit constructed in our laboratory. A 300 J short arc Xenon flash lamp (Heimann®) was mounted in an elliptical reflector and driven by a modified Metz® 60 CT 4 photo flash unit up to 240 J input energy and 4 ms flash duration. A 20 1 cuvette containing a test solution was placed in a complementary elliptical reflector. An ion selective calcium electrode was used to measure the free calcium concentration $[Ca^{++}]$ before and after flash in test solutions containing 1.00 mM Nitr5 in combination with different added $[Ca^{++}]$'s. Using this technique we estimated that 1 flash on 1.00 mM Nitr5 increased the free $[Ca^{++}]$ from 10^{-7} to $1.1*10^{-5}$ M. When the added $[Ca^{++}]$ was less than $2.3*10^{-4}$ M, the used Nitr5 behaved as a strong calcium chelator because 23% of it was unloaded with calcium. It is concluded that a physiologically relevant change in free $[Ca^{++}]$ can be evoked by photolysis of Nitr5 using a low cost (approximately $1500) Xenon flash unit, and that ion selective Ca electrodes can be adequately used to monitor the resulting changes in $[Ca^{++}]$.

Introduction

Photolabile calcium chelators have been designed to study intracellular calcium dependent processes (1,2). These "caged" calcium compounds are useful tools to bypass rate limiting steps in muscular excitation-contraction coupling (3,4,5). When using the chelators intracellularly (6,7,8), it is possible to evoke a stepwise increase in the intracellular calcium concentration $[Ca^{++}]$ by exposing the cells to high intensity ultra-violet (U.V.) light. The minimum energy density required for photolysis of the caged calcium compound Nitr5 is approximately 250 mJ/cm² in a wavelength band from 320 - 370 nm (9,10). The commonly used frequency doubled ruby laser (6,7) meets these specifications in a flash duration of 25 ns, but is very expensive. When a longer flash duration, ± 4 ms, is acceptable, the commercially available xenon flashlamp developed by Rapp and Güth(11) can be used. At one fourth of the price of the laser, this is still not a very economical alternative. We decided to develop a U.V. light source for the release of caged Ca based on a standard photo flashlamp, costing one tenth of the price of the commercially available Xenon flash unit.

The efficacy of the developed UV light source was quantified by measuring the increase in free calcium after exposure of a 20 μl sample of caged calcium

Materials and Methods

Ultra-violet light source

A modified Metz® 60 CT 4 flash unit was used as an ultra-violet (U.V.) light source for the photolysis experiments. When this unit is used for photographic applications, the U.V. light from the flashtube is absorbed by a filter in the front window.

This front window was removed and the 70 mm long flashtube was replaced by a 300 J/flash, 120 W, type DG 8907 ST II Xenon flashtube manufactured by Heimann®, Wiesbaden, Germany. This short arc lamp (arc length 7 mm), was placed in the focus of a Melles and Griot®, type 02 REM 001 elliptical mirror.

In order to compensate for the lower impedance of this lamp (20 mohm) as opposed to the original 70 mm tube (1,5 ohm), an extra choking coil of 22 µH was placed in the high power circuit of the Metz unit in series with the short arc tube. The trigger circuit of the driver unit was not altered. The focus size, determined by video tape recording of flashes on a graduated grey plastic screen, was approximately 5 mm in diameter. Flash duration was 4 ms measured by means of a photo detector with amplifier connected to a storage oscilloscope and the input energy was calculated to be 240 J (12,13).

Fluid sample illumination setup

A 20 µl fluid sample was exposed in a 7 mm long quartz tubular container of 1.8 mm inner diameter and 200 µm wall thickness that was placed in the second focus of the elliptical reflector, as shown in Figure 1. In order to gain a more intense and even exposure the container was surrounded by a custom made second elliptical reflector complementary to the 02 REM 001. A cedar wooden mould was made for this reflector using a computerized milling machine. The glass for the reflector was blown inside this mould to a wall thickness of 2 mm. The inside surface of the elliptically shaped glass was
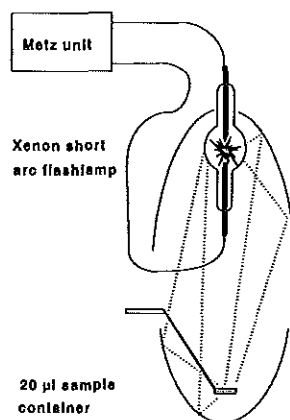

Figure 1: A schematic representation of the fluid sample illumination setup: A short arc Xenon flash lamp was mounted in an elliptical reflector and driven by a modified Metz® 60 CT 4 photo flash unit. A 20 µl cuvette was placed in a complementary second elliptical reflector.

coated with aluminium.

Ion-selective calcium electrode setup

A calcium-selective electrode, Orion® type 9320, was used in combination with a double barrel reference electrode, Orion® type 900200 (inner compartment filled with saturated AgCl solution and outer compartment with 4 M KCl), for the measurement of free [Ca^{++}] in the 20 μl sample. Initially, a setup was tested in which a continuous flow of fluid was pumped via the Ca selective electrode past the reference electrode with a syringe pump. A simpler assembly however, showed far more stable potentials: In this setup, shown in Figure 2, the Ca electrode was positioned upside down and a teflon spacer ring with a thickness of 0.3 mm (inner diameter 6 mm and outer diameter 12 mm) was placed around the 6 mm diameter Ca sensitive membrane. The 20 μl fluid sample was applied centrally in the ring on the membrane. The reference electrode was gently lowered onto the membrane and loaded with a mass of 1.5 kg, so that a fluid film over the teflon ring made contact with the peripheral junction of the reference electrode. The potential between both electrodes was measured using a Consort® pH-mV meter and recorded on a W+W® chart recorder. Values were read after allowing 20 seconds for stabilization. The calcium-sensitive membrane, the ring and the reference electrode were rinsed extensively with de-ionised water and dried with a clean tissue between measurements.
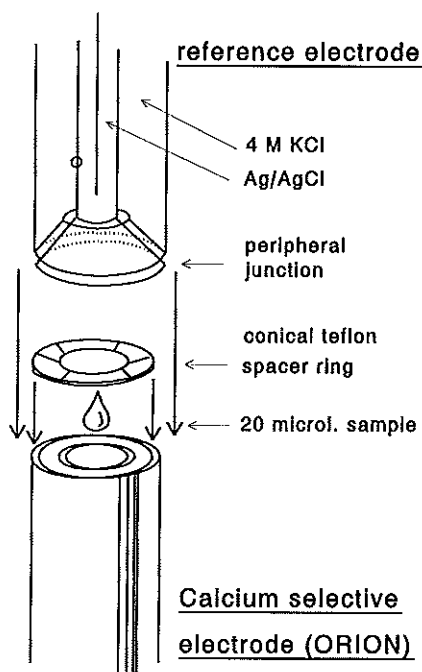

Figure 2: A schematic representation of the ion selective calcium electrode setup: The calcium selective electrode was positioned upside down, the 20 μl sample was applied centrally on the membrane and the reference electrode was lowered so that a fluid film over the ring made contact with the peripheral junction of the reference electrode.

Solutions

For calibration, standard buffer solutions were made containing saturated Ca-EGTA and EGTA in proportions calculated so that free $[Ca^{++}]$ of 10^{-8}, 10^{-7}, 10^{-6} and 10^{-5} M were established at pH 6.8; total EGTA concentration was 3 mM.

Standards with 10^{-4} and 10^{-3} M free $[Ca^{++}]$ were made by diluting a $2*10^{-3}$ M $CaCl_2$ (Merck®) standard solution with de-ionised water ($[Ca^{++}]$ $2*10^{-6}$). The solutions containing Nitr5 (Calbiochem®) were composed of 1.00 or 3.00 mM Nitr5 and 10 mM KCl, the KCl was added to adjust the ionic strength (according to Orion® Ca^{++} selective electrode manual). $CaCl_2$ was added in order to obtain solutions with 11 different added $[Ca^{++}]$'s: 10^{-7}, 10^{-6}, 10^{-5}, $5*10^{-5}$, 10^{-4}, $1.5*10^{-4}$, $2*10^{-4}$, $2.5*10^{-4}$, $3*10^{-4}$, $5*10^{-4}$, 10^{-3} M.

Measurement protocol

Ion-selective electrode (I.S.E.) potentials were measured five times in the 6 different free Ca standard solutions in ascending order. Before and after a series of measurements using Nitr5, the electrode response was checked with 3 different standards: 10^{-6}, 10^{-5}, and 10^{-4} M Ca. The free $[Ca^{++}]$'s of the solutions containing 1.00 mM Nitr5 were measured 5 times in both flashed and unflashed condition for each of the solutions with different added $[Ca^{++}]$'s. The 10^{-7}, 10^{-6}, 10^{-5} and 10^{-4} M added $[Ca^{++}]$ solutions, the 10^{-4}, $1.5*10^{-4}$, $2*10^{-4}$, $2.5*10^{-4}$, $3*10^{-4}$ M $[Ca^{++}]$ solutions and the $3*10^{-4}$ and 10^{-3} M $[Ca^{++}]$ solutions were measured in separate sessions with intermediate reloading of the Ca electrode in high $[Ca^{++}]$. Solutions containing 3 mM Nitr5 were analyzed 3 times, in both flashed and unflashed condition in 3 different solutions with added $[Ca^{++}]$ 10^{-4}, $5*10^{-4}$ and 10^{-3} M. The unflashed Nitr5 solutions were incubated in the 20 µl container in front of the flash lamp for the same period of time as the flashed solutions. Both flashed and unflashed solutions were transferred to the
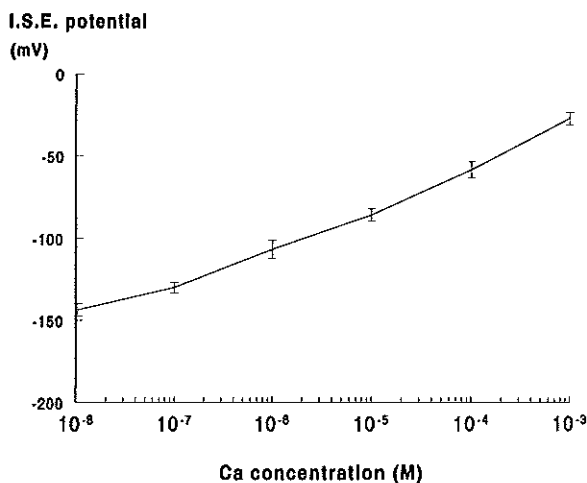

Figure 3: Calcium electrode calibration curve showing the mean ion selective electrode (I.S.E.) potential ± standard error of the mean (S.E.M.) for 6 different calcium standard solutions with free $[Ca^{++}]$ of 10^{-8} to 10^{-3} M.

Ca^{++} measurement site with a 20 µl Hamilton® syringe approximately 1 minute after the flashes. Between measurements both syringe and container were cleaned thoroughly by flushing several times with de-ionized water. All solutions were flashed 5 times in order to obtain a better readability of the responses. In a separate series (N=3) responses to 1 and 5 flashes were compared using a Nitr5 solution with an added $[Ca^{++}]$ of $2.3*10^{-4}$ M . This solution was also used in a series (N=3) to test Ca release with and without the complementary second elliptical mirror and with and without a 3 mm thick UG11 (Schott®) glass filter (80% transmission peak between 320 and 370 nm wavelength).

Results

The I.S.E. potential as a function of the free $[Ca^{++}]$, measured in 6 different calcium standard solutions is shown in Figure 3. Figure 4 shows on a double logarithmic scale the free $[Ca^{++}]$ in the Nitr5 buffer solution as a function of the total $[Ca^{++}]$, which is the sum of added $[Ca^{++}]$ and the calcium initially bound to the 1.00 mM Nitr5. Mean ± standard error of the mean (S.E.M.) for 1.00 mM Nitr5, unphotolysed (solid line) and photolysed (dashed line) are plotted.

Figure 4 also shows a theoretical curve (0% dotted line) representing the relation between total $[Ca^{++}]$ and free $[Ca^{++}]$ in a 2 buffer system (see APPENDIX) This curve is characterized by a steeply increasing free $[Ca^{++}]$ around a total $[Ca^{++}]$ equal to the [Nitr5] as a result of the 1:1 Ca^{++} binding to Nitr5 at saturation. Such a steep part in the curve was also seen in the experimental data measured at different added $[Ca^{++}]$'s. In these data, total $[Ca^{++}]$ in the solutions equaled the added $[Ca^{++}]$ plus the $[Ca^{++}]$ bound initially to the chelator. The amount of Ca^{++} bound initially to the chelator was estimated from the horizontal shift between the steep part of the experimental data curve and the comparable part of the theoretical curve. A best fit of both curves was obtained at a value of 0.77 mM $[Ca^{++}]$ being bound to the 1.00 mM Nitr5. Total $[Ca^{++}]$ values in the Nitr5 solution were therefore calculated by adding 0.77 mM $[Ca^{++}]$ to the added $[Ca^{++}]$. The 77% Ca^{++} loading of Nitr5 was verified by measuring free $[Ca^{++}]$ in 3mM Nitr5 with 10^{-4}, $5*10^{-4}$ and $1*10^{-3}$ M added $[Ca^{++}]$'s. In this 3 fold higher [Nitr5] the steep rise in free $[Ca^{++}]$ was expected at a 3 fold higher total $[Ca^{++}]$. Consequently a 3 fold higher amount of added $[Ca^{++}]$ was expected to be necessary to saturate the Nitr5 i.e. 0.69 mM. In a limited series of measurements (N=3) the steep free $[Ca^{++}]$ increase was indeed shifted to a value between 0.50 mM and 1.00 mM added $[Ca^{++}]$.

Figure 4 shows that after exposing samples with a total $[Ca^{++}]$ between 0.92 and 1.07 mM to 5 flashes from the flash unit, a significant increase in free $[Ca^{++}]$ was detected. The free $[Ca^{++}]$ was increased by a maximum of approximately $2.6*10^{-5}$ M in response to the flashes in a total $[Ca^{++}]$ of 1.02 mM.
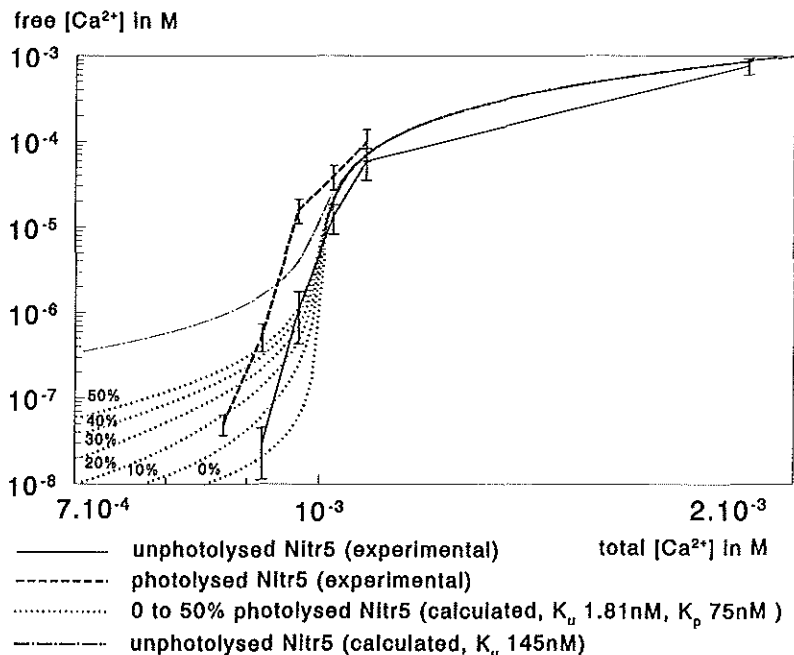
free [Ca²⁺] in M

---------- unphotolysed Nitr5 (experimental)　　　total [Ca²⁺] in M
- - - - - - - - photolysed Nitr5 (experimental)
················ 0 to 50% photolysed Nitr5 (calculated, K_u 1.81nM, K_p 75nM)
—·—·—·— unphotolysed Nitr5 (calculated, K_u 145nM)

Figure 4: Free [Ca⁺⁺] as a function of total [Ca⁺⁺] i.e. added [Ca⁺⁺] plus the calcium bound initially to the 10^{-3} M Nitr5. The solid line represents average values ± S.E.M. for a solution containing 1.00 mM Nitr5. The thick dashed line shows the values for 1.00 mM Nitr5 after exposure to 5 U.V. light flashes. The 6 dotted lines show calculated data for six different degrees of photolysis (from 0% to 50% in steps of 10%) of a theoretical two-buffer system, containing unflashed and flashed Nitr5 with dissociation constants for calcium of 1.81 nM (K_U) and 75 nM (K_P). The dot-dashed line represents a calculated line for unflashed Nitr5 using a K_U of 145 nM (published dissociation constant at 100 mM ionic strength (1)).

The effects of 5 flashes, 1 flash, omission of the complementary elliptical reflector and addition of a UG11 filter in a solution containing 1.00 mM Nitr5 in 1.00 mM total [Ca⁺⁺] are compared in Figure 5. One flash released 67% of the amount of Ca⁺⁺ compared to the amount that was released by 5 flashes. Without a complementary second elliptical reflector 5 flashes released 55% of the amount released with this reflector. Five flashes with a UG11 filter released 97% of the amount released without this filter.

Discussion

A low cost Xenon flash unit was constructed as an alternative for more expensive light sources such as an U.V. laser or a commercially available Xenon flashlamp to photolyse caged calcium. The driver and trigger circuit of a Metz®

flash unit, which is widely employed in professional photography, was used after slight modification. An additional advantage of this system is that it is battery powered, thus avoiding interference on the power lines. The external trigger system of the photoflash unit could easily be used for synchronisation. The original flashtube was replaced by a short-arc xenon flashlamp, which is a more concentrated light source. The UV light emitted by the flashlamp was concentrated using a dual elliptical mirror arrangement, which provided a high efficacy and an even illumination of the preparation. The light spot in the focus was larger in diameter than one would expect from a lamp with 7 mm arc length. This effect was due to the fact that the discharge was not only limited to the arc beteen the anode and cathode but more or less extended through the whole 15 mm diameter bulb of the Xenon lamp. A frame by frame analysis of images recorded on videotape of the flash on a graduated grey screen in the focus revealed that an intense spot in the focus with a diameter of 5 mm was surrounded by a larger less intense spot with a total diameter of 30 mm. This halo was reflected back to the preparation with the complementary elliptical reflector.

The efficacy of the light source was determined by measuring the free $[Ca^{++}]$ before and after flash in a 1.00 mM Nit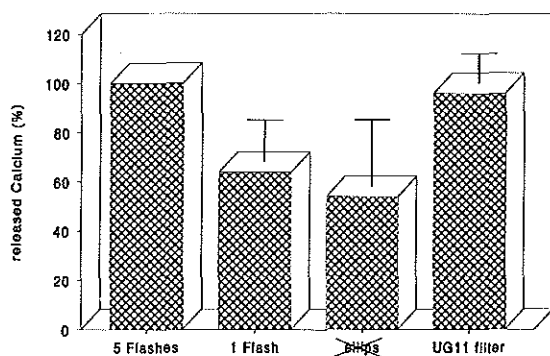r5 solution using a Ca selective electrode. This method had the advantage of multidirectional sensitivity as opposed to most electronic detectors, which are sensitive in one direction only. A disadvantage of the arrangement could be a gradient in Ca release from the surface towards the middle of the container, which was earlier described by Lando and Zucker (9). However this would imply that the measured calcium release is a

Figure 5: The relative increase in free $[Ca^{++}]$ evoked by 1 flash, omission of the second complementary elliptical mirror and addition of a Schott® UG11 filter expressed as a percentage ± S.E.M. of the effect of 5 flashes.

conservative estimate as the diameter of a muscle preparation would be at least a factor 10 less.

Using a calcium selective electrode in combination with a peripheral junction reference electrode and a spacer ring (Fig 2) enabled the analysis of a very small sample while preventing the efflux of the reference solution from directly influencing the contents of the sample.

It was found that the performance of the electrode depended on the order in which measurements were done if free [Ca^{++}]'s were far apart. Therefore the low free [Ca^{++}] range, the high free [Ca^{++}] range and the steep part in the curve (Fig 4) where saturation of Nitr5 occurred were measured in separate sessions to allow for intermediate Ca^{++} reloading and stabilization of the electrode. In solutions containing 1.00 mM Nitr5 and added [Ca^{++}]'s below 10^{-4} M the free [Ca^{++}] was reduced dramatically. The differences between the potentials measured in standard Ca solutions and those obtained in solutions with a low added [Ca^{++}] can be explained by the strong Ca buffering capacity of Nitr5. This implies that in muscle experiments cells should be loaded slowly with Nitr5 in order to prevent the intracellular [Ca^{++}] from dropping too low. The buffering effect also explains why in lower added [Ca^{++}]'s the response to a flash was decreased: All released Ca^{++} is directly reabsorbed by empty "cages". The steep rise in free [Ca^{++}] shown in the unphotolysed Nitr5 curve in Figure 4 between 0.87 and 1.07 mM total [Ca^{++}] can be explained by Ca^{++} saturation of the empty cages of Nitr5 in this region. Therefore a flash evokes the lagest increase in free [Ca^{++}] in this region. As each Nitr5 molecule can contain 1 Ca^{++} molecule, the horizontal position of this saturation region in the free [Ca^{++}]-total [Ca^{++}] plot indicates the point where total [Ca^{++}] equals [Nitr5]. This was used as described in RESULTS to estimate that 1.00 mM of Nitr5 initially contained 0.77 mM Ca^{++}.

Figure 4 shows that 5 flashes increased the free [Ca^{++}] markedly in the range between 0.92 and 1.07 mM total [Ca^{++}]. The amplitude of the calcium jump, which can be read from the y axis, was variable along this range. By interpolation we can estimate that at a free [Ca^{++}] of 10^{-7} M, which corresponds approximately to the intracellular [Ca^{++}] of a muscle cell in the relaxed state, 5 UV flashes would evoke an increase in free [Ca^{++}] to $1.7*10^{-5}$ M. Such an increase in free [Ca^{++}] in the 20 μl sample is similar to or greater than the physiological calcium jump that has been measured intracellularly upon stimulation (14). At 0.97 mM total [Ca^{++}] which corresponds to 10^{-6} M free [Ca^{++}] a maximum response to 5 flashes of $2.6*10^{-5}$ M free [Ca^{++}] was found. The fact that the free [Ca^{++}] increase in response to UV flashes was variable along the range of added [Ca^{++}] values can partly be understood by describing the tested solution as a system of two competing buffers i.e. unflashed Nitr5 and flashed Nitr5. It was attempted to estimate the amount of Nitr5 that was photolysed to give the effect shown in Figure 4 by using the equations for this system described in the APPENDIX. The six dotted lines show simulated data based on a total [Nitr5] of 1.00 mM and depict different ratios of unphotolysed Nitr5 to photolysed Nitr5. The degree of photolysis increases from 0 to 50% in steps of 10%. To realize a closer resemblance of the experimental and the calculated data it was necessary to decrease the dissociation constants Kd of both flashed and unflashed Nitr5 used in other studies (1). It can be seen in Figure 4 that experimental data from unflashed controls resembled closely a line

calculated using a Kd of 1.81 nM, which is a factor 80 less than the dot-dashed line calculated using a Kd of 145 nM (1). Similarly, the dissociation constant for flashed Nitr5 was decreased to 7 nM. The lower Kd values can be explained by the factor 10 lower ionic strength that was used in the present experiments as compared to the ionic strength (100 mM) for which the Kd values were determined in other studies (1). The present experiments were performed at this low ionic strength (10 mM) in order to be able to measure lower $[Ca^{++}]$'s, according to the Orion® Ca^{++} selective electrode manual. For EGTA (15) it has been shown that the Kd value decreases with decreasing ionic strength. By using the formula described by Thomas (15), we calculated that the Kd for Nitr5 would decrease twofold with a 10 fold decrease in ionic strength. It can thus be questioned whether the formula (2.11 in (15)) properly describes the relationship between Kd and ionic strength, considering the very low Kd value in the present experimental data. When comparing the calculated dotted lines in Fig 4 with the lines representing the experimental data, a more or less similar shape is seen. In the lowest range of the theoretical curve experimental data could not be collected because free $[Ca^{++}]$'s lower than 10^{-8} M could not be measured with the used electrode and total $[Ca^{++}]$'s lower than 0.77 mM could not be attained as this amount was bound to the 1.00 mM Nitr5. When comparing photolysed to unphotolysed curves, it seems, other than in the theoretical curves, that the shape of both curves is similar but that the experimental photolysed curve is more shifted to the left. This effect can be observed most clearly around 1.00 mM total $[Ca^{++}]$ in Fig. 4 and is more likely due to a reduction of overall buffer capacity than to an altered Kd of the same buffer. This could be the case when the UV light destructs the cages rather than changes the buffering properties. In the light of these uncertainties it is not possible to calculate a precise ratio of photolysed to unphotolysed Nitr5 in this manner.

It can be concluded that the effect of photolysis on free $[Ca^{++}]$ is critically dependent upon the total $[Ca^{++}]$, as can be seen in both experimental and calculated data in Figure 4. The Figure also shows that there is a very small range of total $[Ca^{++}]$ values in which free $[Ca^{++}]$ values similar to intracellular $[Ca^{++}]$ values can be attained. This indicates that the strong buffering capacity of Nitr5 intracellularly, i.e. when loaded as the Nitr5-acetoxymethyl ester, makes high demands on the calcium homeostasis mechanism of the cell, and might even interfere to a large extent with this mechanism.

In order to obtain a more distinct effect of the UV exposure initially 5 flashes were applied instead of 1 flash. In later experiments, it was shown that the effect of 5 flashes measured in 1.00 mM Nitr5 with a $2.3*10^{-4}$ M added $[Ca^{++}]$ was not 5 times but only 1.5 times higher than the effect of 1 flash (see Fig 5). So as opposed to a $1.7*10^{-5}$ M Ca^{++} jump in response to 5 flashes a $1.1*10^{-5}$ M Ca^{++} jump would be attainable in response to 1 flash. Also the effect of the complementary second elliptical mirror was investigated. With this second mirror the response was twofold enhanced, which can be exactly explained by

the illumination of the preparation from both sides. A 3 mm thick Schott® UG11 filter decreased the increase in free $[Ca^{++}]$ by 3%, which indicates that the effect measured is mainly evoked by U.V. light with a wavelength between 320 and 370 nm.

This study indicates that it is possible using one flash from a low-cost UV flash unit (\$ 1500) to evoke a physiological $[Ca^{++}]$ jump, from 10^{-7} to $1.1*10^{-5}$ M, in a 20 µl sample containing 1.00 mM Nitr5. It is most likely that the effect in a smaller sized (smooth) muscle preparation will be more distinct. Measurement of the free $[Ca^{++}]$ increase using an ion selective electrode appears to be a useful tool to analyze both the behaviour of Nitr5 and the efficacy of the flash for photolysis.

Appendix

The relation of total $[Ca^{++}]$ to free $[Ca^{++}]$ in a solution containing two competing buffers, in this case photolysed and unphotolysed Nitr5, can be described according to Zucker and Steinhardt (16).

In such a solution the total calcium concentration ($[Ca_T]$) consists of free calcium ($[Ca_F]$) and calcium bound to both buffers:

$$[Ca_T] = [Ca_F] + [Ca^{++}] \text{ bound to unphotolysed Nitr5 +}$$
$$[Ca^{++}] \text{ bound to photolysed Nitr5} \qquad Eq.1$$

by introducing a dissociation constant K_U for calcium binding to unphotolysed Nitr5 with a concentration of $[N_5U]$:

$$[Ca^{++}] \text{ bound to unphotolysed Nitr5} = \frac{[Ca_F]\,[N_5U]}{Kd + [Ca_F]} \qquad Eq.2$$

and a similar dissociation constant K_P for calcium binding to photolysed Nitr5 with concentration $[N_5P]$, equation 1 can be rewritten as follows:

$$[Ca_T] = [Ca_F] \left(1 + \frac{[N_5U]}{K_U + [Ca_F]} + \frac{[N_5P]}{K_P + [Ca_F]} \right) \qquad Eq.3$$

Reduction to one denominator gives:

$$[Ca_F]^3 + (K_U + K_P - [Ca_T] + [N_5U] + [N_5P])[Ca_F]^2$$

$$+ (K_P [N_5U] + K_U [N_5P] - [Ca_T](K_U + K_P) + K_UK_P)[Ca_F]$$

$$- K_UK_P[Ca_T] = 0 \qquad\qquad \text{Eq.4}$$

Using the computer program MATLAB® total $[Ca^{++}]$'s were calculated for 100 equally spaced free $[Ca^{++}]$ values between 10^{-8} and 10^{-3} M and 6 different ratio's of $[N_5U]$ and $[N_5P]$. Kd values (for 10mM ionic strength) of 1.81 nM and 75 nM were used. For comparison an extra curve was calculated using the dissociation constant for unphotolysed Nitr5 at 100 mM ionic strength (1). The curves were plotted on logarithmic axes, as shown in Figure 4. The steeply increasing part of the experimental data curve was shifted to coincide with the calculated data curve by addition of $7.7*10^{-4}$ to the added $[Ca^{++}]$ values which represents the $[Ca^{++}]$ bound to 1.00 mM Nitr5.
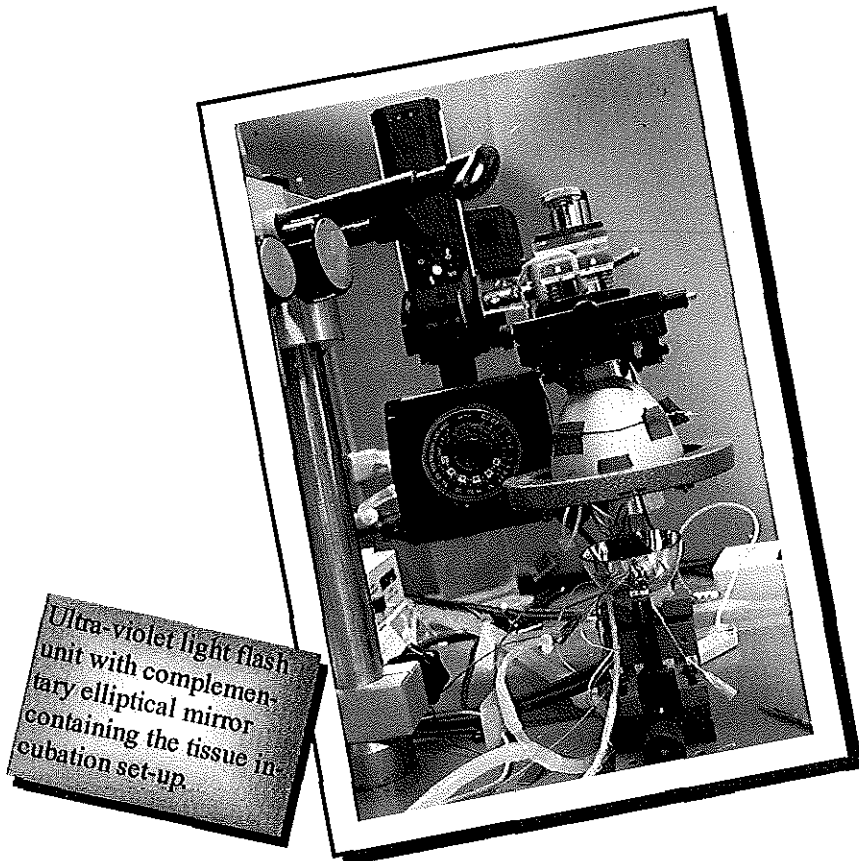
References

1. **Gurney, A.M., R.Y. Tsien and H.A. Lester.** (1987) Activation of a potassium current by rapid photochemically generated step increases of intracellular calcium in rat sympathetic neurons. *Proc.Natl.Acad.Sci.USA.* 84:3496-3500.
2. **Malenka, R.C., J.A. Kauer, R.S. Zucker and R.A. Nicoll.** (1988) Postsynaptic calcium is sufficient for potentiation of hippocampal synaptic transmission. *Science* 242:81-84.
3. **Lea, T.J. and C.C. Ashley.** (1990) Ca^{2+} release from the sarcoplasmatic reticulum of Barnacle myofibrillar bundles initiated by photolysis of caged Ca^{2+}. *J.Physiol.Lond.* 427:435-453.
4. **Lea, T.J., M.J. Fenton, J.D. Potter and C.C. Ashley.** (1990) Rapid activation by photolysis of nitr-5 in skinned fibres of striated adductor muscle from the scallop. *Biochim.Biophys.Acta.* 1034:186-194.
5. **Van Koeveringe, G.A. and R. van Mastrigt.** (1991) Excitatory pathways in smooth muscle investigated by phase-plot analysis of isometric force development. *Am.J.Physiol.* 261:R138-R144.
6. **Näbauer, M. and M. Morad.** (1990) Ca^{2+} induced Ca^{2+} release as examined by photolysis of caged Ca^{2+} in single ventricular myocytes. *Am.J.Physiol.* 258:C189-C193.
7. **Niggli, E. and W.J. Lederer.** (1990) Voltage-independent calcium release in heart muscle. *Science* 250:565-568.
8. **Valdeolmillos, M., S.C. O'Neill, G.L. Smith and D.A. Eisner.** (1989) Calcium-induced calcium release activates contraction in intact cardiac cells. *Pflügers Arch* 413:676-678.
9. **Lando, L. and R.S. Zucker.** (1989) "Caged Calcium" in Aplasia pacemaker neurons. Characterization of calcium-activated potassium and nonspecific cation currents. *J.Gen.Physiol.* 93:1017-1060.
10. **Tsien, R.Y. and R.S. Zucker.** (1986) Control of cytoplasmic calcium with photolabile tetracarboxylate 2-nitrobenzhydrol chelators. *Biophys.J.* 50:843-853.
11. **Rapp, G. and K. Güth.** (1988) A low cost high intensity flash device for photolysis experiments. *Pflügers Arch.*, 411:200-203.

12. **Edgerton, H.E.** (1979) Electronic flash, strobe. Cambridge, MA; M.I.T. press, pp 6-47.
13. **Phillips, R.** (1983) Sources and applications of ultraviolet radiation. London, Academic Press Inc., ; pp 303-331.
14. **Yagi, S., P.L. Becker and F.S. Fay.** (1988) Relationship between force and Ca^{2+} concentration in smooth muscle as revealed by measurements on single cells. *Proc.Natl.Acad.Sci.USA.* 85:4109-4113.
15. **Thomas, M.V.** (1982) Techniques in calcium research. London, Academic press Inc., ; pp 40-45.
16. **Zucker, R.S. and R.A. Steinhardt.** (1978) Prevention of the cortical reaction in fertilized sea urchin eggs by injection of calcium-chelating ligands. *Biochim.Biophys.Acta.* 541:459-466.

CHAPTER 6

Ultra-violet light induces calcium release from intracellular stores in urinary bladder smooth muscle

Ultra-violet light flash unit with complementary elliptical mirror containing the tissue incubation set-up.

Gommert A. van Koeveringe and Ron van Mastrigt

Summary

In this study the accidental finding that in smooth muscle micro-strips of the pig urinary bladder reproducible contractions can be evoked by an ultraviolet light flash is explored. The rate of force development in these contractions is faster than in contractions evoked by field stimulation but slower than in spontaneous contractions. Ultra-violet (UV) flash induced contractions are inhibited by ryanodine, an agent that reduces the availability of calcium from intracellular stores, and also partially by tetrodotoxin (TTX) and atropine. It is suggested that UV light increases the intracellular calcium level by triggering the fast release of calcium from the intracellular stores rather than causing influx of extracellular calcium, which was in previous research shown to be a relatively slow process. UV light stimulation will provide a new way to study smooth muscle mechanics and the function of intracellular calcium stores. The latter probably play a role in spontaneous muscle contractions underlying the clincal syndrome of the "unstable bladder".

Introduction

Smooth muscle contraction is initiated by a rise in the intracellular calcium concentration. In vivo such a rise can occur spontaneously or result from activity of nerves. In vitro it may be triggered by electrical fields or pharmacological agents. Two different mechanisms contribute to the increase in calcium concentration in the muscle cell: Influx of extracellular calcium (12,21,22) and release of calcium from intracellular stores. The intracellular stores can be stimulated to release calcium in several ways e.g. through the inositol 1,4,5-trisphosphate (IP3) receptor channel (2,18) and via the intracellular ryanodine receptor channel located on the intracellular store (calcium induced calcium release: CICR) (9,17). Recently, we suggested that the influx of extracellular calcium is a rate limiting process in the excitation-contraction and pharmaco-mechanical coupling of urinary bladder smooth muscle (28). A similar rate limiting effect of extracellular calcium influx was shown in a study on guinea pig intestine by Himpens & Somlyo (13) In order to confirm the hypothesis that intracellular calcium release is a faster process than extracellular influx, we started a study in which "caged calcium" (Nitr5/AM) was introduced into the cell to bypass the extracellular calcium influx. An ultra-violet (UV) light flash was used to degrade the intracellularly loaded "caged calcium" (25,26). In the course of our experiments it appeared that the UV light flash also reproducibly evoked contractions in muscle preparations that were not loaded with caged calcium. This new contractile effect was the subject of the present study. In contrast a

smaller time constant than electrical field stimulation, the UV light was suspected to stimulate an intracellular process communicating rapidly to the contractile units. Therefore, the effect of ryanodine (a natural plant alkaloid from Ryania Speciosa), which reduces the availability of calcium from the intracellular stores (14,16,20,24) was tested. In order to detect if the UV sensitivity originated in nerve or in muscle cells, the contractile effect was studied in the presence of tetrodotoxin (TTX) and atropine. Additionally, the time constant of isometric force development in response to field stimulation or UV light stimulation was compared to the time constant of spontaneous contractions.

Methods

Tissue preparation.

Fresh pig urinary bladders were obtained from the local slaughterhouse. From each bladder one strip was used from a standardized locus at the dorsal side of the bladder dome. Smooth muscle micro-strips with a maximum diameter of 200μm and a length of 1 to 2 mm were cut using a binocular microscope. Care was taken that the muscle fibres were running longitudinally in the preparation. The strips were prepared in modified aerated Krebs solution and transported to the organ bath in a small container prevent desiccation.

Solutions.

The strips were incubated in modified Krebs solution: NaCl, 118 mM; KCl, 4.7 mM; $NaHCO_3$, 25 mM; KH_2PO_4, 1.2 mM; $CaCl_2$, 1.8 mM; $MgSO_4$ 1.2 mM; glucose, 11 mM; pH 7.4; aerated with 95% O_2 / 5% CO_2. A solution called "ryanodine" was prepared from modified Krebs with 10μM ryanodine (Calbiochem®). A "TTX" solution consisted of modified Krebs with 10μM tetrodotoxin (Sigma®) and the "atropine" solution consisted of modified Krebs with 10μM atropine.

Incubation.

The strips were incubated (Fig. 1) in a 20 μl drop of modified Krebs fluid (with 95% O_2 / 5% CO_2 being blown over the drop's surface) which was continuously refreshed using separate in- and outflow syringe pumps (HOSPAL® Dasco S.p.A. 41036, Medolla, Italy) at a rate of 40μl min⁻¹. Two platinum ring electrodes at either end of the strip were used for electrical stimulation and support of the drop by surface tension. Temperature was kept at 37 C using infrared radiation from a halogen lamp (Philips®,12V,20W,6 ,type
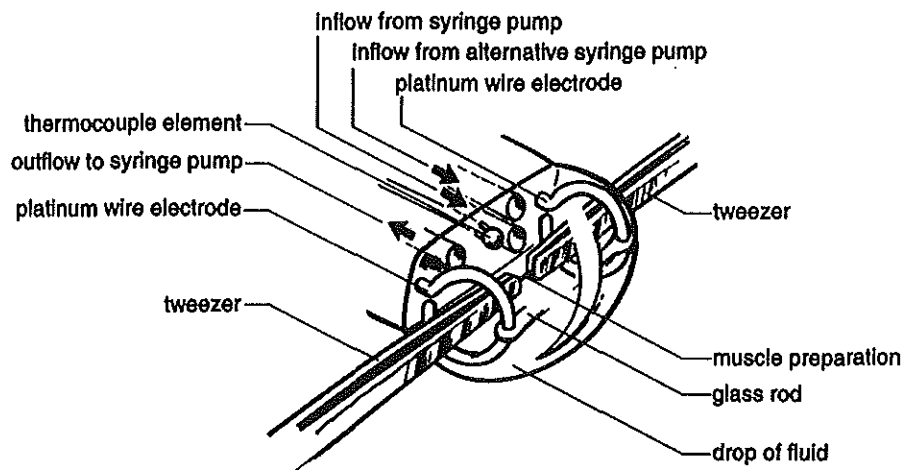
Figure 1: Tissue incubation set-up: A drop of 20µl Krebs fluid was supported by two plati-
num wire electrodes attached to a small Perspex block. The drop remained in position through
surface tension and was stabilised by a glass rod connecting the two electrodes. The Krebs
solution was continuously refreshed using an in- and an outflow syringe pump. The muscle
preparation (length ± 1 mm; diameter 200 µm) was positioned in the centre of the drop bet-
ween two micro tweezers.

6483), controlled using a 200 µm diameter thermocouple (Omega®, Stamford,
CT 06907, U.S.A.) in the drop. The strips were mounted between two tweezers,
400 µm diameter, one of which was attached to a KG3 force transducer
connected to a BAM3 amplifier (Scientific instruments®, Heidelberg,
Germany). In the drop the strips were exposed to electrical field stimuli: 100Hz,
4V alternating polarity pulses of 5ms duration, or UV flashes from a device
described below. The fluid in the drop could be replaced quickly by switching to
an alternative inflow pump unit and increasing in and outflow rate 10 times. The
incubation in a suspended drop of fluid enabled the exposure of the preparation
from all directions and minimized the transients between air, glass, water and
tissue to allow a much UV light as possible to reach the preparation.

UV flash lamp.

In order to produce a high intensity UV light flash at a minimal budget, a
setup described by Van Koeveringe & Van Mastrigt (29) was used. A 300
J/flash, 120 W, type DG 8907 ST II short arc Xenon flash tube (EG&G/
Heimann®, Wies baden, Germany) was mounted in a Melles and Griot® (Irvine,
Ca 92714, U.S.A.) type 02 REM 001 elliptical mirror and driven by a modified
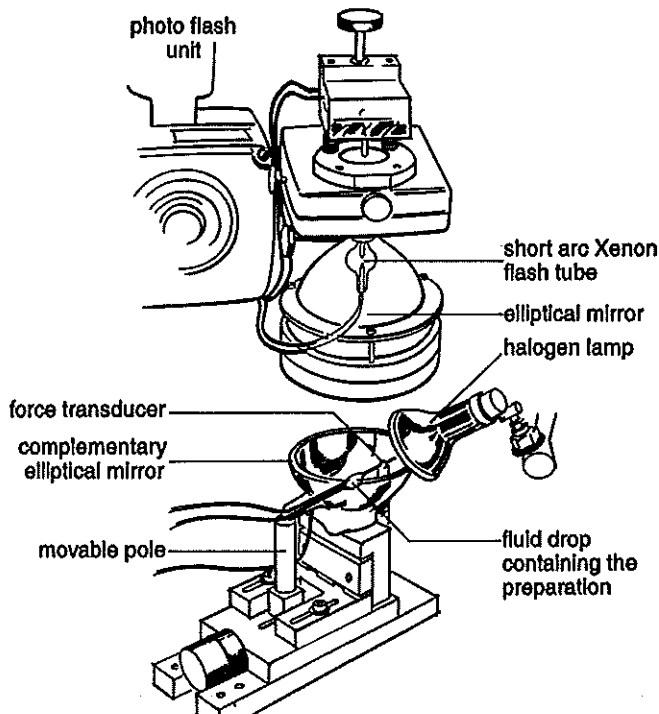
Figure 2: UV flash lamp: A modified photoflash unit was used to drive a short arc xenon flash tube in an elliptical mirror. The fluid drop containing the preparation (see Fig. 1) was placed in a complementary elliptical mirror. One tweezer was attached to the force transducer the other to a movable pole. The fluid drop was heated by an infrared halogen lamp.

Metz® (Metz-werke GmbH, 8510, Furth/Bay.1, Germany) 60 CT 4 photo flash unit up to 240 J input energy and 4 ms flash duration. The fluid drop that contained the preparation was placed in the focus of a home made complementary elliptical mirror (Fig. 2) (29) made of aluminium coated glass blown in a wooden mould. By means of a 3mm thick Schott®, UG 11 glass filter, only UV light in a wave length band between 320 and 370 nm was transmitted to the preparation.

Measurement protocol.

All strips were of a similar size. Strips were not stimulated at l_0, the length at which maximum isometric force is developed, because in this type of smooth muscle passive tension is very high at that length (see Fig. 5 in (30)), which causes rapid degradation of the strips. As an alternative the strips were pre-stretched to an initial passive force of 20 μN. Two test stimulus protocols were applied, one 2 minutes after the pre-stretch and one after another 10 minutes of

equilibration time. Each stimulus protocol consisted of two successive stimulations: an electrical field and one minute later a UV flash stimulation. If any of the four stimuli in the two protocols evoked a contraction amplitude smaller than 40μN, the strip was considered to be in a too bad condition and was discarded. Otherwise, after allowing 5 minutes waiting time, the stimulus protocol was repeated at 5 minute intervals. In 7 strips, each from a different bladder, 5 sequential stimulus protocols were applied. After the first of these 5 protocols the solution in the drop around the prepartion was replaced by the Krebs solution containing 10μM ryanodine. Another 7 strips, in which 5 stimulus protocols were applied without adding ryanodine, served as controls.
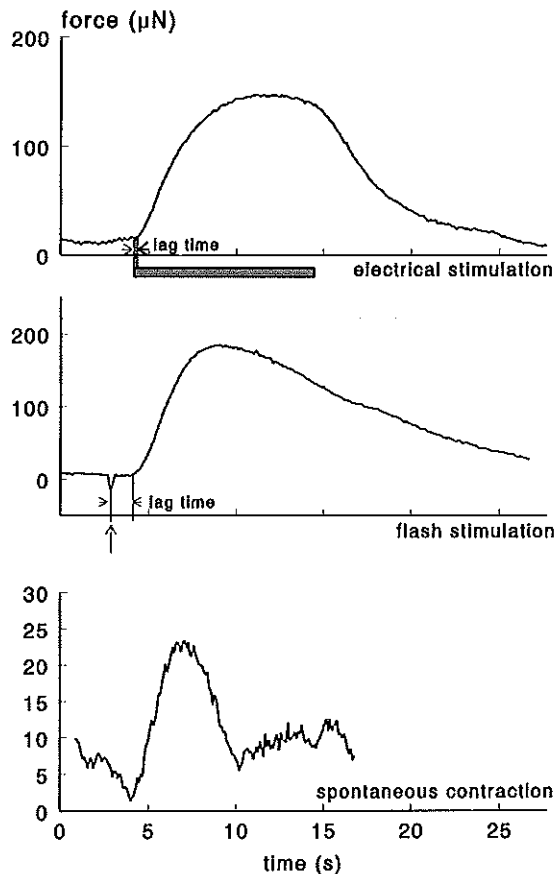

Figure 3: Force as a function of time of a typical electrically stimulated, a flash stimulated and a spontaneous contraction, all recorded in the same micro-strip. (A) Electrical stimulation (100 Hz, 4V alternating bipolar pulses of 5ms) for 10 seconds evoked a contraction with an amplitude of 140 μN. (B) A 180 μN contraction in response to a 240 J flash (arrow) after a lag time of approximately 1 second. (C) A 20 μN spontaneous contraction.

Unfortunately, the possible reversibility of the ryanodine effect could not be tested, because ryanodine remained in the preparation for a duration extending its viability.

In 7 strips, after the first stimulus protocol, the solution was replaced by the TTX solution. After 10 minutes waiting time the next stimulus protocol was applied. The drop preparation was then thoroughly washed with normal Krebs fluid and after another 10 minutes the third and last stimulus protocol was applied. In 7 strips, the first stimulus protocol was followed by 10 minutes incubation in a 10µM atropine solution, after the second protocol the preparation was thoroughly washed and 10 minutes later a last stimulus protocol was applied. In 11 of the 28 strips spontaneous contractions, large enough (>10µN) for processing, were observed before any pharmacological agent was added to the perfusion solution. By definition a contraction (>10µN) was called a spontaneous contraction if no stimulation, neither electrical nor flash, was applied in the previous minute. Spontaneous contractions were statistically compared to the subsequent electrical and flash stimulated contractions.

Data processing.

The measured contraction force signal and the stimulus signal were sampled (at a rate of 10Hz) with a Commodore® 386sx computer equipped with a PCL818 (Advantech Corp .Ltd, Taipei, RC) A/D converter card using multichannel data acquisition software (MKR: developed by the CDAI dept. Academic Hospital Rotterdam, Netherlands), see Fig. 3. From all contractions, the maximum extrapolated isometric force (F_{iso}) and the time constant for isometric force development (C) were determined using phase plot analysis. A phase plot of isometric force development is a plot of the rate of change of the force (dF/dt) as a function of the force (F) (28,31), see Chapter 4: Fig. 1. For the greater part such a phase plot can be characterized by a straight line, representing a mono-exponential force development. The force axis intercept of this line is the isometric force that would have been attained after infinitely long stimulation and was called F_{iso}. The negative reciprocal value of the slope of the line is the time constant in isometric force development (C). Phase plots were calculated and processed in the Matlab® (Math Works inc., Natick, Mass. 01760, U.S.A.) computer programming environment. The lag time, which was defined as the time between the start of the stimulus and the subsequent onset of force development, was visually estimated from the recorded signals (see Fig. 3). In each strip the F_{iso} values were normalized by dividing each value by the corresponding value in the first stimulus protocol, the time constants were not normalized. Mean values and standard errors of the mean were determined for the normalized F_{iso} values and time constants in each set of seven strips subjected to the same treatment.

An unbalanced repeated measures analysis of variance with a customized

analytical model (using BMDP® (5v module), BMDP statistical software, Cork, Ireland) was used to test the significance of the following sources of variance in F_{iso} and the time constant: the type of stimulation (field or flash), the treatment (Krebs or ryanodine) and the elapse of time. A Wilcoxon matched-pairs signed ranks test (using SPSS®, SPSS inc., Chicago, Illinois, U.S.A.) was used to test the differences between the responses to field and flash stimuli in normal Krebs solution in 28 strips i.e. in the measurements made in all strips before pharmacological agents were applied. The same test was used to test for differences between field and flash stimuli and spontaneous contractions in 11 strips that showed spontaneous activity. In both tests the un-normalized F_{iso} and time constant values were used. A Mann-Whitney U test was used to test for differences in the normalized values of F_{iso} and un-normalized values of the time constant between ryanodine, TTX, atropine and control treatments.
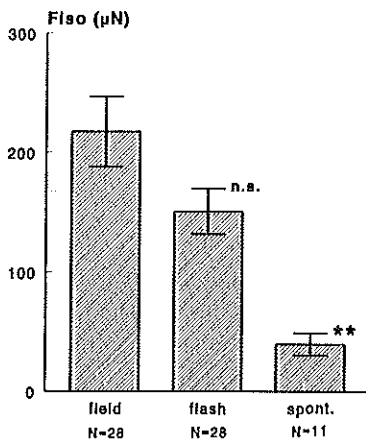

Figure 4: Maximum extrapolated isometric force (F_{iso}) values. Mean ± S.E.M. for contractions in response to electrical field and UV flash stimulation in 28 strips and during a spontaneous contraction in 11 strips, that showed spontaneous activity in normal Krebs solution. The mean values after electrical field and UV flash stimulation in all 28 strips were similar to those in 11 strips. Significances of diferences with the value after field stimulation are indicated by: n.s. = not significant and ** = p<0.01.
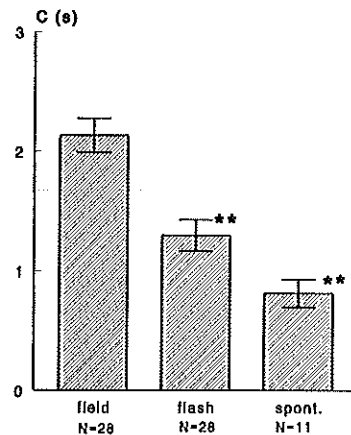
Figure 5: Time constant values. Mean ± S.E.M. for contractions in response to electrical field and UV flash stimulation in 28 strips and during a spontaneous contraction in 11 strips, that showed spontaneous activity in normal Krebs solution. The mean values after electrical field and UV flash stimulation in all 28 strips were similar to those in 11 strips. Significances of diferences with the value after field stimulation are indicated.

Results

UV flash stimulation evoked contractions with an amplitude comparable to electrically stimulated contractions (Fig. 3). The use of a high pass (> 400 nm) UV blocking filter completely abolished the flash-induced contractions. The flash caused a small (< 1 °C) temperature increase at the location of the preparation in the drop.

lag time (s)

Figure 6: Mean lag time (time from start of stimulation to the onset of force development) ± S.E.M. for electrically and flash stimulated contractions. Significances of diferences with the value after field stimulation are indicated.
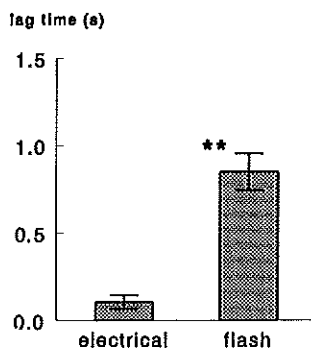
UV flash stimulated contractions compared to field stimulated and spontaneous contractions.

Strips from 11 of the 28 bladders studied showed spontaneous contractions during the first 15 minutes of the experiments before any treatment agent was added. The mean F_{iso} (maximum extrapolated isometric force) of the 11 contractions was significantly smaller than that after electrical field (p<0.005) or flash (p<0.01) stimulation (Fig. 4). The F_{iso} values of the field stimulated and UV flash stimulated contractions in all 28 bladders were not significantly different. The spontaneous contractions (N=11) had a smaller time constant i.e. a faster force development than both the electrical field stimulated contractions (p < 0.005) and the flash stimulated contractions (p < 0.005) (Fig. 5). In turn, the UV stimulated contractions (N=28) were significantly faster (p<0.0001) than the field stimulated contractions. Figure 6 shows that the lag time after a flash was approximately 10 times longer than the lag time after the start of a field stimulation; lag times are illustrated in Figure 3. As the lag time could only be determined with a resolution of 0.1 s (the sample rate), the accuracy of the short lag time after electrical stimulation is limited. Nevertheless a significant difference with the considerable lag time after a UV flash is obvious.

Effect of ryanodine.

In the course of 5 sequential stimulus protocols performed in 7 strips, each from a different bladder, in normal Krebs solution the tissue showed a slight decrease in force development, more prominent for flash stimulated contractions than for field stimulated contractions (Fig. 7 , solid lines). In the 7 more strips, which were incubated in 10µM ryanodine after the first of the 5 stimulus sequences, a more rapid decrease in F_{iso} of the flash induced contractions was
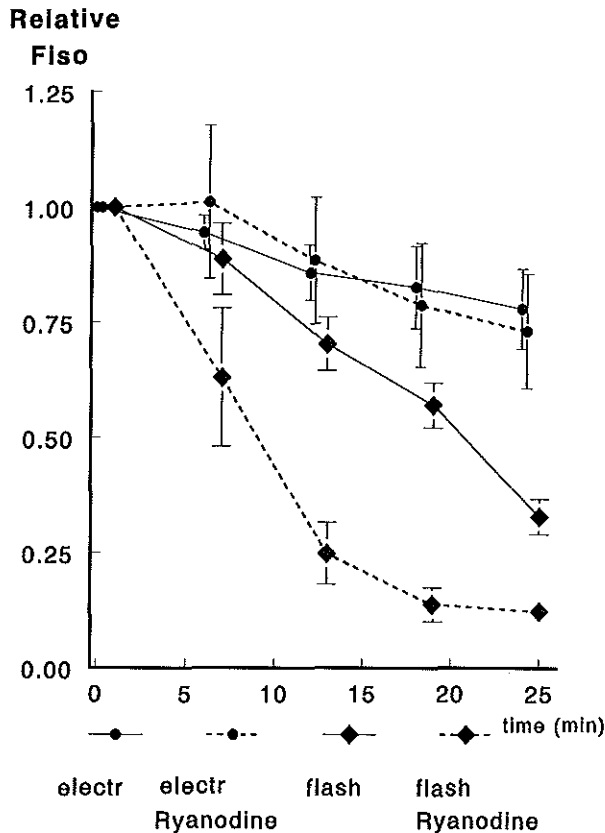
Relative Fiso

Figure 7: Mean ± S.E.M. of F_{iso} in response to electrical (solid line) and UV flash (solid line with diamond signs) stimulation are shown in 5 sequential contractions in normal Krebs solution (N=7). In another 7 strips ryanodine was added to the superfusion solution after the first contraction (dashed lines).

observed (Fig. 7, lines with diamond signs). The significance of this observation was tested using an unbalanced repeated measures analysis of variance with a customised analytical model. A model describing F_{iso} as a logarithmically decreasing variable in time multiplied by a variable determined by treatment (Krebs, ryanodine) and stimulus (field, flash) was used. This analysis showed that elapsed time (p<0.0005), stimulus (p<0.05) and the interaction treatment-stimulus-time (p<0.01) were significant sources of variance. The interactions treatment-time (p=0.3) and treatment-stimulus (p=0.1) were not significant as sources of variance. The stimulus-time interaction was also a significant source of variance (p<0.0005).

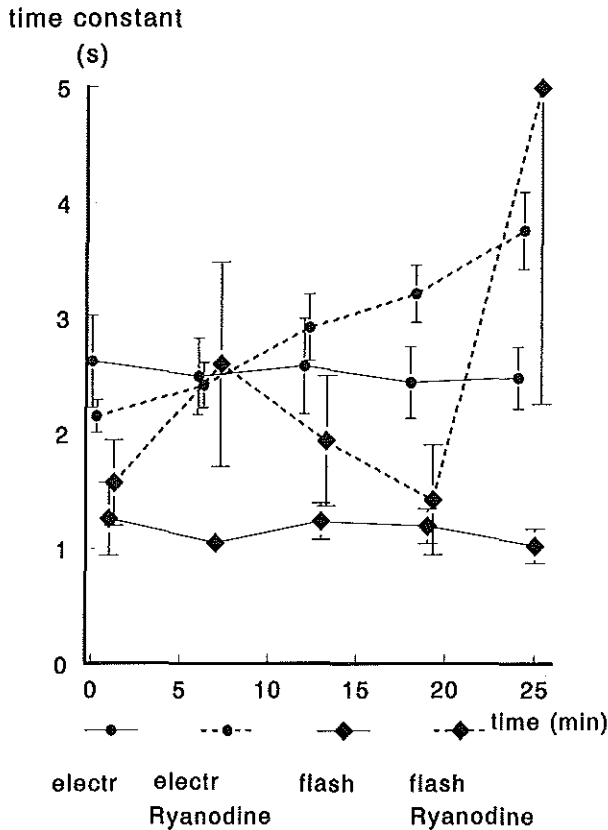When the second contraction (third stimulus protocol, at 15 min. in Fig.7)

Figure 8: Mean time constant values ± S.E.M. in response to electrical (solid line) and UV flash (solid line with diamond signs) stimulation are shown in 5 sequential contractions in normal Krebs solution (N=7). In another 7 strips ryanodine was added to the superfusion solution after the first contraction: The resulting mean ± S.E.M. are shown in the dashed lines.

in ryanodine was compared to the control flash stimulated contraction at the same time in normal solution a significantly (Mann-Whitney U test) smaller mean F_{iso} was shown (see Fig. 9; p<0.005). At this time, the F_{iso} values in flash stimulated contractions were also significantly smaller (p<0.005) than values in electrically stimulated contractions. The field stimulated contractions did not show a significant difference in mean F_{iso} values between in Krebs and ryanodine.

In control Krebs solution the time constants for both flash and field stimulated contractions remained constant throughout the experiment from the 1st to the 5th contraction (Fig. 8). In the ryanodine solution a gradual increase of

the time constant could be seen for field stimulated contractions (Fig. 8). The significance of the effect of ryanodine on the time constant of both field and flash stimulated contractions was tested using the unbalanced repeated measures analysis of variance. As the large variability in the time constants of flash stimulated contractions in ryanodine caused large artifacts in the stimulus-treatment interactions, a group field stimulated and a group flash stimulated contractions were analysed separately. In both groups a linear time dependent model was used to determine the significance of the following sources of variance: time, treatment and time-treatment interaction. For the field stimulated contractions, time alone and the time-treatment interaction were significant sources o variance: for both $p<0.0001$. Treatment alone was not a significant source of variance. For the flash stimulated contractions, time alone was a contributing but not a significant source of variance ($p=0.08$). Treatment alone and time-treatment interaction were not significant sources of variance. In contrast a Mann-Whitney U test, when applied to the third stimulus protocol (10 minutes after adding ryanodine), did not show a significant difference in mean time constant during field stimulation in ryanodine and normal Krebs solution.

Comparison of effects of ryanodine, TTX and atropine

The effects of different treatments on the F_{iso} in response to field and flash stimuli is illustrated in Fig. 9. All values are averages of values normalized by dividing by the corresponding value before treatment ± S.E.M.. The control bars represent the normal decay of the response during 10 minutes incubation. For field stimulation the responses to any treatment (ryanodine, atropine or TTX) were not significantly different from the normal decrease of the response.

A significant reduction in F_{iso} was found in flash stimulated contractions when ryanodine ($p=0.004$), atropine ($p=0.02$) or TTX ($p=0.01$) treatment was compared to control treatment. In ryanodine ($p=0.004$), atropine ($p=0.009$), and TTX ($p=0.02$), F_{iso} values in response to flash stimulation were significantly smaller than in response to field stimulation. There were, however, no significant mutual differences between ryanodine, atropine or TTX treatments for flash stimulation. After wash-out of atropine or TTX the F_{iso} values were not significantly different from controls for either stimulus.

Spontaneous activity was clearly enhanced by atropine treatment in 4 of the 7 strips. This effect was not present in any of the TTX or ryanodine treated strips.

Figure 10 illustrates the effect of the different treatments on the time constants of force development following field and flash stimulation. In normal Krebs solution (control, $p=0.001$), and in atropine ($p=0.05$), the flash stimulated contraction had a significantly smaller time constant. In ryanodine there seemed to be a difference, but this was not significant. In TTX, no significant difference was found. The differences between treatments for each stimulus were not significant, except when TTX treatment was compared to control treatment, a

significantly larger (p<0.05) time constant was found after flash stimulation.

After wash-out of TTX, the time constant returned to a value similar to the control.

Discussion

Small strips of the urinary bladder smooth muscle were exposed to ultraviolet light flashes in a study designed to investigate the rate of isometric force development using photolysis of caged calcium. The UV light evoked a contraction with a maximum extrapolated isometric force F_{iso} (Fig.4) similar to an electrical field stimulated contraction but with a smaller time constant, i.e. it developed faster (Fig.5). As control preparations, not loaded with caged calcium, also contracted upon UV light exposure it was not certain that caged calcium was effectively photo lysed in the caged calcium loaded preparations.

The nature of the flash induced contractions was studied first by excluding possible artefacts. The contractions were completely abolished by a high pass (> 400 nm) UV blocking filter, which did not block visible light, infrared light or electromagnetic artefacts. It was therefore concluded that the flash-induced contractions were neither mediated by heat from the lamp nor by an electrical artefact.

It seemed that the aim of the designed study, i.e. development of a stimulation method bypassing the rate limiting process in excitation contraction, could be met without using caged calcium. The UV flash appeared to address a faster excitatory pathway, more directly related to the contractile units. This finding, combined with the earlier finding that the influx of extracellular calcium is the rate limiting step in the excitation-contraction coupling (13,28) in this tissue, supported the hypothesis that the flash did induce intracellular calcium release.

To test this hypothesis the effect of ryanodine, an inhibitor of calcium induced calcium release (CICR) from the intracellular stores, was studied in strips that were stimulated both electrically and with UV flashes.

The gradual decrease of F_{iso} values (Fig. 7) in control, normal Krebs, solution might be due to the UV light causing damage to the calcium binding molecules in the intracellular stores or to the depletion of a UV sensitive substrate molecule for an intracellular messenger.

In order to analyse the difference in curvature of the clearly visible time dependent decrease of F_{iso} with and without ryanodine an unbalanced repeated measures analysis of variance with a customized analytical model was performed. Time was a significant source of variance in F_{iso}: a general decrease in F_{iso} can be seen in Figure 7. The treatment-stimulus interaction alone was not a significant source because the changes in the contractions over time were too large, thus causing a major unexplained variation source. The treatment-
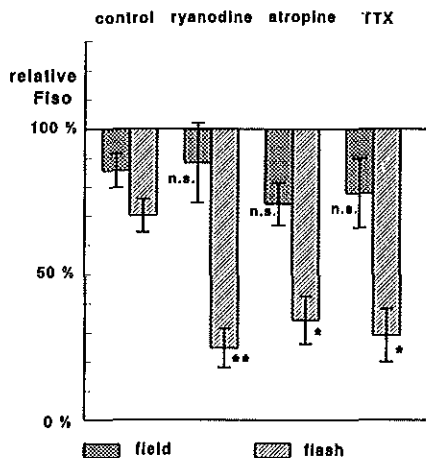
Figure 9: Relative F_{iso} values after 10 minutes incubation in ryanodine, atropine and TTX solutions both for field and flash stimulation. Values are relative to those before any agent was added. The control values (first set of bars) show the normal decay of the tissue in 10 minutes time in normal Krebs solution. Significances of diferences with the corresponding value after field stimulation are indicated: * = p<0.05
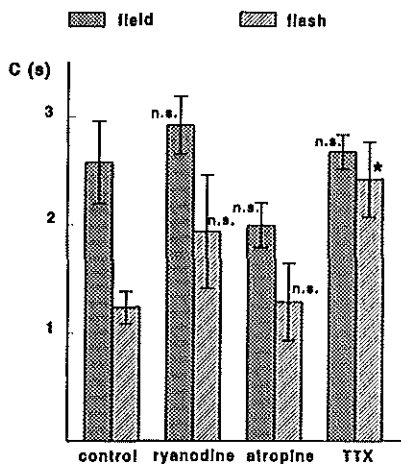
Figure 10: Time constants (C) of responses field and flash stimulation during ryanodine, atropine and TTX treatment. The contrⁱrol values (first set of bars) are values measured after 10 minutes in normal Krebs solution. Significances of diferences with the corresponding value after field stimulation are indicated.

stimulus-time interaction was shown to be a significant source of variance (p<0.01). This indicates that ryanodine produces a significant variance in F_{iso}, when the elapse of time and the different stimuli are taken into account. The finding that the ryanodine alkaloid inhibited flash stimulated contractions, indicates that the UV light stimulation method is likely to exert its effect by depleting intracellular calcium stores. Field stimulated contractions were not affected by ryanodine (Fig.7), so that it can be concluded that calcium release from intracellular stores via the ryanodine receptor (CICR) is not necessary to generate the maximum isometric force in this type of smooth muscle.

Using the same unbalanced repeated measures analysis of variance, the significant sources of variance in the time constant of isometric force development were tested. When analysing both stimulus modalities, flash and field, in one group, it was not possible to perform a representative analysis of variance i.e. the relatively most important source of variance was the stimulus mode, eliminating all other sources. The analysis was corrupted because in the flash stimulated group during ryanodine treatment responses were so small that the time constants could not reliably be determined. Therefore, the flash

stimulated and field stimulated contractions were analysed separately. In the flash stimulated contractions time-treatment interaction and treatment alone were not significant sources of variance, which indicates that ryanodine did not significantly affect the time constant. When interpreting this result, it should be kept in mind again that flash stimulated contractions in ryanodine were so small in amplitud that the phase plot analysis might have been less reliable. This is signified by the large standard error of the mean in Figure 8. The time constant during field stimulation increased (Fig.8) in ryanodine. This was indicated by the time-treatment interaction being a significant source of variance in the field stimulated group (p<0.0001). When ryanodine treated and control values of the time constants were compared at separate times using the Mann-Whitney U-test, no significant differences could be demonstrated. The increasing time constant value suggests that normally during field stimulation a fast ryanodine sensitive excitation-contraction coupling process is involved. As the extrapolated maximum isometric force was not significantly reduced, it is probable, that these values are true maxima limited by the capacity of the contractile proteins. This would imply that, in the measurements made, the intracellular calcium concentration reached a saturation level regardless of the activity of the intracellular stores. The activity of these stores then would only influence the rate at which this saturation level is reached. When the fast process of CICR from intracellular stores was inhibited during ryanodine treatment, slower processes, such as IP3 mediated intracellular calcium release or either depolarisation or receptor operated influx of extracellula calcium would then be more prominent.

In contrast to a UV light induced contraction, a UV light induced relaxation due to release of nitric oxide has been demonstrated in mesenteric arteries (32). As nitric oxide has been shown to be involved in solely muscle relaxing mechanisms by increase of guanylate cyclase activity a similar contraction inducing mechanism is is not likely in bladder muscle. However a regulation of the ryanodine receptor by cyclic-ADP-ribose, via guanylate cyclase and via nitric oxide was suggested by Berridge (1). A possible mechanism for the excitation of the muscle cell UV light flashes might be the UV evoked synthesis of a stimulatory agent instead. NAD^+ is one of the candidates for a UV sensitive intracellular substrate. Spectrophotometrical analysis in a small pilot study showed that during UV exposure NAD^+ degraded (personal communication Dr. H.R. de Jonge, Dept. Biochemistry, Rotterdam). As possible degrading product might be cyclic-ADP-ribose, which has a proven effect on the ryanodine receptor (1,10,11). More research has to be done to clarify this matter.

The role of nerve mediated processes in the excitation-contraction coupling upon UV light stimulation was investigated by stimulating the strips in the presence of TTX or atropine.

The maximum isometric force (F_{iso}) in response to field stimulation was similar in normal Krebs and TTX solution. This confirms that stimulation with a

repetition frequency of 100 Hz, 4 V alternating polarity pulses of 5 ms duration evoked direct muscle stimulation to a saturation level in this kind of preparation. The F_{iso} in response to flash stimulation was reduced in both TTX and atropine solutions. This finding suggests that rather then muscle cells, nerve cells were primarily stimulated by the UV light. These nerve cells must stimulate muscarinic receptors in the muscle cells in view of the inhibition by atropine. If this pathway would have been addressed exclusively, TTX would have inhibited the complete flash effect, which it did not. Therefore, another smaller direct effect of the UV flash on the muscle cell itself must be assumed. This pathway must have a similar time constant as the direct field stimulation pathway, in view of the fact that the time constant in TTX treatment was similar to that in control treatment (Fig. 10). A possible alternative hypothesis is that the flash only stimulated intracellular stores in muscle cells, but that a propagation of the contraction through the preparation occurred which is inhibited by TTX and atropine. An alternative could be that nerve action is a necessary condition to potentiate intracellular calcium release in the smooth muscle cell. More research will be necessary to clarify this matter.

The lag time between stimulation and the onset of force development is approximately 10 times longer in flash evoked contractions than in contractions evoked by field stimulation (Fig. 6). Although the molecular basis of these phenomenons has not been clarified in this study, the lag time could be due to a chemical reaction in the cell initiated by the UV light in which the concentration of the product (e.g. cyclic-ADP-ribose), has to reach a certain threshold level.

The flash stimulated contractions were also compared to spontaneous contractions. In 4 of the 7 strips undergoing atropine treatment, spontaneous activity was either induced or increased in amplitude. This probably indicates that cholinergic receptor stimulation inhibits spontaneous activity. TTX, eradicating all nerve activity, did not stimulate spontaneous contractions. Most probably therefore, other neurotransmitters in the bladder, as for example ATP (5,28) in pig bladder, stimulate while acetylcholine inhibits spontaneous activity. In the recorded spontaneous contractions force developed even faster than in the flash stimulated contractions, suggesting a mechanism even more closely related to the contractile units. Although the amplitude of the spontaneous contractions was small, a synchronisation of a group of cells is necessary to generate forces of this magnitude. An unknown fast mechanism of cell-to-cell propagation of the stimulus through the preparation is necessary for this synchronisation in order to cause a contraction with such a small time constant. This propagation mechanism will be the aim of a future research project.

Light induced calcium release from intracellular stores has been described previously for optic rod cells (6). A similar mechanism in the bladder is physiologically illogical. Other techniques like calcium imaging and testing of several inhibitors of cellular processes might be helpful to provide a better understanding of the origin of the flash induced intracellular calcium release but

lead beyond the scope of this article. It would also be interesting to investigate if this phenomenon is present in other non-skinned smooth muscle preparations or persists following skinning.

It must be concluded that the UV light sensitivity of bladder smooth muscle still has a largely unexplained physiological basis. Nevertheless this study indicates that this newly discovered stimulation method, with a fast, at least partly, nerve mediated pathway to the contractile units, is a useful tool to provide a more direct stimulation of the nerve or muscle cells in muscle mechanics research. It is also a most helpful tool in studying the function of intracellular calcium stores. As these stores probably play a role in spontaneous activity of bladder muscle (8,15,27), which in certain patients leads to functional problems, such studies are clinically relevant (3,4,19).

References

1. Berridge, M.J. (1993) A tale of two messengers. *Nature* 365,388-389.
2. Berridge, M.J. (1993) REVIEW: Inositol trisphosphate and calcium signalling. *Nature* 361, 315-325.
3. Blaivas, J.G. (1988) Pathophysiology and differential diagnosis of benign prostatic hypertrophy. *Urology* 32(Suppl. 6), 5-11.
4. Bosch, R. (1990) Instability of the bladder: Pathophysiology Unknown? A synopsis of Clinical Points of Interest. *Neurourology and Urodynamics* 9, 563-565.
5. Brading, A.F., J.L. Mostwin, G.N.A. Sibley, and M.J. Speakman. (1980) The role of smooth muscle and its possible involvement in diseases of the lower urinary tract. Clin. Sci. Lond. 70:229-240.
6. Campbell, A.K. (1983) *Intracellular Calcium, its Universal Role as a Regulator*. John Wiley & Sons Ltd. Chichester, UK .
7. Deliconstantinos, G., Villotou V. & Fassitas, S. (1992) Ultraviolet-irradiated human endothelial cells elaborate nitric oxide that may evoke vasodilatory response. *Journal of Cardiovascular Pharmacology* 20(Supp. 12), S63-S65.
8. Downie, J.W. & Slack, B.E. (1983) Sensitivity to indomethacin of tetrodotoxin-resistant contractions of smooth muscle from the base of rabbit bladder. *British Journal of Pharmacology* 79, 334-336.
9. Fabiato, A. (1983) Calcium release of calcium from cardiac sarco plasmic reticulum. *American Journal of Physiology* 245, C1-C14.
10. Galione, A. (1993) Cyclic ADP-Ribose: A New Way to Control Calcium. *Nature* 359, 325-326.
11. Galione, A., White, A., Willmott, N., Turner, M., Potter, B.V.L. & Watson, S.P. (1993) cGMP mobilizes intracellular Ca2+ in sea urchin eggs by stimulating cyclic ADP-ribose synthesis. *Nature* 365, 456-459.
12. Ganitkevich, V.Ya. & Isenberg, G. (1991) Depolarization-mediated intracellular calcium transients in isolated smooth muscle cells of guinea-pig urinary bladder. *Journal of Physiology* 435, 187-205.
13. Himpens, B. & Somlyo, A.P. (1988) Free-Calcium and force transients during depolarization and pharmaco-mechanical coupling in Guinea-pig smooth muscle. *Journal of Physiology* 395, 507-530.
14. Katsuyama, H., Ito, S., Itoh, T. & Kuriyama, H. (1991) Effects of ryanodine on

acetylcholine-induced Ca2+ mobilization in single smooth muscle cells of porcine coronary artery. *Pflügers Arciv* 419, 460-466.

15. **Levin, R.M., Ruggieri, M.R., Velagapudi, S., Gordon, D.,Altman, B. & Wein ,A.** (1986) Relevance of spontaneous activity to urinary bladder function: an in vitro and in vivo study. *The Journal of Urology* 136, 517-521.

16. **Meissner, G.** (1986) Ryanodine Activation and Inhibition of the Ca2+ Release Channel of Sarco plasmic Reticulum. *Journal of Biological Chemistry* 261, 6300-6306.

17. **Niggli, E. & Lederer, J.** (1990) Voltage-Independent Calcium Release in Heart Muscle. *Science* 250, 565-568.

18. **Parker, I. & Ivorra, I.** (1990) Localized all-or-none Calcium liberation by Inositol Trisphosphate. *Science* 250, 977-979.

19. **Sibley, G.N.A.** (1984) A comparison of spontaneous and nerve-mediated activity in bladder muscle from man, pig and rabbit. *Journal of Physiology* 354, 431-443.

20. **Smith, J.S., Imagawa, T., Fill, J.M.M., Campbell, K.P. & Coronado, R.** (1988) Purified ryanodine receptor from rabbit skeletal muscle is the calcium release channel of sarco plasmic reticulum. *Journal of General Physiology* 92, 1-26.

21. **Somlyo, A.P.** (1985) Excitation-contraction coupling and the ultrastructure of smooth muscle. *Circulation Research* 57, 497-507.

22. **Somlyo, A.P. & Himpens, B.** (1989) Cell calcium and its regulation in smooth muscle. *The FASEB journal* 3, 2266-2276.

23. **Steg, G.P., Rongione, A.J., Gal, D., DeJesus, S.T., Clarke, R.H. & Isner, J.M.** (1989) Pulsed ultraviolet laser irradiation produces endothelium-independent relaxation of vascular smooth muscle. *Circulation* 80, 189-197.

24. **Sutko, J.L. & Kenyon, J.L.** (1990) Actions of Ryanodine. *Journal of General Physiology* 96, 439-441.

25. **Tsien, R.Y. & Zucker, R.S.** (1986) Control of cytoplasmic calcium with photo labile tetracarboxilate 2-nitrobenzhydrol chelators. *Biophysical Journal* 50, 843-853.

26. **Valdeolmillos, M., O'Neill, S.C., Smith, G.L. & Eisner, D.A.** (1989) Calcium-induced calcium release activates contraction in intact cardiac cells. *Pflügers Arciv* 413, 676-678.

27. **Van Koeveringe, G.A., Mostwin, J.L., Van Mastrigt, R. & Van Koeveringe, B.J.** (1993) Effect of Partial Urethral Obstruction on Force Development of the Guinea Pig Bladder. *Neurourology and Urodynamics* 12, 555-571.

28. **Van Koeveringe, G.A. & Van Mastrigt, R.** (1991) Excitatory pathways in smooth muscle investigated by phase plot analysis of isometric force development. *American Journal of Physiology* 261, R138-R144.

29. **Van Koeveringe, G.A. &** (1994) Photolysis of caged calcium using a low cost flash unit: efficacy analysis with a calcium selective electrode. *Cell Calcium* 15, 423-430.

30. **Van Mastrigt, R.** (1988) The length dependence of the series elasticity of pig bladder smooth muscle. *Journal of Muscle Research and Cell Motility* 9, 525-532.

31. **Van Mastrigt, R. & Glerum, J.J.** (1985) Electrical stimulation of smooth muscle strips from the urinary bladder of the pig. *Journal of Biomedical Engineering* 7, 2-8.

32. **Wigilius, I.M., Axelsson, K.L., Andersson, R.G.G., Karlsson, J.O.G. & S. Ödman** (1990) Effects of sodium nitrite on ultraviolet-induced relaxation and ultraviolet light dependent activation of guanylate cyclase in bovine mesenteric arteries. *Biochemical and Biophysical Research Communications* 169 No1, 129-135.

CHAPTER 7

Length dependency of the force-velocity relation in smooth muscle fibers of the urinary bladder

Tissue incubation set-up on the linear displacement device
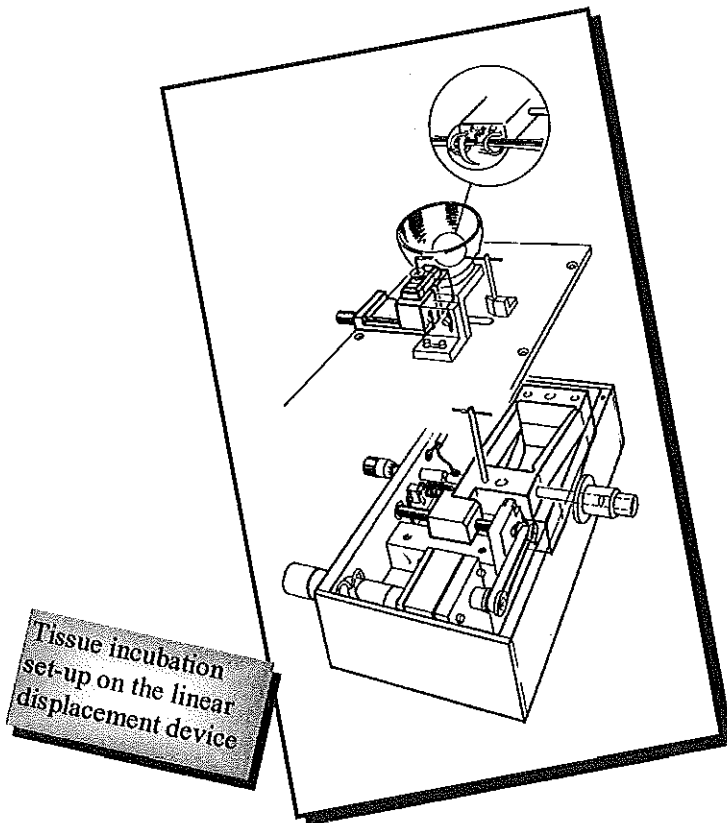
Gommert A. van Koeveringe and Ron van Mastrigt

Summary

The maximum shortening velocity v_{max} and the maximum isometric force were determined at different muscle lengths in small smooth muscle strips of the urinary bladder of the pig. Aim of the study was to determine if v_{max} depended on muscle length. Instead of the frequently used quick release technique, a "stop test" was applied: Linear shortening at different rates was imposed on the tissue during maximum activation until a preset muscle length was reached. A hyperbolic force-velocity relation (Hill curve) was fitted to the resulting force responses so that the maximum shortening velocity v_{max} at different muscle lengths could be estimated. With increasing muscle length v_{max} increased significantly from 0.23 to 0.40 strip lengths per second, in parallel with the well-known length dependent increase in isometric force. This phenomenon could be explained by either an up-regulation of cross-bridge cycling or a changed geometric orientation or contents of intracellular contractile proteins.

Introduction

The maximum shortening velocity of smooth muscle is variable (10, 18, 19, 22). It is thought to be directly dependent on the cross-bridge cycling rate (2, 13, 17). In smooth muscle this rate is regulated by the intracellular Ca^{++}, which forms a complex with calmodulin and then binds to myosin light chain kinase causing myosin light chain phosphorylation(1, 2, 12, 20, 30). Thin filament proteins can also affect the cross-bridge cycling rate (11). Calponin, one of the thin filament proteins, has a marked effect on contraction velocity by reducing the cross-bridge detachment rate (11, 13). Other studies indicate that new thick filaments are formed or activated when the length of the muscle is increased (4, 5, 21). All these mechanisms could result in changes in maximum isometric force, cross-bridge cycling rate and maximum contraction velocity.

Aim of our study was to determine the resulting length dependence of the maximum contraction velocity v_{max} of smooth muscle. Of all smooth muscle tissues, the detrusor muscle has the largest ability to adapt to length changes. The volume of the urinary bladder can be reduced 500-fold within one minute (23). This reflects a 7-fold change in bladder circumference. For this reason the smooth muscle of the urinary bladder is the primary choice for studying the length dependence of smooth muscle contractility. In previous studies (28) large whole thickness bladder strips were used. Consequently, connective tissue and orientation of the muscle bundles might have influenced the findings. The present study was done in very small strips of pig urinary bladder muscle tissue. In this way the effect of the series elasticity of the surrounding connective tissue

was avoided.

Two methods can be used to determine maximum shortening velocity: the quick release technique and the stop test. In the quick release technique a muscle strip is subjected to a series of preset after-loads during maximal stimulation at L_0 (the length at which maximum force is generated). An arbitrarily selected time after quickly releasing the tissue tension to a preset after-load, the velocity of shortening is measured. A disadvantage of this quick release technique is that measurements at different after-loads are taken at different lengths of the muscle. A length dependence of shortening velocity can thus not accurately be determined. Another disadvantage is that the quick release technique does not discriminate active and passive force components. Especially in urinary bladder tissue passive forces are very significant at longer lengths (6, 28).

In the stop-test method the force at a preset length is measured during linear shortening of the muscle. Passive force at this length is measured separately and subsequently subtracted. Using this technique maximum shortening velocity can be determined at high passive forces associated with longer lengths and at high velocities. A clinical equivalent of the stop-test has been used in urology: Urine flow during micturition was suddenly interrupted, while intra vesical pressure was measured (6). Apart from its physiological relevance, the present study is therefore also of interest for the interpretation of clinical urological data.

Materials and Methods

Tissue preparation.

Fresh pig urinary bladders were obtained from the local slaughterhouse. Smooth muscle micro-strips with a maximum diameter of 200μm and a length of 1 to 2 mm were cut from a standardized locus at the dorsal side of the bladder dome using a binocular microscope. Care was taken that the muscle fibers were running longitudinally in the preparation. The strips were prepared in modified aerated Krebs fluid and transported to the organ bath in a small container in order to prevent desiccation.

The modified Krebs solution contained: NaCl, 118 mM; KCl, 4.7 mM; $NaHCO_3$, 25 mM; KH_2PO_4, 1.2 mM; $CaCl_2$, 1.8 mM; $MgSO_4$ 1.2 mM; glucose, 11 mM; pH 7.4; aerated with 95% O_2 / 5% CO_2.

Incubation

The strips were incubated (Fig. 1, top sub-figure) in a 20 μl drop of modified Krebs fluid (with 95% O_2 / 5% CO_2 being blown over the drop's surface) which was continuously refreshed using a separate in- and outflow syringe pump (HOSPAL®) at a rate of 40μl / min (24). Two platinum ring
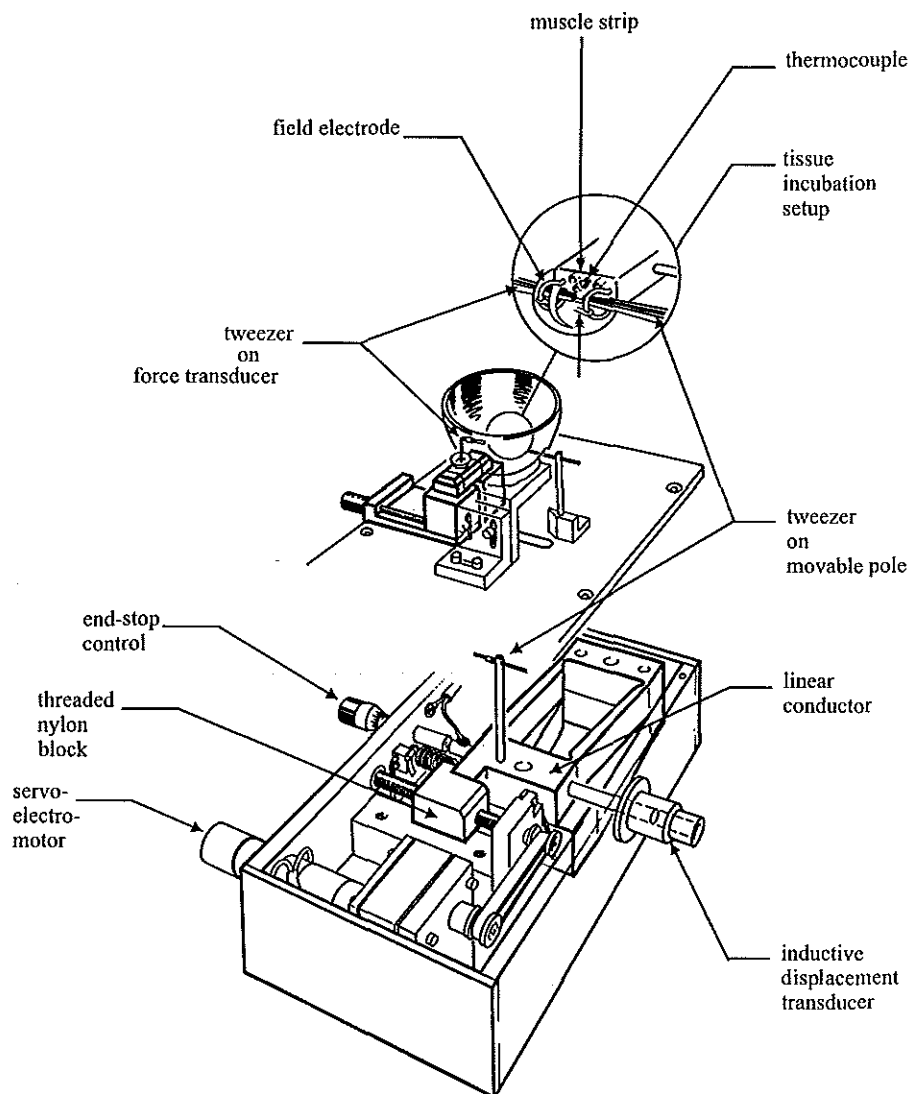
muscle strip

thermocouple

field electrode

tissue incubation setup

tweezer on force transducer

tweezer on movable pole

end-stop control

linear conductor

threaded nylon block

servo-electro-motor

inductive displacement transducer

Figure 1: (Top subfigure) Tissue incubation setup: A drop of 20µl Krebs fluid is supported by two platinum wire ring electrodes extending from a small perspex block. The Krebs fluid is continuously refreshed using an in- and an outflow syringe pump. The muscle preparation is positioned in the centre of the drop between two micro tweezers. The tissue incubation setup is placed in an elliptical reflector to allow heating by an infrared halogen lamp. One tweezer is connected to a linear conductor which is driven by a servo-electro-motor. The other tweezer is connected to a force transducer.

electrodes on either end of the drop were used for electrical stimulation. The drop remained in position through surface tension and was at the outer end stabilized by a glass rod mounted between the two electrodes. Temperature was kept at 37°C using infrared radiation from a halogen lamp (Philips®,12V,20W,6°,type 6483), controlled via a 200 μm diameter thermocouple (Omega®) in the drop. The strips were mounted between two tweezers, 400 μm diameter, one of which was attached to a KG3 force transducer connected to a BAM3 amplifier (Scientific instruments®, Heidelberg, FRG). The other tweezer was attached to a pole connected to the linear displacement device described below. In the drop the strips were exposed to electrical field stimuli: 100Hz, 4V alternating polarity 5ms pulses during 16 seconds.

Linear displacement device.

The movable tweezer was connected to a linear displacement conductor (Fig 1). The linear conductor was composed of two identical quadruple hinged nylon parallelograms. The conductor was connected to an inductive displacement transducer (MERA®), which measured the exact length of the strip. Using a spring, the conductor was pressed against a threaded nylon block which was driven by a servo-electro-motor via a gear-belt. When shortening was applied the conductor, containing pole and tweezer, moves at constant velocity until it was stopped by a preset end-stop. The displacement device was controlled using a Commodore® 386sx computer equipped with a PCL818 A/D and D/A converter card using modified multichannel data acquisition and measurement control software (MKR computer program: developed by the CDAI dept. Academic Hospital Rotterdam).

Measurement protocol.

The incubated strips were stretched to a "measurement length" 1.3 times the initial strip length, which was the in-situ length of an empty bladder. After a waiting interval of 10 minutes two electrical test stimuli were applied with a rest interval of 5 minutes. When a contraction smaller than 100 μN was recorded in response to either of the two test stimuli, the strip was considered to be in a poor condition and discarded. In 9 strips from 9 different bladders a subsequent measurement protocol was applied. In a preliminary study, it was found that transients in the linear displacement of the device did not extend beyond a start-up period of two seconds. Therefore each measurement protocol started with a pre-stretch at a rate of 10μm/s to a velocity dependent pre-shortening length, allowing a subsequent shortening duration of 2 seconds. After a waiting interval of 5 minutes, the strip was linearly shortened for two seconds without stimulation to measure the passive force response. Next the strip was again slowly (at a rate of 10μm/s) stretched to the pre-shortening length. After a waiting interval of 1 minute, field stimulation was applied for a total duration of

Figure 2: An example of the measured signals. The top trace shows the measured force, the bar in the middle trace represents the electrical field stimulus and the lower trace shows the length of the tissue preparation. $F_{r.active}$ and $F_{r.passive}$, as indicated in the figure are approximate values of the fitted variables: $F_{rec.active}$ and $F_{rec.passive}$
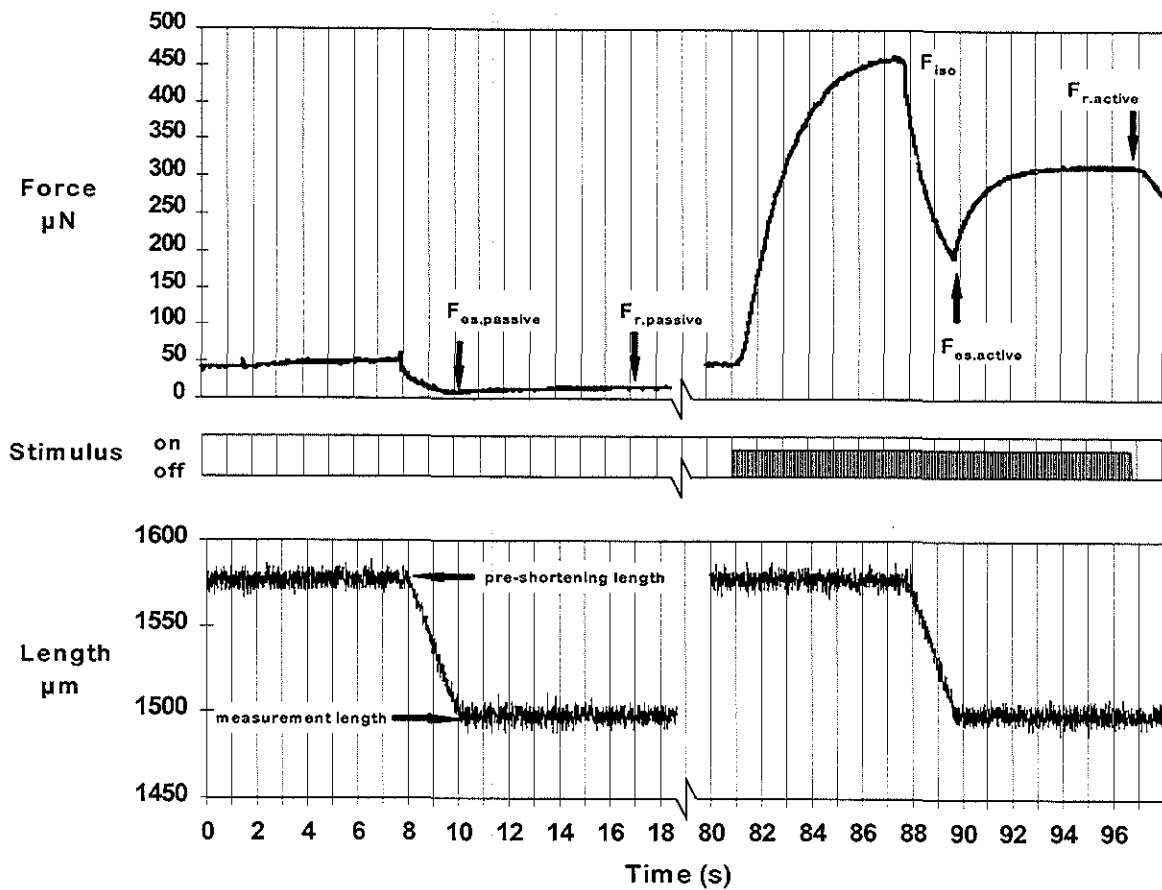
6 seconds. After 7 seconds of stimulation, during which a maximum contraction force was reached, linear shortening was applied for 2 seconds, ending at the end-stop. Stimulation continued for another 7 seconds. The described measurement protocol was repeated at another shortening velocity after a waiting period of 5 minutes. After testing five different shortening velocities, i.e., 10, 20, 40, 100 and 250 µm/s, the whole sequence was repeated at a higher measurement length (Fig. 2) following a waiting interval of 10 minutes. A total of four different measurement lengths, i.e., 1.3, 1.6, 1.9 and 2.2 times the initial strip length were tested. The measured force, binary stimulus signal, and the displacement signal (see Fig. 2) were sampled with a Commodore® 386sx computer equipped with a PCL818 A/D converter card using multi-channel data acquisition sftware (MKR: developed by the CDAI dept. Academic Hospital Rotterdam).

Data processing.

Data were processed in MATLAB®. At all preset velocities the actual shortening velocity just before reaching the end-stop was calculated from the displacement transducer output. The maximum isometric force (F_{iso}), before application of shortening, was determined at each pre-shortening length. In each strip, F_{iso} was normalized by dividing by the F_{iso} value at the first contraction in the measurement protocol i.e. excluding the two contractions after the test stimuli. The pre-shortening length was determined from the displacement signal and normalized by dividing by the initial strip length.

As a consequence of the different pre-shortening lengths necessary to allow a constant shortening duration of two seconds at different velocities, F_{iso} values were measured at a spectrum of different lengths. For this reason a mean F_{iso} value was calculated for 6 different length categories between 1 and 2.7 times initial strip length. To derive a force velocity relation from the measured force signals (see Fig. 4), the following procedure was applied. The force measured when shortening during stimulation stopped at the end-stop ($F_{es.active}$, see Fig. 2) and the force after recovery ($F_{rec.active}$, see Fig. 2) were corrected for changes in the passive force. This was done by subtracting the forces measured at the same instants during the passive shortening sequence ($F_{es.passive}$ and $F_{rec.passive}$, see Fig. 2). The quotient of these corrected force values was called the relative force f_{rel}. These relative force values were plotted as a function of the applied shortening velocity.

Artefacts in the measured force signals leading to outlier values were re-analysed manually and corrected if possible. For every strip, 4 different sets (at different strip lengths) with each 5 different force velocity data points were processed separately.

The hyperbolic Hill force-velocity relation (14) was rewritten in the following form:

$$f_{rel} = f_{rel\,0} * a/f_0 * (v_{max} - v) / (v + a/f_0 * v_{max})$$

where $f_{rel\,0} = f_{rel}$ at zero shortening which is not a force , as in the original Hill equation, but a dimensionless relative force, a/f_0 is a measure for the concavity of the force-velocity curve, v is shortening velocity and v_{max} is extrapolated maximum shortening velocity at zero relative force. This equation was fitted to the measured force-velocity data by adapting the three parameters $f_{rel\,0}$, a/f_0 and v_{max} using a least squares fitting method (27)

In addition to the curve fitting with 3 variable parameters, curve fitting was
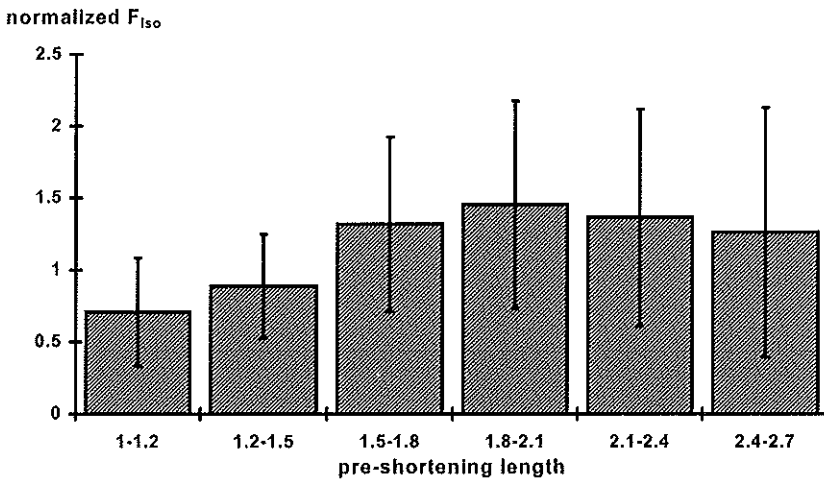
normalized F$_{Iso}$

Figure 3: Normalized F_{iso} as a function of normalized pre-shortening strip length. Both values were normalized by dividing by the appropriate value at the start of the experiment.

performed using a modified equation with only 2 variable parameters, where $f_{rel\,0} = 1$, and an equation with only one variable parameter, where $f_{rel\,0}$ was locked at 1 and a/f_0 at 0.25. The "sum of squares"(S_{sq}) values resulting from fitting equations with 1, 2 and 3 variable parameters to each data set were normalized by dividing by the S_{sq} value found by fitting the one parameter equation. The mean S_{sq} values were plotted as a function of the number of parameters fitted.

A 1 parameter fitting was performed 19 times using a fixed $f_{rel\,0} = 1$ and 19 different a/f_0 values between 0.05 and 0.45 with regular intervals. Mean S_{sq} of all data sets normalized to the S_{sq} value at = 0.25 was plotted as a function of a/f_0 and the minimum mean S_{sq} was determined. Similar plots of the mean S_{sq} value as a function of a/f_0 were made for each of the four different measurement lengths used. Using this technique an optimum a/f_0 was determined for each measurement length. The Hill equation was fitted again with only one variable

parameter (v_{max}) and a locked a/f_0 value optimized for the appropriate measurement length. The significance of muscle length as a source of variance in v_{max} and a/f_0 was tested using a one-way analysis of variance (using SPSS statistical analysis software). The mutual differences between parameters measured at different strip lengths were tested using the Mann-Whitney U test.

Results

Figure 2 shows an example of the signals measured in one measurement. It can be seen that the maximum isometric force F_{iso} was reached before shortening was applied. The mean F_{iso} value in all strips was 574 µN. As the maximum strip diameter was 200 µm, the strips generated a mean stress of at least 1.8 N/cm². It
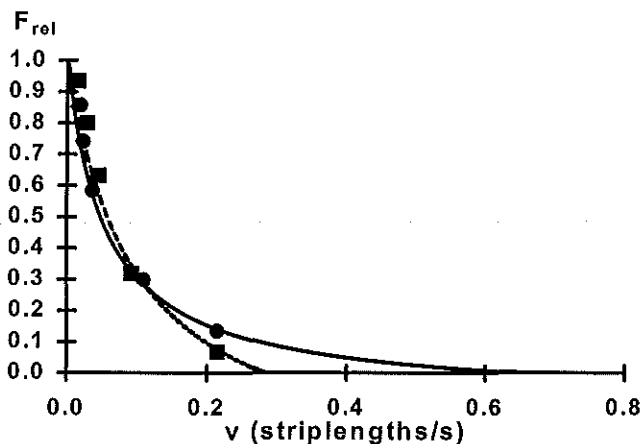

Figure 4: An example of two force-velocity data sets at different measurement lengths in one strip.

can be seen in the bottom trace that shortening was linear. When the shortening stopped a minimum force level F_{es} was reached, subsequently force rerose to a new maximum level F_{rec}. Figure 3 shows the mean F_{iso} values in six different length categories. A maximum normalized F_{iso} was found at a normalized strip lenght between 1.8 and 2.1. The large standard errors of the mean at longer striplengths indicate the increasing variability of F_{iso} with length.

An example of two measured force-velocity data sets and the fitted force-velocity curves is shown in Figure 4.

Figure 5 shows that, as was expected, the normalized sums of squares (S_{sq}) values decreased with the number of parameters that was fitted. Figure 6 shows a Box plot of v_{max} values as a function of the number of parameters fitted. It is
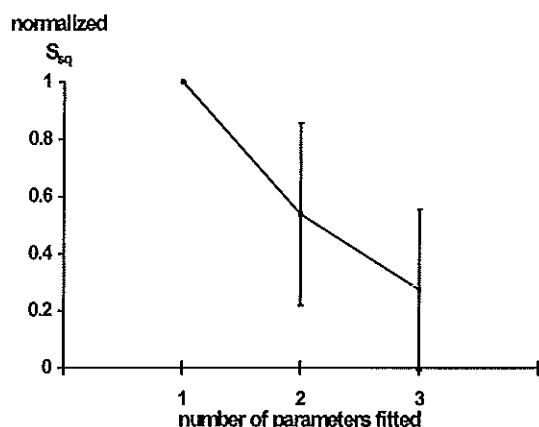
Figure 5: Mean ± standard deviation of the normalized sum of squares S_{sq} as a function of the number of parameters in the force-velocity equation that was fitted. S_{sq} values were normalized by dividing by the values resulting from fitting a one parameter equation.

obvious that when an equation with 2 (a/f_0 and v_{max}) or 3 parameters ($f_{rel\ 0}$, a/f_0 and v_{max}) was fitted, the variability in v_{max} increased ramatically.

Figure 7 indicates that the best fit with the smallest S_{sq} value occurred at decreasing a/f_0 values when strip length increased. In a subsequent one parameter (v_{max}) fitting procedure a/f_0 values were tuned to the strip length according to the minima found in Figure 7. a/f_0 was set to 0.25 , 0.2 , 0.2 and 0.15 for the measurement lengths 1.3 , 1.6 , 1.9 and 2.2. This procedure resulted in v_{max} values that were significantly more reproducible, compare error bars in Fig. 8 and Fig. 6, note the different scales! The average v_{max} values were now found to increase significantly with increasing strip length as shown in the figure. Analysis of variance showed that strip measurement length was a a significant source of variance in v_{max} ($p<0.005$). A significant difference was found between v_{max} values at measurement lengths of 1.3 and 1.6 ($p<0.05$), at lengths of 1.3 and 1.9 ($p<0.05$) and between v_{max} values at lengths 1.3 and 2.2 ($p<0.01$).
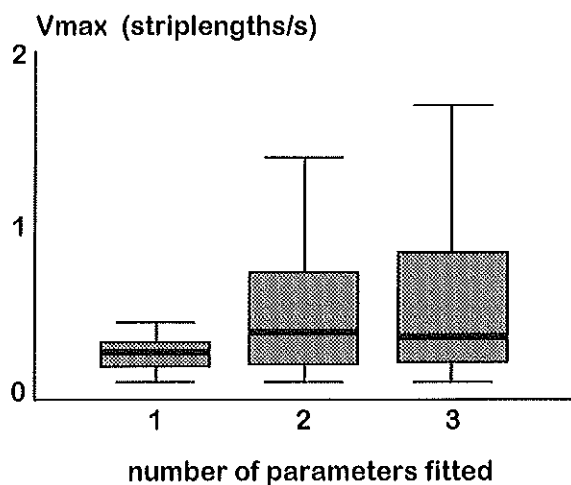

Figure 6: A Boxplot which represents the values of v_{max} as a function of the number of parameters in the force velocity equation that was fitted. Values in the box are between the 25th and 75th percentile. The error bars indicate cases that range within 1.5 box length from either edge of the box.
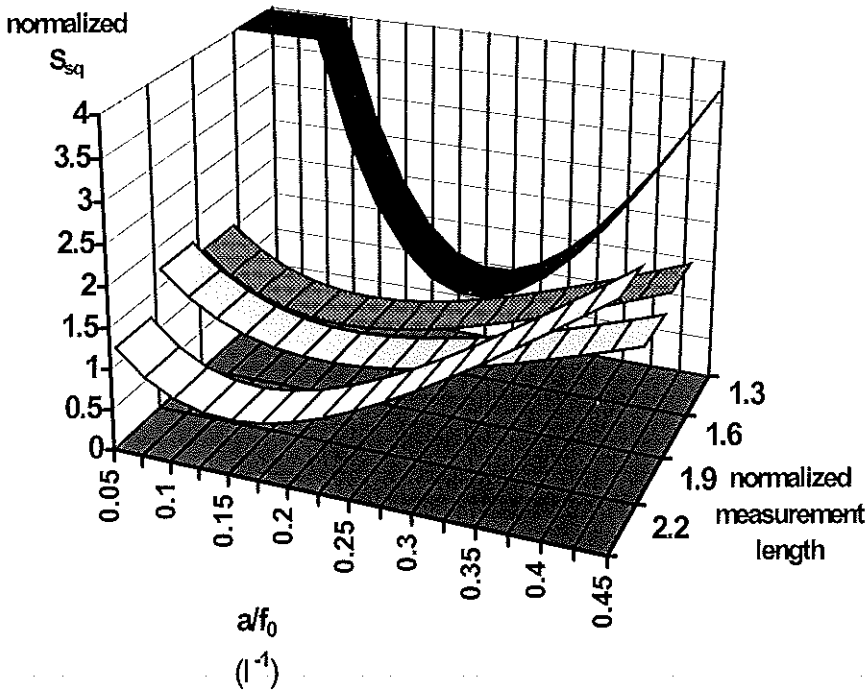
Figure 7: Mean normalized sum of squares (S_{sq}) resulting from repeatedly fitting of a force-velocity equation with one (v_{max}) variable parameter and different locked a/f_0 values. S_{sq} values in the y direction are plotted as a function of the a/f_0 values in the x direction at the 4 different measurement lengths represented in the z direction.

Discussion

In smooth muscle, maximum shortening velocity can be determined by either the quick release technique or the stop test. Using the quick release technique it is not possible to correct for changes in passive force. With increasing length, passive force can reach values that equal or even exceed the active force in urinary bladder tissue (28). Furthermore, in the quick release technique tension is released to several different after loads during a sustained contraction. In order to apply different after-loads, the amplitude of the release has to be adapted, which results in measurements at different lengths to be used in one force-velocity relation. Both problems make it impossible to use the quick release technique to study the length dependence of maximum shortening velocity in smooth muscle.

The stop test was used in our measurements to determine the maximum

shortening velocity value from sets of measurements during shortening at different velocities to one pre-set measurement length. Additionally the stop test allowed to eliminate passive contributions to the measured force. The same shortening protocol was applied with and without stimulation, which allowed subtraction of passive from total force. A disadvantage of the stop test was that shortening had to be applied for at least 2 seconds. This implied that muscle strips had to be pre-stretched to long pre-shortening lengths, sometimes well above L_0 , when higher shortening velocities were applied. Theoretically, damage of the tissue at such long lengths is possible. In order to estimate this possible damage, several strips were stretched to 3 times initial length, after completion of the measurements. This resulted in an increase of passive force well beyond the active force, but only in a slight decrease in active force, indicating that not much damage had been done to the tissue in the used length range.

In order to perform the stop test measurements, a device, illustrated in Figure 1, was designed. Using this device, linear shortening could be applied to one end of a small smooth muscle strip, while on the other end instantaneous force was measured. The shortening was applied during maximal electrical field stimulation (Fig. 2). Previous research from our group has shown that reliable estimates of the maximum shortening velocity v_{max} of a smooth muscle
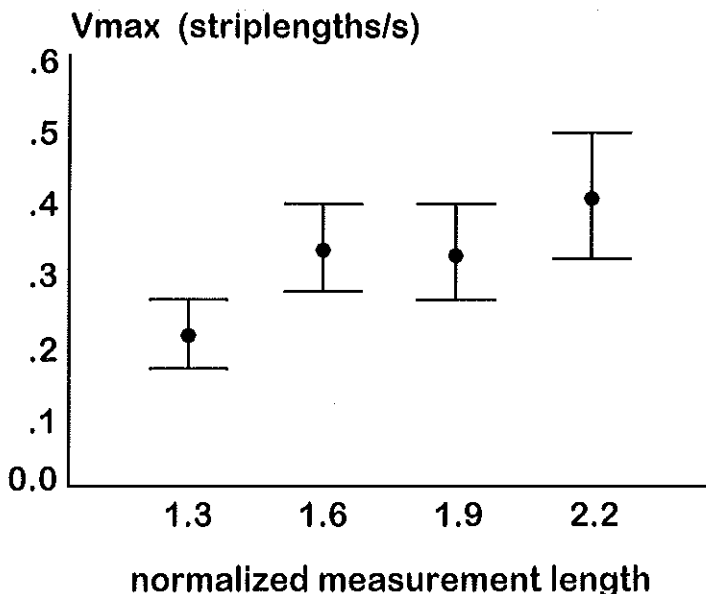

Figure 8: Mean ± standard error of the mean of maximum shortening velocity v_{max} as a function of the measurement length of the muscle strip. Results obtained by fitting a force-velocity relation with only one variable parameter (v_{max}) and a/f_0 values corrected for differences in measurement length.

preparation can be derived from such a measurement (29). It was also shown previously, that electrical field stimulation with the described parameters stimulated the muscle maximally (24,26). Recently Gunst *et al.* (10) showed a difference in v_{max} values measured during phasic and tonic contractions. Shortening velocity was reduced in sustained contractions. In our study phasic contractions were studied because these are most relevant for the physiological function of the urinary bladder.

The estimated maximum active stress of 1.8 N/cm^2 in strips with a diameter of 200 μm is low compared to values of 12.5 N/cm^2 measured in rabbit urinary bladder (23). Apart from a difference in species, this can be explained by the preparation technique of the very small strips. It is likely that only part of the muscle bundles in a fibre are mechanically attached to the tweezers at both ends and generate measurable force. Other bundles may have been cross-sectioned or damaged at the perimeter of the bundle. To enable comparison of different strips, F_{iso} values were normalized to those measured in response to a standard test stimulus at the beginning of the measurement protocol.

The F_{iso} values that were measured before shortening was applied confirm the length dependence of force development in this smooth muscle preparation (28). Although the measurement protocol was far from optimal for studying this length dependence, which is reflected in the large standard errors in Figure 3, a similar curve is seen as in a previous study performed on full thickness bladder wall strips (28). The maximum isometric force is found at approximately twice the measurement length. At this optimum length L_0 large passive forces corrupt the measurements of active isometric forces by causing a continuous lengthening of the contractile element. These large passive forces are the main cause of the large standard errors in Figure 3.

In the measurement protocol the measurements were sequenced in such a way that the length of the strips generally increased, except for some relatively small shortening velocities. Had measurements at longer muscle lengths been done first, much longer incubation times would have been necessary to allow the preparation to adapt to the shorter muscle lengths by a relatively slow passive muscle shortening. These long incubation times would probably have affected the condition and viability of the preparations, resulting in less reliable measurements.

In previous studies it was shown that the duration of shortening greatly influenced the rate and amplitude of force re-development, which was ascribed to shortening deactivation (7,8,10,19). Therefore a small pilot study was conducted in which different shortening velocities were applied to the preparation for different durations of time. The normalized force f_{rel} decreased with time during the first second of shortening. For all shortening velocities, f_{rel} reached a plateau after 2 seconds of imposed shortening, indicating a state of mechanical equilibrium. Therefore a fixed shortening time of 2 seconds was chosen for the main study and strips were pre-stretched to a length that allowed

exactly 2 seconds of shortening before the end-stop was reached. The observed shortening time dependence is apparently, in contrast to the theory suggested by Gunst *et al.* (10), not dependent on the magnitude of the length change but merely on the duration of shortening. This could be due to the presence of latch bridges at maximal activation which need a long detachment time (3,19)

The force velocity data were described with a hyperbolic (Hill) equation with 2 variable parameters one representing the horizontal intercept v_{max} , and one representing the curvature of the equation a/f_0; the vertical intercept of the equation equaled one, as force readings were normalized. When both parameters were optimized simultaneously, v_{max} was often grossly overestimated, as can be seen in Figure 6. Therefore a stepwise approximation method was used. For 17 different a/f_0 values the mean sum of squares S_{sq} for each striplength was determined and presented graphically. A clear minimum in the S_{sq} value was found as shown in Figure 7. This minimum decreased with increasing muscle length. Minimum S_{sq} at 1.6 times measurement length was 0.175, at 1.9 times measurement length was 0.2, at 1.3 times measurement length was 0.25 and at 2.2 times measurement length 0.15, which suggests a linear dependence of a/f_0 on muscle length. The confidence interval of a/f_0 was at least $\pm$ 0.05. Subsequently, maximum contraction velocity values were determined by fitting an equation with only one variable parameter, v_{max}, while the a/f_0 value in the equation was fixed at 0.25 , 0.2 , 0.2 and 0.15 for measurement lengths of 1.3 , 1.6 , 1.9 and 2.2 respectively. This procedure resulted in reproducible v_{max} values, that significantly increased with increasing muscle length.

An increase in shortening velocity with increasing muscle length can either result from an up-regulation of the cross-bridge cycling or from a changed cell or tissue geometry. An up-regulation of cross-bridge cycling could be caused by an increase in intracellular calcium and a concomittant higher phosphorylation rate of myosin light chain kinase (9,16). This increased intracellular calcium concentration in turn could result from (additional) opening of calcium channels (15) or stretching of the sarcoplasmic reticulum inducing more release of intracellular calcium. An up-regulation of the cross-bridge cycling rate could also result from changing of contents or orientation of a thin filament regulatory protein as for example calponin (11).

Alternatively, the length induced increase in maximum shortening velocity could be caused by changes in cell or tissue geometry. Lengthening results in a change in cell shape from round to more oblong. In a more oblong cell contractile elements, the cross-bridges are more oriented in the direction in which force is generated. This results in a faster rate of shortening velocity and a higher amplitude of the force generated. A possible decrease of v_{max} at lengths beyond L_0, analogous to F_{iso} could not be detected yet in the used length range .

Ford *et al.* (4) introduced the concept of a series to parallel transition of cross-bridges during sustained contraction. Analogously a parallel to series conversion of cross-bridges during muscle lengthening could explain the

demonstrated increase in v_{max}. One would expect that less isometric force would be generated if more cross-bridges act in series. Therefore the fact that in the same length range F_{iso} also increases conflicts with this hypothesis. Rather this finding supports the earlier proposed hypothesis (4,5) that additional myosin is incorporated in the thick filaments during activation at increasing muscle lengths. In addition to cell plasticity changes altered tissue plasticity could contribute to a parallel to series transition of the contractile elements with muscle lengthening. If this were the case new extracellular links would have to be broken and made during lengthening of the tissue in order to allow movement of cells from a parallel to a series organization. Uvelius (23) however has shown that tissue length and cell length are proportional in the urinary bladder, so that the latter hypothesis must be rejected for this kind of tissue.

It is concluded that for measuring the maximum contraction velocity of smooth muscle, the used stop test has several advantages over the more frequently used quick-release technique. Using the stop test, passive force changes during shortening can be eliminated. Moreover the stop test allows force measurements at a range of velocities at the same muscle length, which enables investigation of the length dependency of the maximum shortening velocity. The presented data show that maximum shortening velocity increases with increasing stretched muscle length. The mechanism involved is not clear yet but either an up-regulation of cross-bridge cycling or a changed orientation or contents of intracellular contractile proteins are the most feasible causes of this effect.

References

1. **Arner, A. and Hellstrand, P.** (1983) Activation of contraction and ATPase Activity in Intact and Chemically Skinned Smooth Muscle of Rat Portal Vein. *Circ. Res.* 53: 695-702 .

2. **Barany, M.** (1967) ATPase Activity of Myosin Correlated with Speed of Muscle Shortening. *J. of Gen. Physiol.* 50(part 2): 197-218.

3. **Dillon, P.F., Aksoy, M.O., Driska, S.P. and Murphy, R.A.** (1981) Myosin Phosphorylation and the Cross-Bridge Cycle in Arterial Smooth Muscle. *Science.* 211: 495-497.

4. **Ford, L.E., Seow, C.Y. and Pratusevich, V.R.** (1994) Plasticity in smooth muscle, a hypothesis. *Can. J. of Physiol. and Pharmacol.* 72: 1320-1324 .

5. **Gillis, J.M., Cao, M.L. and Godfraid-de Becker, A.** (1988) Density of myosin filaments in the rat anococcygeus muscle, at rest and in contraction. II *J. Muscle Res. Cell Motil.* 9: 18-28 .

6. **Griffiths, D.J., van Mastrigt, R., van Duyl, W.A. and Coolsaet, B.L.R.A.** (1979) Active mechanical properties of the smooth muscle of the urinary bladder. *Med. Biol. Eng. Comput.* 17: 281-290 .

7. **Groen, J.** Functional modelling of voiding. (1996) *Thesis: Erasmus University Rotterdam, The Netherlands.* April 17 .

8. **Gunst, S.J.** Effect of length history on contractile behaviour of canine tracheal smooth muscle. (1986) *Am. J. Physiol.* 250: C146-C154.

9. Gunst, S.J. (1989) Effects of muscle lengths and load on intracellular Ca^{2+} in tracheal smooth muscle. *Am. J. Physiol.* 256: C807-C812 .

10. Gunst, S.J., Wu, M.F. and Smith, D.D. (1993) Contraction history modulates isotonic shortening velocity in smooth muscle. *Am. J. Physiol.* 265: C467-C476.

11. Haeberle, J.R. and Hemric, M.E. (1994) A model for the coregulation of smooth muscle actomyosin by caldesmon, calponin, tropomyosin, and the myosin regulatory light chain. *Can. J. of Physiol. and Pharmacol.* 72: 1400-1409 .

12. Hai, C.M. and Murphy, R.A. (1989) Ca^{2+}, crossbridge phosphorylation, and contraction. *Annu. Rev. Physiol.* 51: 285-298.

13. Hellstrand, P. (1994) Cross-bridge kinetics and shortening in smooth muscle. *Can. J. of Physiol. and Pharmacol.* 72: 1334-1337.

14. Hill, A.V. (1938) The heat of shortening and the dynamic constants of muscle. *Proc. Roy. Soc. London B.* 126: 136-195.

15. Himpens, B. and Somlyo, A.P. (1988) Free-Calcium and force transients during depolarization and pharmacomechanical coupling in Guinea-pig smooth muscle. *J. Physiol.* (London) 395, 507-530.

16. Kasai, Y., Tsutsumi, O., Taketani, Y., Endo, N. and Iino, M. (1985) Stretch-induced enhancement of contractions in uterine smooth muscle of rats. *J. Physiol. (London)* 486.2: 373-384.

17. Klemt, P. and Peiper, U. (1978) The dynamics of Cross-Bridge Movement in Vascular Smooth Muscle Estimated from a Single Isometric Contraction of the Portal Vein: The Influence of Temperature and Calcium. *Pfluegers Arch.* 378: 31-36.

18. Krisanda, J.M. and Paul, R.J. (1988) Dependence of force, velocity, and O_2 consumption on $[Ca^{2+}]_o$ in porcine carotid artery. *Am. J. Physiol.* 255: C391-C400.

19. Meiss, R.A. (1993) Persistent mechanical effects of decreasing length during isometric contraction of ovarian ligament smooth muscle. *J. Muscle Res. Cell Motil.* 14: 205-218.

20. Peiper, U. and Dee, J. (1994) Smooth muscle contraction kinetics at different calcium concentrations. *Can. J. of Physiol. and Pharmacol.* 72: 1338-1344.

21. Schoenberg, C.F. and Needham, D.M. (1976) A study of the mechanism of contraction in vertebrate smooth muscle. *Biol. Rev.* 51: 53-104.

22. Stephens, N.L. (1994) Smooth muscle contraction: Recent Advances. *Can. J. of Physiol. and Pharmacol.* 72: 1317-1319.

23. Uvelius, B. (1976) Isometric and isotonic length-tension relations and variations in cell length in longitudinal smooth muscle from rabbit urinary bladder. *Acta Physiol. Scand.* 97: 1-12.

24. Van Koeveringe, G.A. and Van Mastrigt, R. (1991) Excitatory pathways in smooth muscle investigated by phase plot analysis of isometric force development. *Am. J. Physiol.* 261: R138-R144.

25. Van Koeveringe, G.A. and Van Mastrigt, R. (1994) Photolysis of caged calcium using a low cost flash unit: efficacy analysis with a calcium selective electrode. *Cell Calcium* 15, 423-430.

26. Van Koeveringe, G.A. and Van Mastrigt, R. (1996) Ultra-violet light induces calcium release from intracellular stores in urinary bladder smooth muscle. *Submitted.*

27. Van Mastrigt, R. (1980) Fitting the Hill equation to experimental data. *IEEE trans. biomed. eng.* Vol. BME-27, NO 7: 413-416.

28. Van Mastrigt, R. (1988) The length dependence of the series elasticity of pig bladder smooth muscle. *J. Muscle Res. Cell Motil.* 9: 525-532.

29. Van Mastrigt, R. and Glerum, J.J. (1985) Electrical stimulation of smooth muscle strips from the urinary bladder of the pig. *J. of Biomed. Eng.* 7: 2-8.

30. **Warshaw, D.M., Work, S.S. and McBride, W.J.** (1987)   Effect of low extracellular Calcium on shortening velocity in isolated single smooth muscle cells. *Pfluegers Arch.* 410: 185-191.

CHAPTER 8

Time constants of isometric force development in smooth muscle fibers of the urinary bladder.

Time constants in stretched and shortenened muscle cells ....
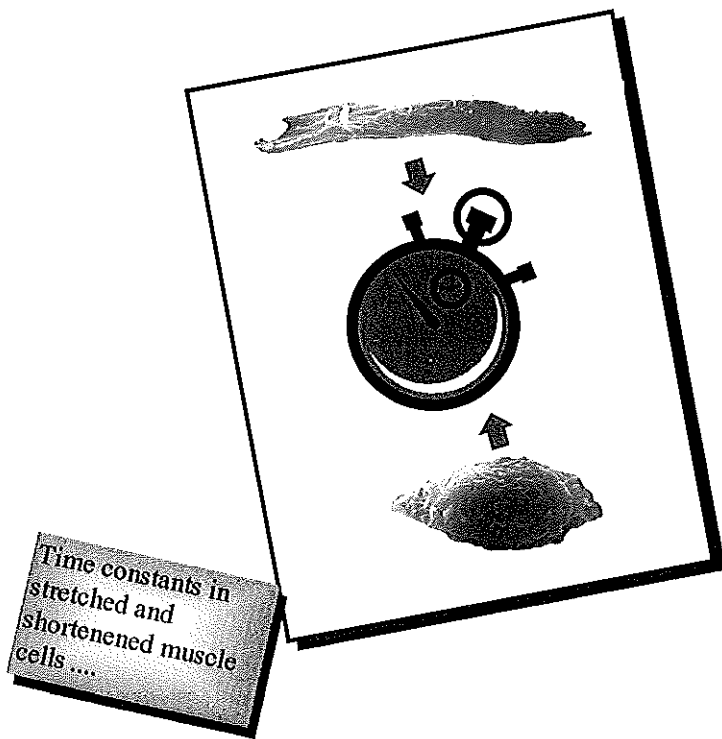
Gommert A. van Koeveringe and Ron van Mastrigt

Summary

        Time constants of isometric force development before and after shortening and maximum shortening velocity v_{max}, indicative of cross-bridge cycling rate, were determined in small strips of pig urinary bladder. v_{max} was measured using the stop test in which linear shortening at different rates was applied until an end stop was reached where force was measured during maximal electrical field stimulation. The time constant of isometric force development before shortening is independent of the cross-bridge cycling rate and of muscle length, indicating a rate limitation by e.g. influx of extracellular calcium. After linear shortening, isometric force (re-)develops faster than before, at a rate that can be defined by a fast and a slow time constant. It is proposed that the fast time constant represents the cross-bridge cycling rate, as directly after shortening the intracellular $[Ca^{++}]$ is still high. The slow component of the recovery contraction is either determined by influx of extracellular calcium, analogous to the time constant before shortening, or by re-attachment of slow-cycling "latch" bridges. A high post-shortening $[Ca^{++}]$, leading to a negative feedback of calcium influx channels and a reduced calcium contribution from intracellular stores could result in a force recovery to submaximal levels and so explain shortening induced deactivation.

Introduction

        A smooth muscle preparation that is supra maximally stimulated develops isometric force at a well defined rate, that can be expressed in terms of a single time constant. There is no consensus on the origin of the underlying mechanism in the literature. Frequently the time constant of isometric force development is related to the series elasticity and the maximum contraction velocity v_{max} (11,12,19) of the preparation. Previous research in our group however indicated that lengthening of the series elasticity at the maximum velocity would lead to force development at a very high rate, that is never measured under physiological circumstances (15, Chapter 2). On the basis of measurements in the presence of various stimulatory and inhibitory substances, it was hypothesized that the normal rate of isometric force development in smooth muscle depends on the influx of extracellular calcium.
        In another previous study (Chapter7) the length dependence of the maximum shortening velocity v_{max} of small bladder muscle strips was studied at different muscle lengths. To this end, analogous to earlier studies by van Mastrigt and Glerum (18), linear shortenings were applied at different rates during maximal stimulation of the preparation while force was measured. In the present study the time constant of isometric force development and v_{max} were

directly compared to investigate underlying mechanisms. Additionally time constants before and shortly after shortening were compared. This comparison gained more insight in shortening induced deactivation, which was earlier described by Meiss (13), Gunst (6) Gunst et.al.(7) and Groen (5).

Methods

Tissue preparation

Fresh pig urinary bladders were obtained from the local slaughterhouse. Smooth muscle micro-strips with a maximum diameter of 200μm and a length of 1 to 2 mm were cut from a standardized locus at the dorsal side of the bladder dome using a binocular microscope. Care was taken that the muscle fibres were running longitudinally in the preparation. The strips were prepared in modified aerated Krebs fluid and transported to the organ bath in a small container in order to prevent desiccation.

The modified Krebs solution contained: NaCl, 118 mM; KCl, 4.7 mM; NaHCO$_3$, 25 mM; KH$_2$PO$_4$, 1.2 mM; CaCl$_2$, 1.8 mM; MgSO$_4$ 1.2 mM; glucose, 11 mM; pH 7.4; aerated with 95% O$_2$ / 5% CO$_2$.

Incubation.

The strips were incubated at 37 °C in a 20 μl set-up shown in Chapter7: Figure 1 and described in more detail in a previous publication (Chapter 7). The strips were mounted between two tweezers, one of which was attached to a KG3 force transducer connected to a BAM3 amplifier (Scientific instruments®, Heidelberg, FRG). The other tweezer was attached to a pole connected to the linear displacement device described below. In the organ bath the strips were exposed to electrical field stimuli: 100Hz, 4V alternating polarity 5ms pulses during 16 seconds.

Linear displacement device.

A displacement device previously described by Van Koeveringe and Van Mastrigt (Chapter 7) was used. The movable tweezer was connected to a linear displacement conductor (Chapter7:Fig 1) with an inductive displacement trans- ducer (MERA®). The conductor was pressed against a threaded nylon block which was driven by a servo electro-motor. When shortening was applied the conductor, containing pole and tweezer, moved at constant velocity until it stopped at a pre-set end-stop. The displacement device was controlled using a computer with multichannel data acquisition and measurement control software

(MKR computer program: developed by the CDAI dept. Academic Hospital Rotterdam).

Measurement protocol.

The incubated strips were stretched to a "measurement length" 1.3 times the initial strip length which was the in-situ length of an empty bladder. After a waiting interval of 10 minutes two electrical test stimuli were applied with a rest interval of 5 minutes. When a contraction smaller than 100 μN was recorded in response to either of the two test stimuli, the strip was considered to be in a too bad condition and discarded. In 9 strips from 9 different bladders a subsequent measurement protocol was applied. Each measurement protocol started with a pre-stretch at a rate of 10μm/s to a velocity dependent pre-shortening length, allowing a subsequent shortening during 2 seconds, which ended at exactly the measurement length (Chapter 7). After a waiting interval of 5 minutes, the strip was linearly shortened for two seconds without stimulation to measure the passive force response. Next the strip was again slowly (at a rate of 10μm/s) stretched to the pre-shortening length. Afer a waiting interval of 1 minute, field stimulation was applied for a total duration of 16 seconds. After 7 seconds of stimulation, during which interval force reached a maximum, linear shortening was applied for 2 seconds, ending at the measurement length. Stimulation continued for another 7 seconds. The described measurement protocol was repeated at another shortening velocity after a waiting period of 5 minutes. After testing five different shortening velocities i.e. 10, 20, 40, 100 and 250 μm/s, the whole sequence was repeated at a higher measurement length following a waiting interval of 10 minutes. A total of four different measurement lengths i.e. 1.3, 1.6, 1.9 and 2.2 times the initial strip length were tested, resulting in 9x5x4=180 measurements. The measured force signal, a binary stimulus signal, and the displacement signal (see Chapter7:Fig. 2) were recorded digitally.

Data processing

Data were processed using MATLAB®. To the isometric contractions that were measured before shortening was applied a mono exponential curve of the following form was fitted:

$$F = F_{iso} [1 - \exp(-t/C_{iso})] \qquad \text{Eq.1}$$

where: F = measured force
           t = time
           F_{iso} = maximum extrapolated isometric force
           C_{iso} = time constant

At all pre-set velocities the actual shortening velocity just before reaching

the end-stop was calculated from the displacement transducer output. Pre-shortening length was determined from the displacement signal and normalized by dividing by the initial strip length. At each pre-shortening length the maximum extrapolated isometric force (F_{iso}, see Chapter7:Fig.2), before application of shortening was determined and normalized by dividing by the F_{iso} value at the first contraction in the measurement protocol i.e. excluding the two test contractions. As a consequence of the different pre-shortening lengths necessary to allow a constant shortening duration of two seconds at different velocities, F_{iso} values were thus measured at a spectrum of different lengths.

To derive a force velocity relation from the measured force signals, the following procedure was applied. The force measured when shortening during stimulation stopped at the end-stop ($F_{es.active}$, see Chapter7:Fig. 2) and the force after recovery ($F_{rec.active}$, see Chapter7:Fig. 2) were corrected for changes in the passive force. This was done by subtracting the forces measured at the same instants during the passive shortening sequence ($F_{es.passive}$ and $F_{rec.passive}$,see Chapter7:Fig. 2). The quotient of these corrected force values was called the relative force f_{rel}. The relative force values were plotted as a function of the applied shortening velocity. Artefacts in the measured force signals leading to outlier values were re-analysed manually and corrected if possible. For each of the 9 strips, 4 different sets (at different strip lengths) with each 5 different force velocity data points were processed separately. One set of 5 measurements and 5 single measurements had to be excluded from further processing because due to problems with either stimulation or displacer, resulting in 170 valid measurements out of 180.

Equation 1 was also fitted to the isometric force recovery immediately following the linear shortening (90<t<96 s in Chapter7:Fig. 2). The resulting parameters were called F_{rec}, the maximum extrapolated isometric force after recovery and C_{rec}, the time constant for isometric force development during recovery. Measurements with values for F_{rec} smaller than 10μN or larger than 1.5 * F_{iso} were excluded from further processing. F_{rec} and C_{rec} could thus be determined for subgroup of 161 out of the 180 measurements. Note: F_{iso} and the F_{rec} values were not read from the traces as shown in Chapter7:figure 2 but determined by curve fitting of eq. 1.

As it appeared that the force development during the recovery period consisted of an early fast force development and a later slower force development to a saturation level a dual exponential curve:

$$F = F_{rec1} [1 - \exp(-t/C_{rec1})] + F_{rec2} [1 - \exp(-t/C_{rec2})] \qquad \text{Eq.2}$$

was also fitted to the data. Again, outliers where F_{rec1} or F_{rec2} were smaller than 10μN or larger than 1.5 * F_{iso} or where either C_{rec1} or C_{rec2} were < 0 or larger than 21 s (3 times the measurement duration) were excluded from further processing. F_{rec1}, F_{rec2}, C_{rec1} and C_{rec2} could thus be determined for a subgroup of

126 out of the 180 measurements.

In order to determine v_{AX} for the 9 different strips at the 4 different measurement lengths, the hyperbolic Hill force-velocity relation (9) was rewritten in the following form (16):

$$f_{rel} = a/f_0 * (v_{max} - v) / (v + a/f_0 * v_{max}) \hspace{3cm} \text{Eq.3}$$

where f_{rel} is not a force, as in the original Hill equation, but a dimensionless relative force, a/f_0 is a measure for the concavity of the force-velocity relation, v is shortening velocity and v_{max} is the maximum contraction velocity. This equation was fitted to the data by varying only one parameter (v_{max}), using a least square criterion. A preset a/f_0 value optimized for the appropriate 4 measurement lengths, as described by Van Koeveringe and Van Mastrigt (Chapter 7), was used.

In three measurement sets the generated force declined sharply before all five shortening velocities were applied. Therefore v_{max} could only be determined in 33 out of the 36 (9 strips, 4 measurement lengths) data sets.

Multi variate analysis of variance was applied separately in the different subgroups to determine the significance of measurement length and the applied linear shortening velocity as a source of variance in the measured parameters. Mean values of the evidently velocity independent parameters, F_{iso}, F_{rec1}, C_{iso}, C_{rec}, C_{rec1} and C_{rec2} were determined for each measurement set (of 5 measurements which were used to determine one v_{max} value) at each measurement length in each strip. In each strip, the mean values of these parameters were correlated with v_{max}, using Spearman's rank correlation coefficient.

Spearman's correlation coefficient was also determined for the correlation between C_{iso} and C_{rec}. A Wilcoxon signed ranks test was used to determine the significance of the pairwise difference between C_{iso} and C_{rec}. Also the significance of the difference between C_{iso} and either C_{rec1} or C_{rec2} was determined using the Wilcoxon signed ranks test.

At different measurement lengths mean values of parameters, which were proven length dependent by analysis of variance, were compared using a Mann-Whitney U test.

Results

In Chapter7, Figure 2 shows an example of the signals measured in one measurement protocol. It can be seen that the maximum isometric force F_{iso} was reached before shortening was applied. The mean F_{iso} value in all strips was 574 µN. At a maximum strip diameter of 200 µm, the maximum active tension was at least 1.8 N/cm². It can also be seen that shortening was linear as shown in the bottom trace. When the shortening stopped a minimum force level F_{es} was

Tabel 1: Mean parameter values for v_{max} and the isometric force development parameters before and after shortening. Mean ± SEM.

	mean	S.E.M	N
v_{max} (l/s)*	0.328	0.02	33
F_{iso} (μN)	573	45.8	170
F_{rec} (μN)	210	19.6	161
F_{rec1} (μN)	63.5	11.1	126
F_{rec2} (μN)	211	19.2	126
C_{iso} (s)	2.74	0.06	170
C_{rec} (s)	1.51	0.06	161
C_{rec1} (s)	0.49	0.04	126
C_{rec2} (s)	3.13	0.20	126

*: l/s = striplengths/s

reached, subsequently force rerose to a new maximum level F_{rec}.

Table 1 shows descriptive statistics for unnormalized values of all parameters. Mean C_{iso}, the pre-shortening time constant of isometric force development and mean C_{rec}, the time constant of isometric force recovery, equaled 2.77 and 1.51 sec. C_{iso} and C_{rec} were weakly correlated (Spearman's correlation coefficient: 0.185 (2-tailed p<0.05)). A pairwise comparison of measurements using a Wilcoxon signed ranks test showed a significant difference of C_{iso} and C_{rec} values (N=161; p<0.001).

Figure 1 illustrates that the pre-shortening time constant of isometric force development C_{iso} was not length dependent (Spearman's corr.coeff. 0.076). F_{iso}, however correlated significantly with measurement length (corr. 0.297; p<0.001), which was illustrated in a previous report (Chapter7:Fig. 3). Multi variate analysis of variance showed that the imposed linear shortening velocity was a significant source of variance in F_{rec} (p<0.001) but not in C_{rec} and that measurement length (see Chapter7:Fig 2) was a significant source of variance (p 0.001) in both F_{rec} and C_{rec}. Figure 2 shows values for C_{rec} together with values for C_{rec1} and C_{rec2} at different measurement lengths. The C_{rec} value at a normalized measurement length of 1.9 or 2.2 was significantly higher than that at lengths 1.3 and 1.6 (p<0.01). When a dual-exponential curve was fitted and mean values of C_{rec2} at measurement lengths 1.3
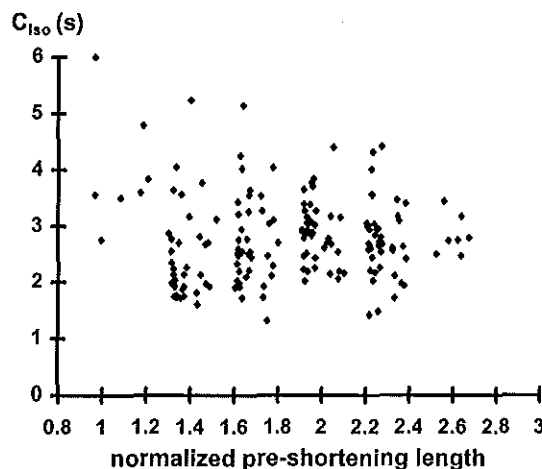

Figure 1: Scatterplot of pre-shortening time constant C_{iso} as a function of pre-shortening length.
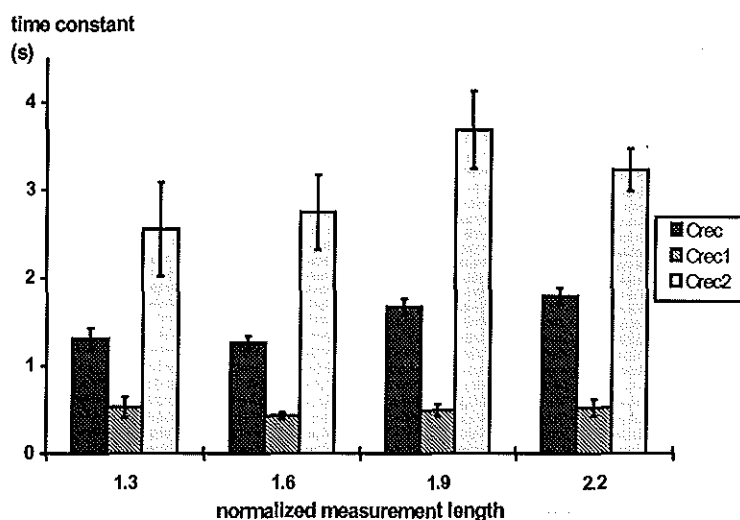
Figure 2: Mean ± standard error of the mean of the mono-exponential time constant of force recovery C_{rec} and the dual-exponential time constants C_{rec1} and C_{rec2} as a function of the normalized measurement length.

or 1.6 were compared with those at measurement lengths 1.9 or 2.2, a significant difference (p 0.01) was found. No significant differences were found when mean C_{rec1} values at different measurement lengths were compared. Multi variate analysis of variance showed that for neither C_{rec1} nor C_{rec2}, imposed linear shortening velocity or measurement length was a significant source of variance. Figure 3 however shows a decrease in the value of C_{rec2} with the lowest 3 shortening speeds. Mean values of C_{rec2} after shortening with a velocity of 10 µm/s were significantly different from those after shortening with 40 µm/s (p=0.01), 100 µm/s (p<0.05) and 250 µm/s (p<0.01). No significant differences were found between mean values of C_{rec} and C_{rec1} after different shortening velocities.

As was expected from the Hill equation (9, Chapter7) the amplitudes of isometric force rede-

Table 2: Correlations between v_{max} and the isometric force development parameters before and after shortening.

	v_{max}	sign. (2 tailed)*
F_{iso}	0.549	<0.01
F_{rec1}	0.654	<0.01
C_{iso}	0.133	n.s.[†]
C_{rec}	-0.357	<0.05
C_{rec1}	-0.489	<0.01
C_{rec2}	-0.444	<0.05

*: two-tailed significance of the correlation
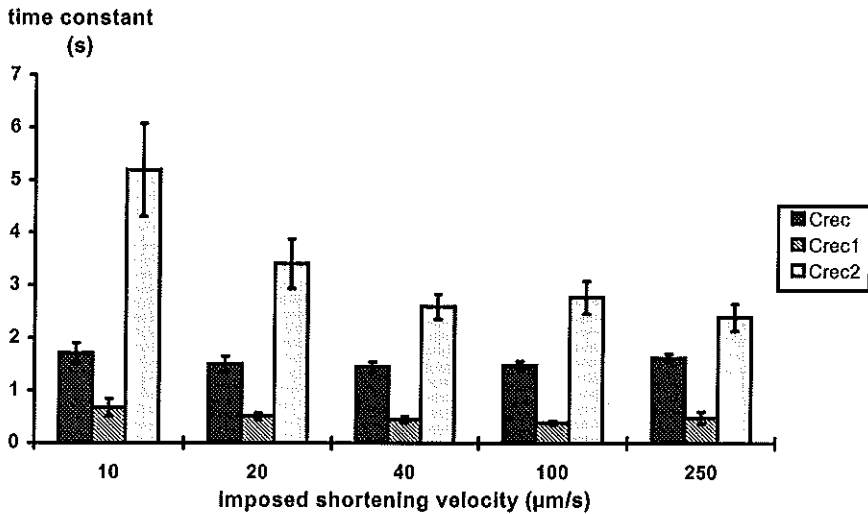[†]: n.s. = not significant

Figure 3: Mean ± standard error of the mean of the mono-exponential time constant of force recovery C_{rec} and the dual-exponential time constants C_{rec1} and C_{rec2} as a function of the previously imposed shortening velocity.

velopment after shortening F_{rec}, F_{rec1} and F_{rec2} depended significantly on the imposed linear shortening velocity. For neither of the amplitudes of isometric force recovery, measurement length was a significant source of variance.

Table 2 shows Spearman's correlation coefficients and 2-tailed significances for the correlation between v_{max} and the isometric force (re)development parameters. F_{iso}, F_{rec1} and C_{rec1} correlated significantly with v_{max} ($p<0.01$). Mean C_{rec} and C_{rec2} correlated significantly with v_{max} ($p<0.05$) but mean C_{iso} did not, which is visualized in Figure 4. Figure 5 shows in a scatter plot the negative correlation of both C_{rec1} and C_{rec2} values with maximum shortening velocity v_{max}.

Discussion

In the literature, the rate of isometric force development of smooth muscle is frequently related to the cross-bridge cycling rate, of which the maximum shortening velocity (v_{max}) is a mechanical index (1,19). The former rate also depends on the pre-stimulus interval and contraction history (17). In the current study we measured the time constant of isometric force development before shortening was applied, C_{iso}, and the time constant of isometric force recovery after shortening, C_{rec}, in pig urinary bladder smooth muscle. The relation between the cross-bridge cycling rate, represented by the maximum shortening velocity measured in the same preparations using a stop-test method (Chapter 7), and the time constants both before and after shortening was explored. Additio-
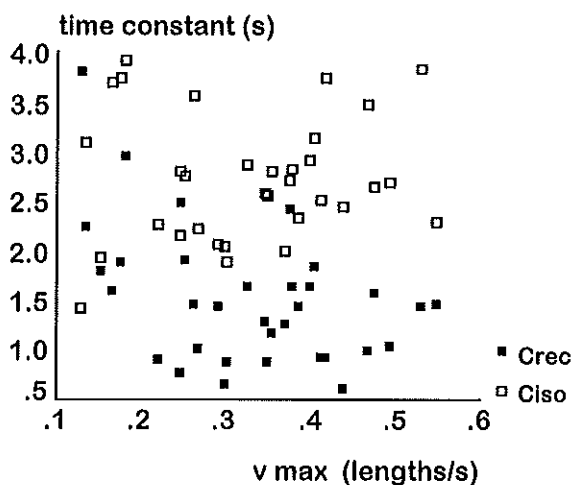
time constant (s)

Figure 4: Scatterplot of the time constant of pre-shortening isometric force development C_{iso} (open squares) and the time constant of isometric force recovery C_{rec} (solid squares) as a function of maximum shortening velocity v_{max}.

nally, the influence of muscle length and the rate of the previously applied shortening on the time constants was investigated.

In previous reports from our group, it was hypothesized that the rate of isometric force development, represented by the time constant C_{iso}, was limited by the influx of extracellular calcium (15, Chapter 2). Both in vitro and in intact urinary bladders (2,5) C_{iso} was smaller when calcium was released from intracellular stores. Himpens and Somlyo (10) monitored intracellular $[Ca^{++}]$ with Fura2 in smooth muscle of the small intestine of the Guinea pig. They showed that a fast high intracellular $[Ca^{++}]$ peak was followed by a "shoulder" of a sustained high intracellular $[Ca^{++}]$, that lasted as long as the stimulation. In normal extracellular $[Ca^{++}]$ an initial fast force rise was followed by an after-contraction during the sustained high intracellular $[Ca^{++}]$, this after-contraction was not seen in low extracellular $[Ca^{++}]$ (10). It is therefore likely that the sustained after-contraction depends on the "shoulder" in the intracellular $[Ca^{++}]$, which is caused by the influx of extracellular calcium. In urinary bladder tissue, the fast initial contraction that was observed in Guinea pig intestine probably merges with the large after-contraction. It is therefore likely that the time constant C_{iso} is determined by the influx of extracellular calcium.

This view is supported by the fact that the mechanical index of cross bridge cycling, v_{max}, was not correlated with the time constant of isometric force development C_{iso} (Fig. 4). Moreover, isometric force development limited by the cross-bridge cycling rate would take place at a considerably higher rate. In contrast to C_{iso}, the time constant of isometric force recovery after shortening C_{rec} was significantly correlated with v_{max}. C_{rec} was at all stretched muscle lengths significantly faster than C_{iso}, which confirms that C_{rec} and C_{iso} represent different mechanisms. C_{rec} was faster at higher v_{max} values (see Fig. 4), indicating that cross-bridge cycling is a major denominator of the rate of force recovery after shortening. Additional support for the view that the rate of force development before and after shortening is limited by different mechanisms is provided by the

fact that the time constant of isometric force development, C_{iso}, did not depend on the stretched muscle length (see Fig. 1). In contrast, C_{rec}, the time constant of isometric force recovery after shortening increased significantly with increasing muscle length (Fig. 2) i.e force re-development after shortening was slower when the muscle was stretched. The difference in rate limitation before and after shortening is most likely caused by the fact that intracellular $[Ca^{++}]$ is already high after shortening and force development is limited by other factors, as for instance cross-bridge cycling. Such a high intracellular calcium concentration directly after an imposed shortening has been described by Gunst (6).

After careful visual examination of the force recovery data, most of the curves seemed to consist of a fast initial force recovery followed by a slower recovery to a saturation level. Therefore, in a second analysis, two separate time constants, C_{rec1} and C_{rec2}, were determined by dual-exponential fitting. In 126 of the 180 measurements the dual-exponential curve could successfully be fitted to the data. Since this dual-exponential fitting was not possible for all valid data and a mono-exponential fitting resulted in an adequate average time constant we decided to present both a mono- and a dual-exponential fitting analysis. Two hypotheses are proposed to explain the dual-exponential time course of force recovery after shortening.
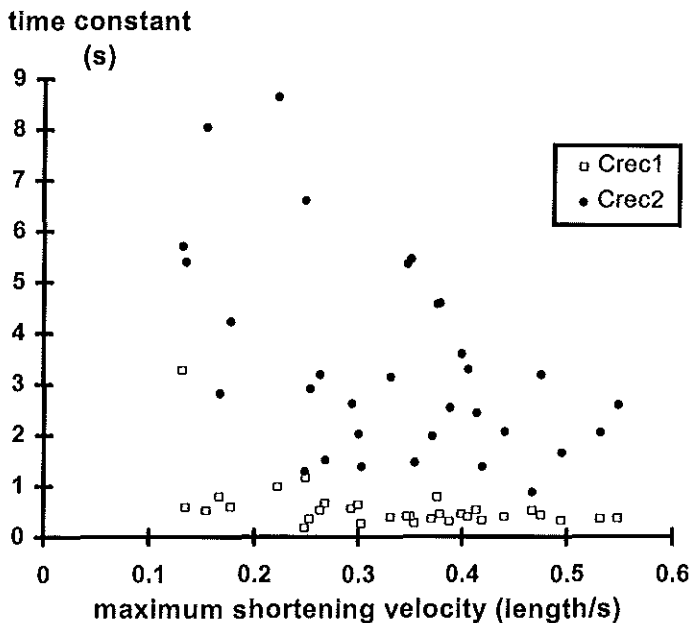

Figure 5: Scatterplot of the time constants C_{rec1} (open squares) and C_{rec2} (solid dots) as a function of maximum shortening velocity v_{max}.

The calcium influx hypothesis

The fast time constant of force recovery C_{rec1} was significantly different from C_{iso} whereas the slow C_{rec2} was not. Therefore, two processes underlie the isometric recovery of force after shortening, the slowest of which is probably identical to the mechanism that limits the rate of isometric force development before shortening, i.e., the influx of extracellular calcium. v_{max} was however significantly correlated with both time constants of isometric force recovery (Fig. 5). Analogously to C_{rec}, both C_{rec1} and C_{rec2} were faster at higher v_{max} values. The correlation coefficient of v_{max} and C_{rec1} of -0.489 was only slightly larger than the coefficient of v_{max} and C_{rec2} of -0.444. This conflicts with our hypothesis that both C_{rec2} and C_{iso} are determined by the same process. A possible explanation is that as a consequence of the dual exponential fitting process C_{rec2} and C_{rec1} are strongly correlated (corr. 0.61, p<0.001), which makes it difficult to differentiate the two on the basis of a correlation. It appeared that C_{rec2}, the slowest time constant, increased significantly with muscle length i.e., became slower (Fig. 2) while the fastest time constant C_{rec1} did not change. Taking this finding together with the finding that v_{max} increases with increasing muscle length (Chapter 7), suggests that the slow time constant C_{rec2} is independent of cross-bridge cycling. The fact that v_{max} did and C_{rec1} did not change with muscle length does not necessarily refute the hypothesis that the fast rate of force development represented by this time constant depends on cross-bridge cycling. With increasing muscle length the contribution of the fast process to the recovery force increased accordingly. In view of the time constant being a quotient of isometric force and v_{max} (Chapter 2) it is possible that an increase of v_{max} with muscle length is compensated by a comparable increase of the isometric force, so that the time constant remains unaffected. It is thus warranted to hypothesize that time constant C_{rec1} represents cross-bridge cycling and that C_{rec2} and C_{iso} represent the influx of extracellular calcium.

The 'latch' bridge hypothesis

In the literature (3) two types of cross bridges are identified, the fast cycling bridges, directly dependent on myosin light chain phosphorylation, and the slow cycling, so called 'latch' bridges, which can maintain force at less energy consumption. According to Meiss (13) and Hellstrand (8) these bridges react differently to preceding shortening. Therefore it could be hypothesized that the time constant C_{rec1} is determined by the cross-bridge cycling rate of fast cycling cross-bridges and C_{rec2} by the reattachment rate of slow cycling "latch" bridges.

In this view, the increase of C_{rec} and C_{rec2} with increasing muscle length results from an increased shortening induced detachment of slowly cycling cross-bridges. This could result from the higher passive forces i.e. higher load on the muscle. In the literature (7,13) it is described that shortening initiated at a

large length caused a relatively greater distortion of the cell structure than shortening at a short length. Consequently, more cross-bridges have to be re-attached, which takes a longer time, if it happens at all (13). Meiss (13) also described the possibility that at larger lengths a relatively higher number of slowly cycling latch bridges reattach, which can explain the finding that C_{rec2} did change with muscle length but C_{rec1} did not. Also, due to a more efficient contraction and a faster cross-bridge cycling before shortening at larger lengths, less energy (ATP) is left in the muscle cell, resulting in a relatively larger contribution of slowly cycling latch bridges to the recovery contraction.

More experiments, for instance in different calcium concentrations or using instantaneous intracellular calcium measurements, are indicated to determine whether the calcium influx or the latch bridge hypothesis provide the final explanation for the observed two time constants of force recovery after shortening.

Shortening deactivation.

Shortening induced deactivation, during persistent stimulation, has been, described extensively for striated and cardiac muscle and in the last decade also for smooth muscle (5,7,13,14).

In order to explain shortening induced deactivation, Meiss (13) introduced a shortening induced detachment of slowly cycling latch bridges, which sparsely or not reattached after shortening. As previously described, this phenomenon could also explain the increase of the time constant (C_{rec} and C_{rec2}) with increasing muscle length.

Moreover, when the current results are combined with the results from a previous study by Ganitkevich and Isenberg (4), another hypothesis can be proposed. After shortening the intracellular calcium concentration is still high, which could explain the fast initial rate of force development (C_{rec1}) after shortening. The calcium channels (presumably L-type) may be affected by a negative feed-back mechanism, which reduces the influx capacity of extracellular calcium. In addition, it is not likely that after shortening an initial fast intracellular calcium release exists, resulting in another relative calcium deficit. These two mechanisms consequently lead to recovery of force to sub-maximal levels.

It can be concluded that in smooth muscle isometric force develops at a well defined rate, that can be characterized by one time constant. This time constant is independent of the maximum shortening velocity, which represents the rate of cross-bridge cycling. It represents a significantly slower rate limiting mechanism, most likely this mechanism is the influx of extracellular calcium. After linear shortening applied during activation of smooth muscle, isometric force (re-)develops faster than before, at a rate that can be defined by two time constants, representing a fast and a slow component. It is proposed that fast

component is more dependent upon cross-bridge cycling rate, as directly after shortening the intracellular calcium concentration is still high. The slow component of the recovery contraction could be determined by influx of extracellular calcium analogously to the time constant of isometric force development before shortening. Alternatively, the slow component in force development could be deermined by re-attachment of slow-cycling "latch" bridges, which would better explain for the muscle length dependence of the force recovery. The high post-shortening calcium concentration could induce a fast re-development of force but it could additionally lead to negative feedback of calcium influx channels. In combination with a reduced post-shortening calcium contribution from intracellular stores, this effect might result in a force recovery to submaximal levels and so explain shortening induced deactivation.

References

1. Barany, M. (1967) ATPase Activity of Myosin Correlated with Speed of Muscle Shortening. *J. of Gen. Physiol.* 50(part 2): 197-218.
2. Damaser, M.S., Kim, K.B., Longhurst, P.A., Wein, A.J. and Levin, R.M. (1997) Calcium regulation of urinary bladder function. *J. Urol.* 157: 732-738.
3. Dillon, P.F., Aksoy, M.O., Driska, S.P. and Murphy, R.A. (1981) Myosin Phosphorylation and the Cross-Bridge Cycle in Arterial Smooth Muscle. *Science.* 211: 495-497.
4. Ganitkevich, V.Y. and Isenberg, G. (1991) Depolarization-mediated intracellular calcium transients in isolated smooth muscle cells of guinea-pig urinary bladder. *J. Physiol.* 435: 187-205.
5. Groen, J., R. Van Mastrigt and R. Bosch. (1996) Shortening induced deactivation in the guinea pig urinary bladder. *Acta Physiol. Scand.* 156: 483-487.
6. Gunst, S.J. (1989) Effects of muscle lengths and load on intracellular Ca^{2+} in tracheal smooth muscle. *American Journal of Physiology.* 256: C807-C812.
7. Gunst, S.J., Wu, M.F. and Smith, D.D. (1993) Contraction history modulates isotonic shortening velocity in smooth muscle. *American Journal of Physiology* 265: C467-C476.
8. Hellstrand, P. (1994) Cross-bridge kinetics and shortening in smooth muscle. *Canadian Journal of Physiology and Pharmacology.* 72: 1334-1337.
9. Hill, A.V. (1938) The heat of shortening and the dynamic constants of muscle. *Proc. Roy. Soc. London B.* 126: 136-195.
10. Himpens, B. and Somlyo, A.P. (1988) Free-Calcium and force transients during depolarization and pharmacomechanical coupling in Guinea-pig smooth muscle. *Journal of Physiology.* 395, 507-530.
11. Klemt, P. and Peiper, U. (1978) The dynamics of Cross-Bridge Movement in Vascular Smooth Muscle Estimated from a Single Isometric Contraction of the Portal Vein: The Influence of Temperature and Calcium. *Pflügers Archiv.* 378: 31-36.
12. Krisanda, J.M. and Paul, R.J. (1988) Dependence of force, velocity, and O_2 consumption on $[Ca^{2+}]_o$ in porcine carotid artery. *American Journal of Physiology* 255: C391-C400.
13. Meiss, R.A. (1993) Persistent mechanical effects of decreasing length during isometric contraction of ovarian ligament smooth muscle. *Journal of Muscle Research and Cell Motility.* 14: 205-218.

14. **Pelper, U. and Dee, J.** (1994) Smooth muscle contraction kinetics at different calcium concentrations. *Canadian Journal of Physiology and Pharmacology.* 72: 1338-1344.
15. **Van Koeveringe, G.A. and Van Mastrigt, R.** (1991) Excitatory pathways in smooth muscle investigated by phase plot analysis of isometric force development. *American Journal of Physiology* 261: R138-R144.
16. **Van Mastrigt, R.** (1980) Fitting the Hill equation to experimental data. *IEEE transactions on biomedical engineering.* Vol. BME-27, NO 7: 413-416.
17. **Van Mastrigt, R.** (1988) The length dependence of the series elasticity of pig bladder smooth muscle. *Journal of Muscle Research and Cell Motility* 9: 525-532.
18. **Van Mastrigt, R. and J.J. Glerum.** (1985) In vitro comparison of isometric and stop-test contractility parameters for the urinary bladder. *Urological Research.* 13:11-17.
19. **Warshaw, D.M., Work, S.S. and McBride, W.J.** (1987) Effect of low extracellular Calcium on shortening velocity in isolated single smooth muscle cells. *Pflügers Archiv.* 410: 185-191.

CHAPTER 9

The temperature dependence of the maximum shortening velocity and time constants of isometric force development in human detrusor biopsies

Small 150 μm muscle strip, as from a human bladder biopsy in an organbath
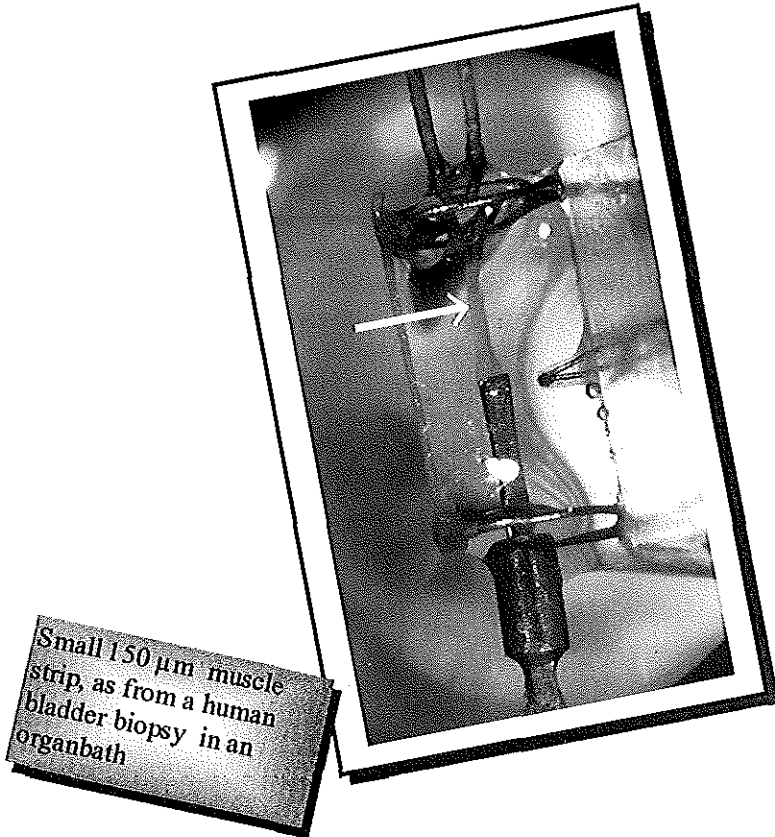
Gommert A. van Koeveringe and Ron van Mastrigt

Summary

Apart from its possible diagnostic impact, a study on maximum shortening velocity in the human detrusor might be used to verify earlier data derived from pig detrusor muscle. Linear shortening at different rates was imposed on smooth muscle strips from small cold cup biopsies during maximum electrical field stimulation until a preset endstop was reached. At different temperatures, maximum shortening velocity v_{max} (mean at 37°C: 0.28 striplengths/s) was determined by fitting the Hill equation to the force, measured at the endstop, as a function of shortening rate. It was found that v_{max} did not show a species difference and increases in the human bladder when temperature increases. As the time constant of isometric force development C_{iso} is independent of v_{max} and increases with decreasing temperature, it is not limited by cross-bridge cycling but by a slower process in the excitation-contraction coupling, the influx of extracellular calcium. The time constant of force recovery directly after shortening C_{rec} is determined by v_{max} and also shows a decrease with temperature. Mean C_{iso}, 3.79 s, was significantly larger than in pig detrusor (2.87 s). A potential diagnostic use needs to be investigated in the near future.

Introduction

The maximum shortening velocity of detrusor smooth muscle has been determined in several species (12, 15, 17). This velocity is directly dependent on the cross bridge cycling rate (2, 9, 20) and differs among the species. Most often the maximum shortening velocity has been measured in rather large strips of animal detrusor muscle. In our research group the pig bladder model was amply used for smooth muscle studies (4, 16, 17, 18). It has recently been shown that it is possible to measure a maximum shortening velocity in human bladder biopsies (1). Measurements on human bladder smooth muscle are valuable for a correct interpretation of clinical data. They enable the study of the role of maximum shortening velocity in human bladder pathology, and its possible diagnostic impact. Therefore we developed a dedicated device (17) to measure the maximum shortening velocity in very small muscle strips from biopsy material of the human bladder. Such biopsies are regularly taken in our department for other purposes.

It is known that in smooth muscle from other species the maximum shortening velocity is much more temperature dependent than force development(13). Also, muscle mechanics experiments in skeletal muscle are generally done at room temperature while smooth muscle experiments have to be done at 37°C as the muscle tends to be very slow at room temperature. Therefore

a smooth muscle specific temperature effect seems to exist. It was the purpose of the present study to quantify the impact of this effect on the maximum shortening velocity in human bladder tissue.

In addition, the time constants of isometric force development were studied. Frequently these time constants are related to series elasticity and the maximum shortening velocity. (10, 11, 21) Previous research in our group however indicated that the normal rate of isometric force development in the pig urinary bladder depends on the influx of extracellular calcium. (16). This was recently confirmed by data from another group for the rabbit(3). Therefore in the present study the time constant of isometric force development describing the rate of isometric force development was measured before and after shortening at different temperatures. The time constants were compared to the maximum shortening velocity.

Materials and Methods

Patients and Biopsy tissue preparation.

Human bladder tissue was obtained by taking one extra cold cup biopsy (2 mm diameter) during an operative procedure in which 6 to 10 random bladder biopsies were taken. Patients were suspected of either recurrent or new transitional cell carcinoma of the bladder and biopsies were necessary to diagnose the pathology. Smooth muscle micro-strips with a maximum diameter of 150μm and a length of approximately 1 mm were cut from the biopsy tissue using a binocular microscope. Care was taken that the muscle fibres were running longitudinally in the preparation. The strips were prepared in modified aerated Krebs fluid and transported to the organbath in a small container in order to prevent desiccation.

The modified Krebs solution contained: NaCl, 118 mM; KCl, 4.7 mM; NaHCO$_3$, 25 mM; KH$_2$PO$_4$, 1.2 mM; CaCl$_2$, 1.8 mM; MgSO$_4$ 1.2 mM; glucose, 11 mM; pH 7.4; aerated with 95% O$_2$ / 5% CO$_2$.

Incubation.

The strips were incubated at 37 C in a 20 μl fluid drop as shown in Chapter7:Figure 1 and described in more detail in a previous publication (Chapter 7). The strips were mounted between two tweezers, one of which was attached to a KG3 force transducer connected to a BAM3 amplifier (Scientific instruments®, Heidelberg, FRG). The other tweezer was attached to a pole connected to the linear displacement device described below. In the drop the strips were exposed to electrical field stimuli: 100Hz, 4V alternating polarity 5ms pulses during 16 to 24 seconds.

Linear displacement device.

A displacement device previously described by Van Koeveringe and Van Mastrigt (Chapter 7, 17) was used. The movable tweezer was connected to a linear displacement conductor (Chapter 7:Fig 1) with an inductive displacement transducer (MERA®). The conductor was pressed against a threaded nylon block which was driven by a servo-electro motor. When shortening was applied the conductor, containing pole and tweezer, moved at constant velocity until it stopped at a pre-set end-stop. The displacement device was controlled using a computer with multichannel data acquisition and measurement control software (MKR computer program: developed by the CDAI dept. Academic Hospital Rotterdam).

Measurement protocol.

The incubated strips were stretched to a "measurement length" 1.6 times the initial strip length. After a waiting interval of 10 minutes two electrical test stimuli were applied with a rest interval of 5 minutes. When a contraction smaller than 100 μN was recorded in response to either of the two test stimuli, the strip was considered to be in a too bad condition and discarded. In 5 strips from 5 different bladders out of 8 tested, a subsequent measurement protocol was applied, first at 37°C.

Each measurement protocol started with a pre-stretch at a rate of 10μm/s to a velocity dependent pre-shortening length, allowing a subsequent shortening during 2 seconds, which ended at exactly the measurement length (17). After a waiting interval of 5 minutes, the strip was linearly shortened for two seconds without stimulation to measure the passive force response. Next the strip was again slowly (at a rate of 10μm/s) stretched to the pre-shortening length. After a waiting interval of 1 minute, field stimulation was applied for a total duration of 16 seconds. After 7 seconds of stimulation, during which interval isometric force reached a maximum, linear shortening was applied for 2 seconds, ending at the measurement length. Stimulation continued for another 7 seconds.

The described measurement protocol was repeated at another shortening velocity after a waiting period of 5 minutes. After testing five different shortening velocities i.e. 10, 20, 40, 100 and 250 μm/s, the whole sequence was repeated at another temperature following a waiting interval of 10 minutes. Four different temperatures i.e. 37, 33, 29 and 25°C were tested.

All protocols started with 37°C, the next three temperatures were tested in a random order. The stimulus duration and the interval after onset of stimulation were adapted to the incubation temperature, i.e., 16, 20, 24 and 24 s at 37, 33, 29 and 25°C respectively. The measured force signal, a binary stimulus signal, and the displacement signal (see Fig. 1) were recorded digitally.
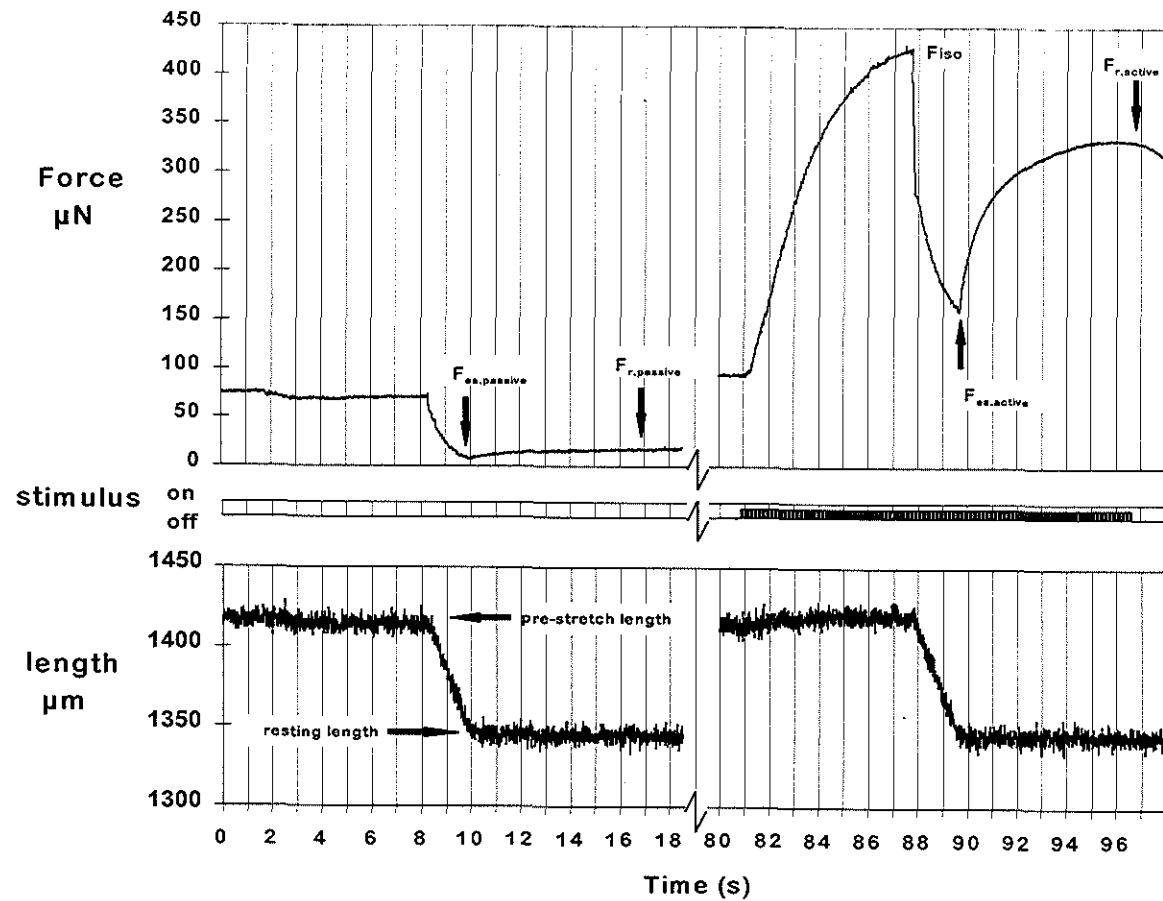
Figure 1: An example of signals measured in a smooth muscle preparation derived from a human bladder biopsy. The top trace shows the measured force, the bar in the middle trace represents the electrical field stimulus and the lower trace shows the length of the tissue preparation.
$F_{r.active}$ and $F_{r.passive}$ as indicated in the figure are approximate values of the fitted variables $F_{rec.active}$ and $F_{rec.passive}$

Data processing.

Data were processed using MATLAB®. To the isometric force rise before shortening, a monoexponential curve of the following form was fitted:

$$F = F_{iso} [1 - exp(-t/C_{iso})] \qquad\qquad Eq.1$$

where: F = measured force
  t = time
  F_{iso} = maximum extrapolated isometric force
  C_{iso} = time constant

At all pre-set velocities the actual shortening velocity just before reaching the end-stop was calculated from the displacement transducer output. Pre-shortening length was determined from the displacement signal and normalized by dividing by the initial strip length. At each pre-shortening length the maximum extrapolated isometric force (F_{iso}, see Fig.1), before application of shortening was determined and normalized by dividing by the F_{iso} value at the first contraction in the measurement protocol i.e. excluding the two test contractions. As a consequence of the different pre-shortening lengths necessary to allow a constant shortening duration of two seconds at different velocities, F_{iso} values were thus measured at a spectrum of different lengths.

Equation 1 was also fitted to the isometric force recovery immediately following the linear shortening ($90<t<97$ s in Fig. 1). The resulting parameters were called F_{rec}, the maximum extrapolated isometric force during recovery and C_{rec}, the time constant for isometric force development during recovery.

To derive a force velocity relation from the measured force signals, the following procedure was applied. The force measured when shortening during stimulation stopped at the end-stop ($F_{es.active}$, see Fig. 1) and the force after recovery ($F_{rec.active}$, see Fig. 1) were corrected for changes in the passive force. This was done by subtracting the forces measured at the same instants during the passive shortening sequence ($F_{es.passive}$ and $F_{rec.passive}$, see Fig. 1). The quotient of these corrected force values was called the relative force f_{rel}. The relative force values were plotted as a function of the applied shortening velocity. Artefacts in the measured force signals leading to outlier values were re-analysed manually and corrected if possible.

For each of the 5 strips, 4 different sets (at different temperatures) with each 5 different force velocity data points were processed separately. In 21 contractions the applied linear shortening was higher than the maximum shortening velocity of the strip, resulting in a relative force zero at the end stop. These contractions were excluded thus leaving 79 valid measurements out of 100.

To calculate the maximum shortening velocity v_{max}, the hyperbolic force-

velocity relation of Hill (8) was rewritten (19) as follows:

$$f_{rel} = a/F_0 * (v_{max} - v) / (v + a/F_0 * v_{max}) \qquad \qquad Eq.2$$

where f_{rel} is not a force, as in the original Hill equation, but a dimensionless relative force, a/F_0 is a measure for the concavity of the force-velocity curve, v is shortening velocity and v_{max} is the maximum shortening velocity at zero relative force. This equation was fitted with only one variable parameter (v_{max}) and a preset a/F_0 value of 0.20 (17).

Analysis of variance was applied to determine the significance of temperature as a source of variance of the measured parameters. Mean values of F_{iso}, C_{iso} and C_{rec} were determined for each set of 5 measurements at each temperature and were correlated with the corresponding v_{max} values for the same sets.

Spearman's rank correlation coefficient was calculated between C_{iso} and C_{rec}. A Wilcoxon signed ranks test was used to determine the significance of the pairwise difference between C_{iso} and C_{rec}.

Mean values of parameters, which were proven temperature dependent by analysis of variance were compared using a Mann-Whitney U test. This test was also used to determine the significances of the differences of parameter values measured in a previous study on pig detrusor (17) and corresponding values measured in the human detrusor.

Results

Figure 1 shows an example of the signals measured in one measurement protocol. It can be seen that the maximum isometric force F_{iso} was reached before shortening was applied, and that shortening was linear as shown in the bottom trace. When the shortening stopped a minimum force level F_{es} was reached, subsequently force rerose to a new maximum level F_{rec}.

Eight biopsies from 8 different patients were obtained. Three strips from 3 different human bladder biopsies showed contractions smaller than 100 µN during the 2 test stimuli and were discarded. The mean F_{iso} value in the 5 remaining strips at 37°C was 577 µN. In view of the maximum strip diameter of 150 µm, this value is comparable with at least a maximum active tension of 3.3 N/cm². Overall, mean values of v_{max} and the time constants C_{iso} and C_{rec} at 37°C (Table 1) were in the same order of magnitude as the corresponding values for pig detrusor strips (17). Maximum shortening velocity v_{max} seems smaller in human bladders (Table 1), however this was not significant. The time constant of isometric force development C_{iso} was significantly larger ($p < 0.05$) in the human bladders indicating a slower isometric force development. Force development at recovery after shortening seemed, although not significantly, faster in human

Table 1: Maximum shortening velocity v_{max}, maximum extrapolated isometric force F_{iso}, the pre- C_{iso} and post- C_{rec} shortening time constants of isometric force development. Mean ± standard error of the mean for human and pig bladder and the significances of differences between the species.

	human bladder	S.E. mean	pig bladder	S.E. mean	sign. diff. human vs. pig
v_{max} (l/s)*	0.278	±0.035	0.334	±0.031	n.s.[†]
F_{iso} (μN)	577	±55	693	±108	n.s.[†]
C_{iso} (s)	3.79	±0.34	2.87	±0.12	<0.05
C_{rec} (s)	1.08	±0.063	1.23	±0.07	n.s.[†]

*: l/s = striplengths/s
†: n.s. = not significant

than in pig bladders despite the lower v_{max} in human bladders.

Table 2 shows the correlation coefficients of v_{max} with F_{iso}, C_{iso} and C_{rec}. A significant correlation could only be demonstrated for v_{max} and C_{rec}. Figure 2 clearly illustrates that v_{max} correlated more with C_{rec} than with C_{iso}.

Temperature was a significant source of variance for all four parameters v_{max} (p=0.01), F_{iso} (p<0.001) C_{iso} (p<0.01) and C_{rec} (p<0.001). Figure 3 depicts the significant increase of v_{max} with increasing temperature. At 29°C (p<0.05), 33°C (p<0.01) and 37°C (p<0.01), v_{max} was significantly increased compared to
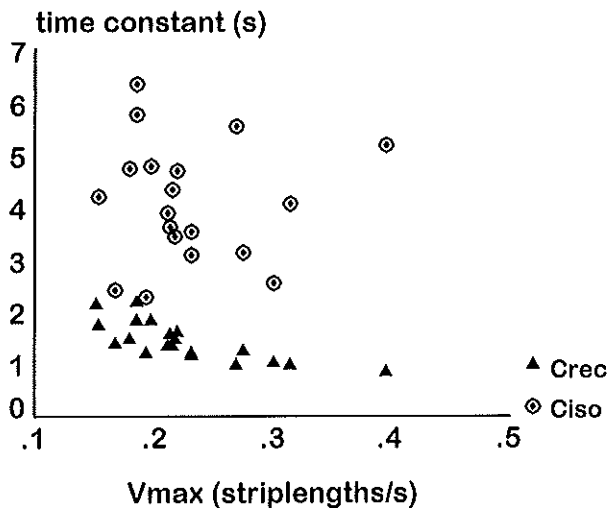
Figure 2: Scatterplot of the pre-shortening time constant of isometric force development C_{iso} and the post-shortening time constant of isometric force recovery C_{rec} as a function of the maximum shortening velocity v_{max}.

Table 2: Spearman's rank correlation coefficients for F_{iso}, C_{iso}, C_{rec} and v_{max}. Two tailed significances of the correlations.

	v_{max}	sign. (2tailed)	N
F_{iso} (µN)	0.286	n.s.[†]	20
C_{iso} (s)	-0.236	n.s.[†]	20
C_{rec} (s)	-0.789	<0.001	20

†: n.s. = not significant

25°C. At decreasing temperature, a decrease of the standard error of the mean can be seen in Fig. 3.

Maximum isometric force was also significantly reduced at lower temperatures, which is illustrated in Fig.4. At 37°C, F_{iso} was significantly increased compared to 25°C (p<0.001), 29°C (p<0.001) and 33°C (p<0.001).Between 25°C and 33°C, F_{iso} did not change significantly.

The time constants of isometric force development before (C_{iso}) and after shortening (C_{rec}) differed significantly (p<0.001). Also, their response to decreased temperature seems different. Figure 5 shows a hyperbolic decrease in C_{iso}, while C_{rec} in Figure 6 seems to decrease linearly with increasing temperature. C_{iso} was significantly increased at 25°C (p<0.01) compared to 37°C. The increase in C_{rec} was significant when temperature was decreased to 33°C (p<0.05), 29°C (p<0.001) and 25°C (p<0.001).

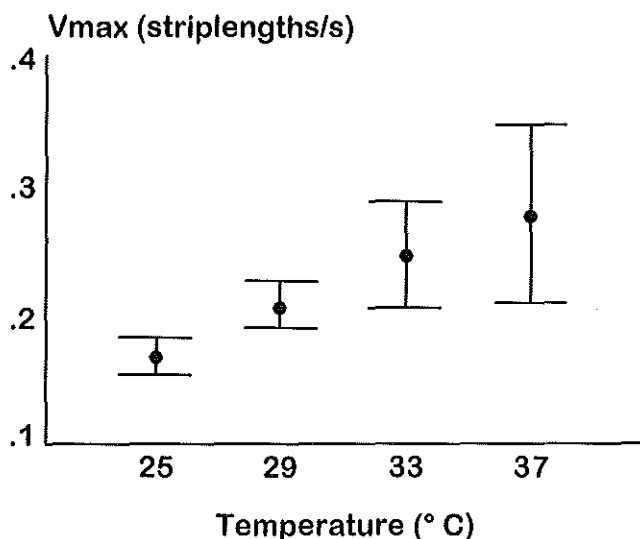**Figure 3:** Mean ± standard error of the mean of the maximum shortening velocity v_{max} as a function of the temperature.
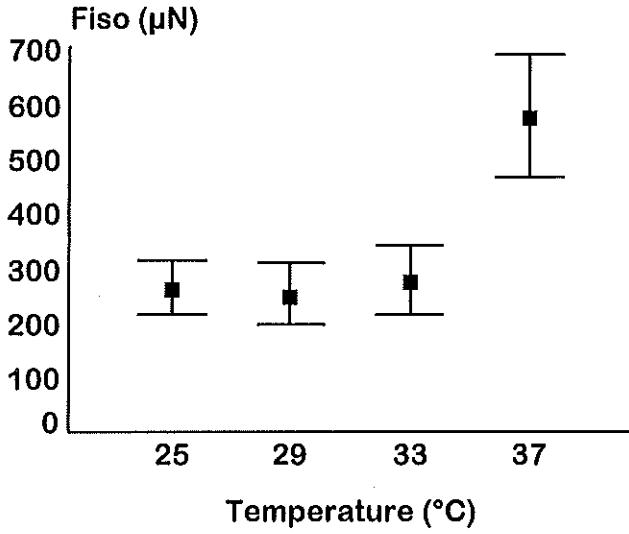
Fiso (µN)

Figure 4: Mean ± standard error of the mean of the maximum isometric force F_{iso} as a function of the temperature.
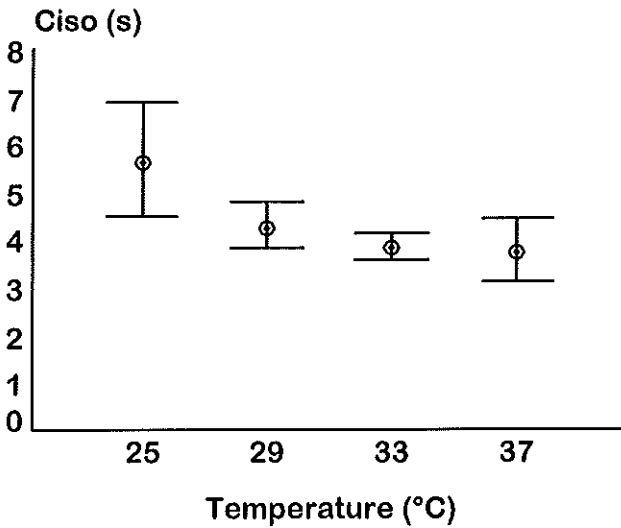
Ciso (s)

Figure 5: Mean ± standard error of the mean of the pre-shortening time constant of isometric force development C_{iso} as a function of the temperature.

Discussion

Functional studies of human detrusor smooth muscle are usually done on material collected during an open surgical procedure. In the present study a very small cold biopsy provided enough material to conduct a complete study in which several force-velocity relations at different temperatures could be measured in each preparation. Random cold cup biopsies are taken regularly in our department in patients with suspected transitional cell carcinoma of the bladder and are a constant source of normal smooth muscle tissue without additional risk to the patient. The present smooth muscle studies did not relate to the patients disease.

Analogous to data published earlier for rat vascular smooth muscle (13) a decrease of the maximum shortening velocity v_{max} of human detrusor smooth muscle with decreasing temperature (Fig. 3) was found. This indicates that cross-bridge cycling was reduced at lower temperatures, most likely due to a lower rate of de-phosphorylation leading to a slower cross bridge detachment. At lower temperature an inter-individual difference of , most likely, tissue metabolism was eliminated as evidenced by a reduced standard error of the mean.

Maximum isometric force also showed a temperature dependence: A steep decrease occurred between 37°C and 33°C. This decrease was markedly different from the slight decrease in v_{max} and the changed rate of isometric force development C_{iso}. Probably a reduced number of contractile units took part in the contraction at temperatures below 37°C or less force was generated by the contractile units. The latter might be caused by a changed activity or orientation of smooth muscle specific light chain proteins (7), as a similar temperature dependence in this temperature range is not seen in striated muscle (14).

The two time constants of isometric force development C_{iso} before and C_{rec} after shortening show a significant difference.

In the literature, the rate of isometric force development of smooth muscle is frequently related to its maximum shortening velocity (v_{max}). In previous studies from our group in pig detrusor muscle, the time constant C_{iso}, which characterizes this rate, showed a dependence on the influx of extracellular calcium (16). The time constant was smaller when calcium was released from intracellular stores. It also depended on the inter-stimulus interval and the contraction history (18). The present study shows that also in the human detrusor, C_{iso} is not significantly correlated with v_{max}, which indicates that it is determined by other factors. C_{rec} however was significantly correlated with v_{max}, indicating cross-bridge cycling to be an important factor that determines the time constant of isometric force recovery. Another factor which confirms this dependence is the linear change of both v_{max} (Fig.3) and C_{rec} (Fig.6) with decreasing temperature. C_{iso} has a significantly higher value than C_{rec} at all temperatures and is hyperbolically related to the temperature which again
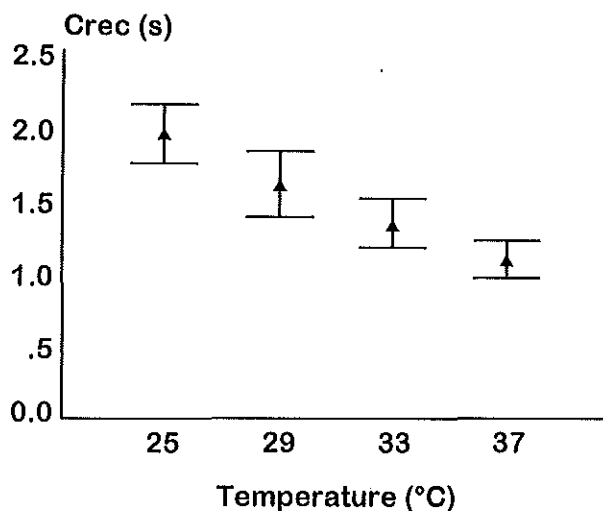
Figure 6: Mean ± standard error of the mean of the post-shortening time constant of isometric force recovery C_{rec} as a function of the temperature.

confirms that cross-bridge cycling is not a rate limiting factor in the rate of force development before shortening.

The parameter values determined in the human bladder in this study were compared to values determined in the pig bladder in other studies (16, 17). The human bladder muscle however is slower than that of the pig. v_{max} seemed to be slower too i.e., 0.278 striplengths/s in human detrusor, which is markedly smaller than the estimated v_{max} value of 0.38 striplengths/s in a previous study on guinea pigs by Groen et al. (5), and 0.334 striplengths/s in pig bladder (17). C_{iso} was higher in the human bladder but the evidence above indicates that mechanisms other than a slower v_{max} have caused this effect. These mechanisms are a changed operation of calcium channels or intracellular calcium stores.

It is concluded that maximum shortening velocity v_{max} in the human bladder increases when temperature increases. As the rate of isometric contraction development is independent of v_{max} and increases hyperbolically with decreasing temperature, another process, slower than cross-bridge cycling is proven to be rate limiting. Earlier, this process has been identified as influx of extracellular calcium (3, 6, 16). In contrast, the time constant of isometric force recovery directly after shortening is determined by v_{max} and shows a linear dependence on temperature. Mean time constant of isometric force development in the human detrusor, 3.79 s, is slower than that in pig bladder (2.87 s). v_{max} did not show a significant species difference, i.e., 0.278 striplengths/s in human and 0.334 striplengths/s in pig bladder. Additionally this study illustrates the power of functional smooth muscle studies in tissue derived from cold cup bladder

biopsies. A potential use of these studies to diagnose intrinsic bladder muscle disorders needs to be investigated in the near future.

References

1. Mark, S.D., P.J. Gilling, R. Van Mastrigt, E.P. Arnold and C.U. Mc. Rae. (1992) Detrusor contractility: Age related correlation with urinary flow rate in asymptomatic males. Neurourol. Urodyn. 11: 314-315.

2. Barany, M. (1967) ATPase Activity of Myosin Correlated with Speed of Muscle Shortening. *J. Gen. Physiol.* 50(part 2): 197-218 .

3. Damaser, M.S., K.B. Kim, P.A. Longhurst, A.J. Wein and R.M. Levin. (1997) Calcium regulation of urinary bladder function. *J. Urol.* 157: 732-738 .

4. Griffiths, D.J., R. van Mastrigt, W.A. van Duyl and B.L.R.A. Coolsaet. (1979) Active mechanical properties of the smooth muscle of the urinary bladder. *Med.Biol.Eng.Comput.* 17: 281-290 .

5. Groen, J., R. van Mastrigt, E. van Asselt, G.A. van Koeveringe, and R. Bosch. (1994) Contractility parameters of the guinea pig bladder in situ: similarity to human bladder. *J. Urol.* 151: 1405-1410 .

6. Groen, J., R. Van Mastrigt and R. Bosch. (1996) The influence of extracellular Ca^{2+} on the time course of isovolumetric pressure development in the guinea pig urinary bladder. *Acta Physiol. Scand.* 156: 475-482 .

7. Haeberle, J.R. and M.E. Hemric. (1994) A model for the coregulation of smooth muscle actomyosin by caldesmon, calponin, tropomyosin, and the myosin regulatory light chain. *Can. J. Physiol. Pharmacol.* 72: 1400-1409 .

7. Hill, A.V. (1938) The heat of shortening and the dynamic constants of muscle. *Proc. Roy. Soc. London B.* 126: 136-195 .

9. Huxley, A.F. (1957) Muscle structure and theories of contraction. *Prog.Biophys.Biophys.Chem.* 7:255-318 .

10. Klemt, P. and U. Peiper. (1978) The dynamics of Cross-Bridge Movement in Vascular Smooth Muscle Estimated from a Single Isometric Contraction of the Portal Vein: The Influence of Temperature and Calcium. *Pflügers Archiv.* 378: 31-36 .

11. Krisanda, J.M. and R.J. Paul. (1988) Dependence of force, velocity, and O_2 consumption on $[Ca^{2+}]$ in porcine carotid artery. *Am. J. Physiol.* 255: C391-C400 .

12. Munro, D.D. and I.R. Wendt. (1993) Contractile and metabolic properties of longitudinal smooth muscle from Rat Urinary bladder and the effects of aging. *J. Urol.* 150: 529-536 .

13. Peiper, U. (1984) What kind of signals are perceived by vascular smooth muscles, including physical factors. *J. Cardiovasc. Pharmacol.* 6 (Suppl. 2) .

14. Podolsky, R.J. and A.C. Nolan. (1971) Cross-bridge properties derived from physiological studies of frog muscle fibers. In: Contractility of muscle cells and related processes. Ed. E.D. Podolsky, Eaglewood Cliffs NJ, Pretence Hall . Pp: 247-260.

15. Uvelius, B. (1976) Isometric and isotonic length-tension relations and variations in cell length in longitudinal smooth muscle from rabbit urinary bladder. *Acta Physiol. Scand.* 97: 1-12 .

16. Van Koeveringe, G.A. and R. Van Mastrigt. (1991) Excitatory pathways in smooth muscle investigated by phase plot analysis of isometric force development. *Am. J. Physiol.* 261: R138-R144 .

17. Van Koeveringe, G.A. and R. Van Mastrigt. (1997) Length dependency of the force-velocity relation in smooth muscle fibers of the urinary bladder. *Submitted* .

18. **Van Mastrigt, R., J.W.B. Koopal, J. Hak, and J. van de Wetering.** (1986) Modeling the contractility of urinary bladder smooth muscle using isometric contractions. *Am.J.Physiol. 251*: R978-RR983 .

19. **Van Mastrigt, R.** (1980) Fitting the Hill equation to experimental data. IEEE trans. biomed. eng. Vol. BME-27, NO 7: 413-416 .

20. **Warshaw, D.M.** (1987) Force:velocity relationship in single isolated toad stomach smooth muscle cells. *J. Gen Physiol.* 89: 771-789 .

21. **Warshaw, D.M., S.S. Work and W.J. McBride.** (1987) Effect of low extracellular Calcium on shortening velocity in isolated single smooth muscle cells. *Pflügers Archiv.* 410: 185-191 .

CHAPTER 10

Summarizing Discussion
and
Conclusions
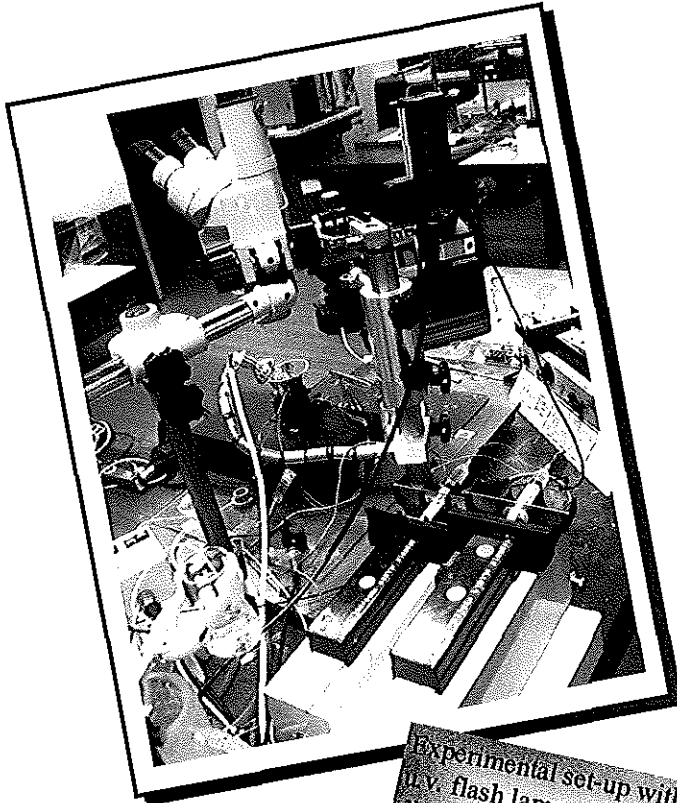
Experimental set-up with
u.v. flash lamp and linear
displacement device
(black box)

.

Summarizing Discussion

Smooth muscle of the urinary bladder is a specialized kind of tissue, that enables the complete evacuation of stored urine. The urine is continuously produced by the kidneys and stored in the bladder until evacuation at a voluntary moment takes place, which is called micturition. Several forms of defective regulation of this process are responsible for a broad area of urological pathology. The keyword in this area of urological disease is "voluntary". Pathological processes usually result in either involuntary urine loss or involuntary urine retention. The smooth muscle of the urinary bladder is controlled by the central nervous system. Disturbed nerve activity, either afferent or efferent, can result in pathological behaviour of the urinary bladder. However, unaffected nerve activity can also coexist with both categories of bladder disorders, involuntary urine loss or involuntary urine retention. In these cases, the disorders can subsequently be either due to an over- or under active bladder muscle, or due to a too wide or an obstructed bladder outlet or a combination of these conditions. Clinical urodynamic studies are essential to distinguish between these pathological processes.

Basic muscle research in order to understand micturition disorders

Micturition disorders due to either primary nervous system pathology or bladder outlet pathology, of which the cause cannot be eliminated, can be alleviated by modulation of the smooth muscle properties of the bladder. New approaches for modulation of smooth muscle or treatment of primary smooth muscle pathology require a better understanding of excitation-contraction coupling, pharmaco-mechanical coupling and the contractile machinery of smooth muscle.

Excitation-contraction coupling and Calcium

In the first part of this thesis, a model for excitation-contraction coupling of urinary bladder smooth muscle is described. The modeled excitatory pathways were addressed using combinations of stimulatory agents and pathway blocking agents. In addition to the maximum isometric force, the time constant of isometric force development was used to differentiate the pathways. The time constant of isometric force development represents the time elapsed until 63 % of the force saturation level is reached and is determined using phase plot analysis. A phase plot is a plot of the first derivative c.q. rate of change of force as a function of the force. In such a plot a straight line represents a monoexponential force development and the negative reciprocal value of the slope of this line is the time constant. In combination with data from previous studies, it was shown that the rate of isometric force development is not limited by

shortening of the series elasticity of the muscle, an inherently fast process. Ratherthe rate of change of force, represented by the time constant, was limited by a slower process. When a contraction was evoked in a calcium free solution or during blocking of calcium channels, a smaller time constant ,i.e., a faster force development was seen. Such a contraction, independent of extracellular calcium, was demonstrated to be most pronounced after stimulation of muscarinic receptors, for example by acetylcholine. It was found that influx of extracellular calcium was under normal circumstances the rate limiting factor in isometric force development.

Caged Calcium

The validity of this hypothesis was further explored by an attempt to bypass the rate limiting influx of extracellular calcium using intracellularly loaded "caged calcium".This had to be photolyzed cq. freed by a high intensity ultraviolet light flash. As an alternative to the commonly used expensive ultraviolet laser, a photo-flash unit was modified to serve the purpose. The performance of this flash unit was tested by exposure of a 20µl solution containing caged calcium (Nitr 5) in a setup with a calcium selective electrode. It was found that the effect of photolysis on the free calcium concentration depended critically on the total calcium concentration. After loading the acetoxy-methyl ester of Nitr5 (caged calcium) into intact cells by incubation, the total calcium concentration is expected to be variable and the very strong calcium buffering capacity of Nitr5 make high demands if not interfered with the calcium homeostasis mechanism of the cell. This means that using this technique in intact cells, theeffect of photolysis on the intracellular free calcium concentration is unpredictable. In a test solution, however, a physiological calcium jump from 10^{-7} to $1.1*10^{-5}$ M could be evoked using the low cost ultraviolet photo flash unit.

In a pilot study an attempt was made to load and photolyze "caged calcium" in the smooth muscle cells of a urinary bladder micro-strip. Marked force development resulted from ultraviolet light illumination, but this effect was also found in control preparations not loaded with caged calcium. The rate of force development upon ultraviolet light stimulation was faster than upon electrical field stimulation, indicating a different excitatory pathway. Therefore this new stimulation method was further investigated.

Ultraviolet light and intracellular calcium stores

In small strips of pig urinary bladder smooth muscle, contractions elicited by electrical field stimulation and an ultra-violet light flash (wave length: 320-370 nm) were compared with spontaneous contractions in terms of maximum isometric force development and time constant. The flash induced contraction was not caused by an electrical or heat artefact as the response could be abolished by a filter that blocked light with wavelengths below 400 nm. The

amplitude of a contraction evoked by an ultraviolet flash was comparable to that during field stimulation. The time constant of isometric force development was smaller after ultraviolet stimulation than during field stimulation, but larger than that during a spontaneous contraction. The time constant after ultraviolet flash stimulation was similar to that of a contraction independent of extracellular calcium, which was measured previously. It was therefore concluded that ultra-violet light evoked release of calcium from intracellular stores rather than influx from extracellular space, which earlier had been shown to be a slower process.

It was shown that ultraviolet light induced contractions were inhibited by ryanodine, an agent which inhibits (calcium induced) calcium release from intracellular stores. Electrical field stimulated contractions were not significantly inhibited by ryanodine. The involvement of calcium induced calcium release indicates that some calcium influx will probably take place during flash stimulation. A long lag time between the flash and the resulting force increase was found, which could be explained by slow influx of calcium to a threshold level. An alternative explanation of the lag time is that another intracellular messenger is formed by ultra-violet light. A possible candidate for such a messenger is cyclic-ADP-ribose which could be formed by disintegration of NAD^+. Disintegration of $[NAD^+]$ by ultraviolet light was shown in a small pilot study. The ultraviolet flash induced contractions were partly inhibited by tetrodotoxin (eradicating all nerve activity) and atropine (blocking muscarinic receptors). Part of the ultraviolet light effect is therefore probably mediated by cholinergic nerve stimulation. Possibly, the ryanodine inhibitable stimulation of intracellular calcium stores occurs at least partly in the nerve cells rather than in the muscle cells. The ultra-violet light stimulation provided a new way to study smooth muscle mechanics and the function of intracellular calcium stores. The latter probably play a role in the syndrome of the unstable bladder as spontaneous contractions have relatively small time constants. Influx of extracellular calcium is probably less important than release of calcium from intracellular stores in the genesis of these spontaneous contractions. This indicates that research for new treatment modalities for the unstable bladder should concentrate more on dvelopment of less toxic, bladder specific, ryanodine like agents and less on calcium entry blockers.

Functional bladder muscle disorders caused by urethral obstruction

Maximum isometric force and the time constant of isometric force development in the pathological bladder secondary to obstruction was studied in a guinea pig model. In this model jeweler's jump rings were placed around the urethra of young animals. With growth a gradual urethral obstruction developed that mimicked the gradual urethral obstruction due to prostatic hypertrophy in men. Like in humans, in the guinea pig different post-obstructive urodynamic

patterns of bladder dysfunction could be identified. Bladders characterized by high voiding pressures, by instable contractions, by low compliance during filling and by decompensation were discriminated. The maximum isometric force and the time constant values were compared between animals with a different duration of the obstruction and those showing the different urodynamic patterns. The animals were sacrificed after 4 or 8 weeks of obstruction and in vitro bladder contractility was assessed. No difference in bladder weight or force development parameters culd be shown between animals that were obstructed for 4 or 8 weeks. There was no change in the rate of isometric force development, cq. time constant. The maximum isometric force, normalized by muscle strip weight, was impaired in obstructed guinea pigs with unstable and decompensated bladders but not those with high voiding pressures. On the basis of increased bladder weight, bladder instability and decompensation were interpreted as more advanced stages of bladder dysfunction as opposed to high pressure voiding. Generally, bladder dysfunction and impaired in vitro force development were associated, and appeared to be more pronounced as bladder weight increased.

Lenght dependence of the cross-bridge cycling rate in smooth muscle

The upper limit to the rate of force development in any smooth muscle type is the cross-bridge cycling rate. The maximum shortening velocity of the muscle is directly associated with this cross-bridge cycling rate and is by definition measured at zero force. The cross-bridge cycling rate has been shown to be independent of the stretched length of the muscle in striated muscle. In smooth muscle the length dependency of maximum shortening velocity has hardly been studied. In many previous studies the quick release technique was used to measure maximum shortening velocity. In this technique, the load on the maximally stimulated muscle is several times quickly reduced to different after loads. In order to compose one force-velocity relation, for determination of one maximum shortening velocity value, the length of the muscle has to be reduced to different values to apply different corresponding after loads. This implies that the maximum shortening velocity measured with the quick release technique cannot be assciated with a certain stretched muscle length. Another disadvantage of the quick release technique is that the high passive forces at longer stretched muscle lengths interfere with the measurements.

An alternative technique was used in order to overcome these disadvantages: the "stop test" technique. In this technique the tissue is linearly shortened at different rates until a preset muscle length is reached. By comparing responses with and without stimulation passive force can easily be subtracted from the active data. A hyperbolic force velocity relation (Hill curve) was fitted to the resulting force responses so that the maximum shortening velocity at different muscle lengths could be estimated. It increased from 0.23 to 0.40 strip·lengths

per second at increasing muscle lengths from 1.3 to 2.2 times the initial length. This increase can be explained by an up-regulation of cross-bridge cycling caused by either increased calcium release from increasingly stretched intracellular calcium stores or by increaed calcium influx from the extracellular space. Stretch induced changes of the regulatory light chain proteins have also been described to cause this effect in smooth muscle. Alternatively a changed geometric orientation or contents of intracellular contractile proteins could explain the increase in maximum shortening velocity with increasing stretched muscle length.

Cross-bridge cycling rate and the rate of isometric force development

The thus measured maximum shortening velocity of the smooth muscle preparations was compared to the time constants of isometric force development before and after the applied linear shortening. The time constant of force recovery after shortening was faster than the time constant of pre-shortening isometric force development. The pre-shortening time constant was independent of maximum shortening velocity and of muscle length, indicating that other effects than cross-bridge cycling, as for example influx of extracellular calcium are rate limiting in force development of this type of smooth muscle. The force recovery after shortening was divided in a fast and a slow component. Time constants of force recovery after shortening showed a significant correlation with the maximum shortening velocity. The fast component is most likely determined by cross-bridge cycling. The slow component of force recovery increased with muscle length and decreased with higher linear shortening velocity. This component could be determined either by influx of extracellular calcium analogous to the pre-shortening time constant or alternatively by rate limiting reattachment of slowly cycling so called "latch" cross-bridges.

Cross-bridge cycling rate determined in human bladder biopsies

In order to create the possibility to determine cross-bridge cycling rate cq. maximum shortening velocity in human bladder tissue in various stages of bladder pathology, a study was performed on human detrusor biopsies. It was found that a very small cold cup biopsy provided enough material to conduct a complete study in which several force velocity relations could be measured. The human bladder was shown to be slower than the pig bladder, as witnessed by the smaller maximum shortening velocity values. A temperature reduction below 37°C reduced the maximum shortening velocity and increased the time constants of isometric force development both before and after shortening. In addition, it was shown that maximum shortening velocity correlated significantly with the time constant after but not with the time constant before shortening. Also in human tissue at all temperatures the time constant after shortening was smaller than before shortening. This again indicates that after shortening cross-bridge

cycling is ate limiting in the force recovery, but that before shortening another process as for example influx of extracellular calcium is rate limiting. From the above findings it follows that the time constant of isometric force development during a clinically performed procedure, in which urine flow is deliberately interrupted during micturition, is related to the maximum shortening velocity. It represents another process than the time constant of isometric force measured without preceding shortening. The latter time constant of isometric force development can be measured during a voluntary contraction before urine loss occurs and its rate is limited by the influx of extracellular calcium.

Conclusions

In the development of new approaches to the modulation of urinary bladder smooth muscle, a good understanding of excitation-contraction coupling, pharmaco-mechanical coupling and fundamental muscle mechanics is essential. The time constant is a useful tool to quantify the time course of isometric force development. In the present study this tool was used to identify rate limiting pathways in the excitation-contraction coupling. The rate of isometric force development in the urinary bladder is limited by the influx of extracellular calcium. A contraction in calcium free medium shows a faster rate of force development. Isometric force recovery after shortening of the muscle shows a similarly fast rate of force development which is significantly correlated to the cross-bridge cycling rate. The cross-bridge cycling rate in urinary bladder smooth muscle was shown to be affected by stretched length and temperature. The length dependence could be due to a changed content or orientation of the intracellular contracile proteins or to an up-regulation of cross-bridge cycling. In the course of this study, a new stimulation method for smooth muscle was discovered with a fast pathway to the contractile units. A new ultraviolet flash device was developed on the basis of a photo flash unit which produced a sufficiently intense ultraviolet light flash to perform photolysis of caged calcium. Surprisingly, smooth muscle preparations not loaded with caged calcium also contracted in response to ultraviolet light illumination. The inhibition of the ultraviolet light stimulation by ryanodine and the fast rate of force development similar to that in spontaneous contractions suggests a stimulation of the intracellular calcium stores. Nerve stimulation might serve as an intermediate in view of the partial inhibition of the effect by tetrodotoxine and atropine. The ultraviolet light flash can serve as a new tool for the investigation of intracellular calcium stores or fundamental smooth muscle mechanics. As major bladder pathology can develop secondary to bladder outlet obstruction, the effect of this condition on isometric force and the time course in force development was investigated in a guinea pig model. In vitro isometric force amplitude was reduced but the rate of force development was unaffected by obstruction mainly in animals showing in vivo unstable or decompensated bladders. In an attempt to measure fundamental smooth muscle contractility parameters of the human bladder, maximum shortening velocity, isometric force and the time constant of isometric force development have successfully been determined in very small cold biopsies. In the human bladder these parameters were in the same order of magnitude as in the pig bladder confirming that the pig is a good animal model for detrusor muscle studies. The presented measurements on human bladder biopsies provide a new tool for the investigation of muscular substrates of urological disorders and for the development of specific treatment modalities for these disorders.

Samenvatting en bespiegeling

Urine wordt voortdurend door de nieren geproduceerd, vervolgens opgeslagen in de urineblaas totdat normaal gesproken op een bewust gekozen moment wordt overgegaan tot een complete ontlediging, het urineren. Hiertoe bevat de urineblaas een speciaal soort spierweefsel, het gladde spierweefsel. Het gladde spierweefsel wordt aangezet tot samentrekken via een uitgebreid regulatie mechanisme. Een slecht functioneren van dit regulatie mechanisme kan verantwoordelijk zijn voor een groot aantal urologische ziekten. De bewuste keuze van het moment van urineren speelt een sleutelrol in deze ziekten. Over het algemeen kunnen de ziekten worden onderverdeeld in processen die resulteren in ongewild urineverlies, de incontinentie, of het niet kunnen plassen, de urine-retentie.

Het gladde spierweefsel van de urineblaas wordt bestuurd door het centrale zenuwstelsel. Verstoorde zenuwactiviteit kan leiden tot afwijkend gedrag van de blaasspier. Een normale zenuwactiviteit kan echter ook gepaard gaan met zowel ongewild urineverlies als retentie. In deze gevallen kan de oorzaak van de afwijking enerzijds liggen in een te sterke of een te geringe activiteit van het blaasspierweefsel zelf of anderzijds in een uitstroombelemmering of een combinatie van deze situaties. Klinische urodynamische metingen, waarbij met een catheter de druk in de blaas tijdens vulling en ontlediging en de uitstroomsnelheid (flow) bij ontlediging wordt gemeten, zijn essentieel om de verschillende bovengenoemde afwijkingen te kunnen onderscheiden.

Het belang van fundamenteel spier onderzoek

Blaasontledigingsstoornissen, bijvoorbeeld die het gevolg zijn van een uitstroombelemmering (bijvoorbeeld ten gevolge van een prostaatvergroting), worden in eerste instantie behandeld door het wegnemen van de onderliggende oorzaak (bijvoorbeeld een deel van de prostaat). Als dit om een of andere reden niet mogelijk is kunnen de symptomen worden verlicht door directe beïnvloeding van de eigenschappen van de blaasspier. Voor de ontwikkeling van nieuwe methoden ter beïnvloeding van gezond glad spierweefsel of behandeling van ziek glad spierweefsel is een beter begrip nodig van de fundamentele werking van dit weefsel. Blaasspiercellen worden in het menselijk lichaam tot samentrekken aangezet door zenuwen. De electrische pulsen in zenuwen veroorzaken vlak bij de spiercellen een afscheiding van een chemische stof die op zijn beurt weer zorgt voor een electrische en/of chemische prikkeling (excitatie) van de structuren in de cel die voor samentrekking (contractie) zorgen. Dit laatste mechanisme wordt excitatie-contractie koppeling genoemd, en het is belangrijk dit mechanisme te onderzoeken omdat kennis hiervan het mogelijk maakt nieuwe medicijnen te ontwikkelen.

Excitatie-contractie koppeling

In hoofdstuk 2 van dit proefschrift wordt een model besproken dat verschillende excitatie-contractie koppeling mechanismen in glad spierweefsel van de blaas beschrijft. De diverse excitatie mogelijkheden werden uitgetest door combinaties van verschillende electrische en chemische prikkels te combineren met stoffen die bepaalde mechanismen blokkeren. De maximale *isometrische* krachtsontwikkeling in varkensblaas spierweefsel en de *tijdconstante* van de krachtsontwikkeling werd gemeten bij excitatie via verschillende paden. *Isometrische* kracht is de kracht die door de spier wordt ontwikkeld zonder dat er samentrekking van de spier optreedt. De *tijdconstante*, een maat voor het tempo van krachtsopbouw is de tijd die nodig is om tot 63 % van de maximale kracht te komen. Deze werd bepaald door *fase-plot* analyse. Een *fase-plot* is een grafiek waarin de verandering van de kracht, wordt uitgezet tegen de kracht zelf. In zo'n grafiek van de krachtsopbouw van glad spierweefsel van de urineblaas is een rechte lijn te zien, de hellingshoek van deze lijn is een maat voor de tijdconstante.

Calcium

Het calcium gehalte in een spiercel is een belangrijke factor in het excitatie-contractie mechanisme. Als een cel eenmaal is geprikkeld door bijvoorbeeld een zenuw begint het excitatie proces binnen in de spiercel met een verhoging van het calcium gehalte, dit kan plaatsvinden door het openen van calciumkanalen in de celwand of door een afgifte van calcium uit voorraden binnen de cel. Deze verhoging van de calcium concentratie in de cel zorgt voor het stimuleren van de samentrekkingseiwitten in de spier. Deze eiwitten maken kruisverbindingen met elkaar, de kruisbruggen. Doordat deze kruisbruggen bij stimulatie continu gemaakt, verkort, en verbroken worden treedt een verkorting van de spier op en wordt een kracht ontwikkeld. In een normale situatie is de calcium concentratie buiten de cel vele malen groter dan binnen de cel. Wanneer een contractie werd opgewekt in een omgeving met een lage calcium concentratie of gedurende blokkade van de calciumkanalen werd een snellere krachtsontwikkeling gezien dan in de normale situatie. Dit fenomeen was het meest uitgesproken bij excitatie met de chemische stof acetylcholine, een stof die van nature door zenuwen bij blaasspierweefsel wordt afgescheiden en die haar werking uitoefent via stimulatie van bepaalde gevoelige plaatsen (receptoren) op de cel. De belangrijkste conclusie uit dit deelonderzoek was dat het tempo van krachtsontwikkeling wordt beperkt wanneer deze receptoren een instroom van calcium van buiten de cel veroorzaken. Als het calcium nodig voor excitatie van de samentrekkings eiwitten uit voorraden binen de cel kwam werd een veel hoger tempo van de krachtsopbouw gezien.

"Caged calcium" en ultraviolet licht

In een vervolg onderzoek werd een poging gedaan de snelheidsbeperkende instroom van calcium van buiten de cel te omzeilen om te bewijzen dat de voorafgaande bewering waar is. Met dit doel werd calcium in de cel ingebracht terwijl het niet-actief was door een binding aan een groter molecuul een "cage" of kooi; dit complex van calcium en dat grote molekuul heet "caged calcium". Het calcium kan worden vrijgemaakt van het grotere molecuul (uit de kooi) door een sterke ultraviolette lichtflits, kortweg wordt dit fotolyse genoemd. In het algemeen wordt hiervoor een zeer dure ultraviolet laser gebruikt, maar voor dit proefschrift werd een goedkoop foto-flits-apparaat aangepast. In hoofdstuk 5 werd aangetoond dat het aangepaste foto-flits-apparaat in staat was calcium vrij te maken uit dit "caged calcium". Er werd aangetoond dat voldoende calcium vrij gemaakt kan worden om in de cel de samentrekkingseiwitten te stimuleren. Wel werd berekend dat de concentratie caged calcium in de cel erg kritisch is voor het succes.

In een voorstudie werd caged calcium ingebracht in gladde spiercellen van de varkensblaas. Belichting met een ultraviolette lichtflits veroorzaakte een sterke contractie. Echter, spierweefsel waarbij vóór de flits geen caged calcium was ingebracht liet een contractie van dezelfde orde-grootte zien. De snelheid van krachtsontwikkeling van deze contractie, zoals die werd bepaald door de tijdconstante, was groter dan wanneer een contractie werd opgewekt door stimulatie met een electrisch veld.

Ultraviolet licht en intracellulaire calcium voorraden

Verder werd onderzocht hoe het komt dat ultraviolet licht het gladde spierweefsel van de urineblaas stimuleert. Dit werd gedaan met behulp van kleine strips van de varkens urineblaas met een diameter van 0,2 millimeter en is beschreven in hoofdstuk 6. Contracties opgewekt met een electrisch veld en met een ultraviolette licht flits (golflengte 320-370 nm) werden vergeleken met soms onwillekeurig optredende (spontane) contracties. De flits contractie werd niet veroorzaakt door warmte of een electrische storing uit de flitser omdat het gehele effect verdwenen was na het plaatsen van een filter, dat niet de ultraviolette straling maar wel zichtbaar licht, warmte straling en electrische storing doorlaat. Zowel electrische stimulatie als flits-stimulatie veroorzaakten een vergelijkbare kracht. Er werd een kleinere tijdconstante gevonden bij een krachtsopbouw veroorzaakt door een ultraviolette lichtflits dan door electrische stimulatie, wat betekent dat de krachtsontwikkeling door een flits-stimulatie sneller plaatsvond.

Een spontane contractie veroorzaakte een nog iets snellere krachtsontwikkeling. De krachtsopbouw door flits-stimulatie had een tempo vergelijkbaar met dat van een contractie in een vloeistof met een laag calcium gehalte zoals die werd gebruikt in hoofdstuk 2. Er werd dus geconcludeerd dat bij een flits-stimulatie het calcium eerder van intracellulaire voorraden afkomstig

moest zijn dan van buiten de cel. Ook werd aangetoond dat de door een flits opgewekte contracties konden worden voorkomen door het toedienen van de stof ryanodine, die de afgifte van calcium uit intracellulaire voorraden blokkeert. De contracties veroorzaakt door electrische stimulatie werden niet voorkomen door ryanodine. Het exacte mechanisme waardoor ultraviolet licht tot een contractie leidt is nog niet geheel duidelijk. Eén mogelijkheid is dat er in de cel een stimulerende stof wordt gevormd door het ultraviolette licht, bijvoorbeeld een pas ontdekte stof in de excitatie-contractie koppeling, het cyclisch-ADP-ribose. Deze stimulerende stof zou dan de calcium voorraden in de cel weer stimuleren. Verder werd echter gevonden dat de door een flits opgewekte contracties ook gedeeltelijk door tetrodotoxine (dat alle zenuw activiteit wegneemt) en atropine (dat selectief de acetylcholine gevoelige receptoren blokkeert) werden geremd. Dit betekent dat een deel van het flits-effect alleen kan plaatsvinden in aanwezigheid van cholinerge zenuwen (dit zijn zenuwen die acetylcholine afscheiden). Mogelijk vindt de intracellulaire calcium afscheiding eerder in zenuwcellen plaats dan in spiercellen.

De nieuwe ultraviolet-licht stimulatiemethode veroorzaakt een snelle krachtsontwikkeling en kan daarom in de toekomst goed gebruikt worden in spier experimenten of om de intracellulaire calcium voorraden te bestuderen. Deze voorraden spelen mogelijk een rol bij onwillekeurige (spontane) contracties van de blaas, die bij de mens vaak een oorzaak zijn van ongewenst urineverlies. Nieuwe behandelwijzen voor deze onwillekeurige contracties of kortweg blaas instabiliteit zouden dan meer gericht moeten worden op het voorkómen van calcium afscheiding uit intracellulaire voorraden dan op het voorkómen van instroom van calcium van buiten de cel. Er zou bijvoorbeeld een minder toxische stof kunnen worden ontwikkeld die op ryanodine lijkt.

Functionele blaasspier veranderingen ten gevolge van obstructie

In hoofdstuk 4 wordt beschreven hoe de maximale isometrische kracht en het tempo van krachtsontwikkeling werden bestudeerd in blazen die door een uitstroombelemmering (obstructie) afwijkend gedrag waren gaan vertonen. Dit onderzoek werd gedaan aan cavia's op de urologie afdeling van Johns Hopkins University in Baltimore, U.S.A. In deze dieren, zoals beschreven in hoofdstuk 3 , werden op jonge leeftijd operatief kleine zilveren juweliersringetjes rondom de plasbuis (urethra) geplaatst. Doordat de cavia's vervolgens groeiden ontwikkelde zich geleidelijk een relatieve plasbuis vernauwing (obstructie), zoals dat ook gebeurd bij mannen met obstructie door prostaatvergroting. In de cavia werden bij urodynamisch onderzoek blaasafwijkingen gezien die ook bij de mens na obstructie worden aangetroffen: hoge blaasdrukken bij de mictie (het plassen), instabiliteit (onwillekeurige contracties), verminderde elasticiteit (lage compliantie) en een overloop blaas (decompensatie). Bij decompensatie wordt de blaas erg vol, kan deze zelf geen druk meer ontwikkelen en staat op een

gegeven moment zo strak gespannen dat lekkage (incontinentie) optreedt. De blaas werd onderzocht 4 en 8 weken nadat de obstructie (de ring) was aangebracht bij de dieren. De maximale isometrische kracht en de tijdconstante van de krachtsontwikkeling werden gerelateerd aan de duur van de obstructie en de urodynamische blaasafwijkingen, zoals boven beschreven. De duur van de obstructie was niet van invloed op het blaasgewicht, de urodynamische blaasafwijkingen, de isometrische kracht of de tijdconstante. De maximale isometrische kracht, per milligram spierweefsel, was verminderd in de blazen die bij urodynamisch onderzoek instabiliteit of decompensatie vertoonden en onveranderd in de blazen die hoge mictie-drukken lieten zien. De tijdconstante veranderde niet door obstructie. Hierdoor kon worden geconcludeerd dat instabiliteit en decompensatie, veroorzaakt door obstructie, verder gevorderde afwijkingen waren dan hoge druk bij de mictie. Algemeen kan gesteld worden dat blaasafwijkingen door obstructie het best gekarakteriseerd worden door verminderde krachtsontwikkeling en een hoger blaasgewicht.

Het fundamentele contractie mechanisme

Van alle besproken excitatie processen die voorafgaan aan krachtsontwikkeling bepaalt de langzaamste het tempo van krachtsopbouw. Zo was in hoofstuk 2 de langzaamste factor bijvoorbeeld de instroom van calcium van buiten de cel. Als alle excitatie processen snel verlopen dan zal uiteindelijk het samentrekkingsmechanisme van de spiercel het tempo van de krachtsontwikkeling beperken. Dit tempo is afhankelijk van de cyclusduur waarin de kruisverbindingen tussen langs elkaar schuivende spiereiwitten gemaakt en verbroken worden, en wordt aangeduid als de cyclusduur van de kruisbruggen (cross-bridge cycling rate). Krachtsontwikkeling en samentrekkings-, oftewel verkortingssnelheid zijn van elkaar afhankelijk. Deze afhankelijkheid kan zichtbaar worden gemaakt in een kracht-snelheidsrelatie grafiek. In deze grafiek (zie hoofdstuk 7, figuur 4) is te zien dat bij een lage verkortingssnelheid veel kracht en bij een hoge verkortingssnelheid weinig kracht wordt ontwikkeld. De grootst mogelijke verkortingssnelheid wordt bereikt op het punt waar geen kracht meer wordt ontwikkeld. Dit punt in de grafiek wordt de maximale verkortingssnelheid genoemd. Deze maximale verkortingssnelheid is een maat voor de cyclusduur van de kruisbruggen.

De lengte afhankelijkheid van de cyclusduur van de kruisbruggen

In skeletspierweefsel is aangetoond dat de cyclusduur van de kruisbruggen onafhankelijk is van de lengte waarover de spier wordt uitgerekt (reklengte). In glad spierweefsel is deze lengte-afhankelijkheid nauwelijks bestudeerd. Om deze lengte-afhankelijkheid van de cyclusduur van de kruisbruggen te bepalen werd in hoofdstuk 7 de stop-test gebruikt. Bij deze techniek laat men een stripje varkensblaas spierweefsel na voor-rekken steeds met een andere snelheid

verkorten tot een zelfde lengte. Op deze lengte wordt de kracht tijdens verkorten gemeten, die dan samen met de verkortings snelheid een punt van de kracht-snelheids relatie grafiek representeert. Nadat bij een aantal snelheden de kracht is gemeten kan de kracht-snelheids relatie grafiek en daarmee de maximale verkortingssnelheid, behorend bij de lengte waartoe de spierstrip werd verkort worden vastgesteld. Bij reklengtes van de spier tussen 1,3 en 2,2 keer de oorsprongkelijke lengte werd een oplopende maximale verkortingssnelheid van 0.23 tot 0.40 spierlengten per seconde gevonden; de maximale verkortingssnelheid steeg dus met oplopende lengte. Dit zou het gevolg kunnen zijn van een versnelde cyclusduur van de kruisbruggen door enerzijds meer calcium uitstroom uit gerekte intracellulaire opslag structuren of anderzijds meer instroom uit de extracellulaire ruimte door rek van de in de celmembraan aanwezige poriën en kanalen. Een andere mogelijke verklaring is dat de vorm of structuur van de samentrekkings eiwitten door rek zo verandert dat er een snellere verschuiving ten opzichte van elkaar kan plaatsvinden. De rek of lengte afhankelijkheid van de cyclusduur van de kruisbruggen betekent voor de blaas dat bij meer vulling dus bij een meer uitgerekte blaasspier de maximale verkortingssnelheid groter is en dus de cyclusduur van de kruisbruggen korter is.

De cyclusduur van de kruisbruggen en het tempo van isometrische krachtsopbouw

In hoofdstuk 8 werd de relatie onderzocht tussen de maximale verkortingssnelheid, gemeten met de bovenbeschreven "stop-test" methode, en het tempo van een isometrische krachtsopbouw voor en na een verkorting. Het tempo van krachtsherstel na een verkorting was sneller dan dat ervoor. De tijdconstante die het tempo van krachtsopbouw voor een verkorting representeert was onafhankelijk van de maximale verkortingssnelheid of van de rek (lengte) van de spier. Dit bevestigt dat andere processen dan het tempo van kruisbruggen beweging, zoals bijvoorbeeld de instroom van calcium van buiten de cel het tempo van deze krachtontwikkeling beperken. Het snellere krachtherstel na verkorting bleek wel te worden bepaald door de cyclusduur van de kruisbruggen. De tijdconstante voor dit krachtherstel zou dus ook als maat voor de cyclusduur van de kruisbruggen kunnen worden gebruikt

Het bepalen van maximale verkortingssnelheid in spierweefsel uit menselijke blaas biopsieen.

Om in de toekomst ziekten en afwijkingen van de menselijke blaasspier in verband te kunnen brengen met mogelijke afwijkingen in het samentrekkingsmechanisme van de spier en de cyclusduur van de kruisbruggen werd in hoofdstuk 9 onderzocht of het mogelijk is de maximale verkortingssnelheid in menselijk weefsel te meten. Een biopsie is een klein stukje blaasweefsel van 2 mm in diameter, dat via een kijk operatie binnen uit de

blaas wordt weggenomen. Er werd aangetoond dat aan een stukje blaasspierweefsel uit een dergelijke kleine biopsie een volledige studie kon worden gedaan waarin verschillende kracht-snelheidsrelatie grafieken konden worden bepaald. De menselijke blaas had een iets tragere maximale verkortingssnelheid dan de varkensblaas. Als de temperatuur van het preparaat werd verlaagd, verminderde ook de maximale verkortingssnelheid en werd het tempo van krachtontwikkeling voor en na een verkorting lager. Ook in deze studie werd aangetoond dat de tijdconstante na een verkorting van de spier werd bepaald door de cyclusduur van de kruisbruggen. Dit betekent dat een herstel van de blaasdruk bij het onderbreken van de straal tijdens het plassen een maat is voor de cyclusduur van de kruisbruggen. De tijdsconstante van drukopbouw vóór de mictie wordt bepaald door de instroom van extracellulair calcium in de spiercel.

Conclusies

Een goed begrip van excitatie-contractie koppeling en fundamentele spier mechanica is onontbeerlijk voor het ontwikkelen van specifieke nieuwe methoden voor het beïnvloeden van de werking van het gladde spierweefsel in de urineblaas. De tijdconstante van de krachtsontwikkeling kan worden gebuikt om het tempo van krachtsontwikkeling te meten en daarmee snelheidsbeperkende processen in de excitatie-contractie koppeling te identificeren. Als de spier niet eerst verkort, wordt het tempo van isometrische krachtsontwikkeling bepaald door de instroom van extracellulair calcium. Wanneer er alleen calcium uit intracellulaire voorraden komt, bij een contractie in een calciumvrije vloeistof, ontwikkelt de kracht zich sneller, wat zichtbaar wordt door een kleinere tijdconstante. Isometrisch krachtsherstel na verkorting resulteert in een tijdconstante in een ongeveer even grote tijdconstante en deze vertoont een direkte samenhang met de fundamentele samentrekkingssnelheid van de contractiele spier eiwitten, bepaald door de cyclusduur van de kruisbruggen. Deze cyclusduur is in glad spierweefsel van de urineblaas afhankelijk van de voorrek-lengte en van de temperatuur. De rek-lengte afhankelijkheid zou veroorzaakt kunnen worden door een veranderde hoeveelheid of een veranderde geometrische orientatie van de contractiele spiereiwitten.

Tijdens deze studie werd een nieuwe stimulatiemethode ontdekt voor het gladde spierweefsel van de urineblaas. Op basis van een foto-flitser werd een ultraviolet lichtflits apparaat ontwikkeld dat genoeg lichtintensiteit kon produceren om calcium vrij te maken uit "caged calcium". Verrassenderwijs contraheerden ook spierstrips die niet waren geladen met "caged calcium" op de ultraviolette lichtflits. Het feit dat deze ultraviolet licht stimulatie geblokkeerd

kon worden door ryanodine, een remmer van de intracellulaire calcium afscheiding, en dat de krachtsontwikkeling snel verliep, betekent dat afscheiding van calcium uit intracellulaire voorraden werd veroorzaakt. Doordat tetrodotoxine en atropine ook remmend werkten op de ultraviolet licht stimulatie, is het waarschijnlijk dat deze stimulatie plaatsvindt door zenuwen. De ultraviolette lichtflits kan goed worden toegepast voor onderzoek van intracellulaire calcium voorraden en fundamenteel glad spierweefsel mechanica onderzoek.

Door obstructie van de blaasuitgang kunnen diverse blaasafwijkingen ontstaan. Het effect van deze obstructie werd bestudeerd aan cavia's. De capaciteit van de blaas om isometrische kracht te ontwikkelen was na obstructie verminderd en het tempo van krachtsopbouw was gelijk gebleven. Dit effect werd vooral gezien samen met verder gevorderde urodynamische afwijkingen ten gevolge van de obstructie zoals instabiliteit of decompensatie. Er werd aangetoond dat zowel de maximale verkortingssnelheid, een indicator voor de cyclusduur van de kruisbruggen, als de maximale isometrische kracht en de tijdconstante van krachtsontwikkeling gemeten konden worden in kleine stukjes biopsie materiaal uit de menselijke blaas. Deze parameters waren in de menselijke blaas van een zelfde grootte-orde als in de varkensblaas, wat de goede bruikbaarheid van varkensblazen voor dit soort onderzoek bevestigt. De mogelijkheid om op deze manier metingen te doen aan menselijk weefsel opent perspectieven voor verder onderzoek naar fundamentele spierweefsel-afwijkingen bij urologische ziekten, en voor de ontwikkeling van nieuwe behandelingsmethoden voor deze ziekten.

Dankwoord   *Acknowledgements*

Het is af.

Dit is het antwoord op de vraag die de afgelopen jaren honderden keren de opening vormde van lange, korte, goede, en minder goede gesprekken. Iedereen met wie ik deze gesprekken heb gevoerd wil ik bedanken voor de niet aflatende belangstelling en het vertrouwen dat ze door het vaak meermalen stellen van die vraag hebben getoond. Dan zijn er diegenen die zich hebben ingezet om dit proefschrift te maken tot wat het nu is. Hen wil ik graag met name noemen:

De meeste dank ben ik verschuldigd aan mijn ouders die de basis hebben gegeven en gevormd voor mijn huidige denken en doen. Jullie gaven mij op de goede momenten de begeleiding of de vrijheid om mij te vormen. Bedankt voor de steun, de sfeer, de belangstelling, de inzet en de middelen.

Prof. Dr F.H. Schröder, mijn promotor en opleider. Professor, bedankt voor de kansen die u mij gaf en geeft: Door uw telefoontje met Prof. Walsh gaf u mij de mogelijkheid een deel van het onderzoek in Baltimore te doen. Door uw actieve inzet kwamen de middelen om zowel mijn gestarte onderzoek uit te breiden tot een promotie onderzoek als ook de deel-onderzoeken op diverse internationale congressen te presenteren. Door u kreeg ik de kans uroloog te worden. Uw stimulerende invloed heeft dit werk zeker in een stroomversnelling gebracht waar ik me uiteindelijk uit geworsteld heb.

Dr Ir. R. van Mastrigt, mijn co-promotor. Ron, jouw altijd structurele en opbouwende kritiek is net zo rechtlijnig als je karakter. Het heeft jaren geduurd voor ik een discussie met jou kon voeren zonder na de eerste zin al te denken "eigenlijk heeft hij gelijk". Bedankt voor het altijd even snel en even rood maken van mijn manuscripten. Je hebt altijd, zelfs in het begin, mijn verhaal écht gecorrigeerd zonder het te gaan herschrijven. Daar heb ik een structurele denkwijze van geleerd. Jij hebt mij anderzijds de kans en de vrijheid gegeven al van student-assistent af een eigen onderzoek te doen waar ik mijn creativiteit in kwijt kon. Van jou mocht ik ook van het begin af aan zelf de artikelen schrijven en zelf de papers presenteren. Daar heb ik de zelfwerkzaamheid van geleerd die jij soms van het begin af van iedereén verwacht. Dit alles heeft wel een boekje opgeleverd waar jij ook trots op mag en moet zijn.

Iedereen die op de afdeling Urodynamica werkt en werkte wil ik danken voor de ontspannende en ook vaak diepgaande lunchdiscussies evenals voor de zo belangrijke ad-hoc hulp en bijstand tijdens het onderzoek. Speciaal wil ik noemen: Dr J.J Glerum, Ko, doordat ik jou kende via de zendclub PI₁GOE ben

eenvoudige maar voor mij zulke lastige problemen.

De afdeling Cardiovasculaire research, bedankt voor het ter beschikking stellen voor mijn onderzoek van het "hart van de urologie". In het bijzonder ook: Dr R. Krams, Rob, bedankt voor de adviezen en discussie. Dr B.C.G. Gho, Ben, bedankt voor het brainstormen over zowel onderzoeks- als andere onderwerpen; daar gaan we zeker mee door.

Drs. T.M. Teune, afdeling Neuro-anatomie, Thea, bedankt voor je hulp en ideeen met betrekking tot de (neuro)-histologische aspecten van mijn onderzoek. Bedankt voor de gezelligheid en je luisterend oor in Baltimore.

Drs. P.G.H. Mulder, afdeling Epidemiologie en Biostatistiek, Paul, bedankt voor je hulp en adviezen voor statistische bewerking van mijn data. Een bezoek aan jou genereerde significant meer werk en dus ook leermomenten.

Prof. C.F. van der Klauw, bedankt voor het ter beschikking stellen van middelen die nodig waren voor het maken van dit proefschrift, de aanmoedigingen en het nageslacht.

Herr Kirchner, Metz GmbH, many thanks for your indispensable advice on how to adapt the photo flash unit to my needs. Herrn P. Strzelczyk dipl.Ing. and R. Zartner, EG&G-Heimann Optoelectronics GmbH, Wiesbaden, Germany, thank you very much for the necessary technical advice on flash lamps that enabled me to increase my ultraviolet light output.

Dr J.L. Mostwin, associate professor of Urology at Johns Hopkins University Baltimore, U.S.A. Jacek, thank you very much for working in your lab, for the discussions, the hospitality, your support and your friendship. I hope that we can continue the cooperation. Prof. Dr P.C. Walsh (Chief of the James Buchanan Brady Urological institute, Johns Hopkins Medical Institutions, Baltimore) thank you for the opportunity to work in your research and clinical department, for sharing the secrets of the radical prostatectomy and for giving me my first operating experience during this operation. Prof. Dr D.S. Coffey, thank you for the interesting Journal clubs, for the experience of your stimulating research influence and for your philosophy on life, death and cancer. T. (Tom) Chang, (in Memoriam), It was good to have known you and to have shared ideas and friendship. Everyone working in the urology research and clinical departments at Hopkins, thanks for the hospitality the good social and research atmosphere. Especially,I would like to mention Shelly Tillman, Steve Ward, Dalal Tonob and the members of friday afternoon's Library club. Mr. O.M.A. Karim, MS, FRCS(urol). Dear Omer, thanks for the fine cooperation, the academic discussion, the social events and your and Helen's hospitality. Always remember my last "STELLING".

Dr H.F. Veen, mijn chirurgisch opleider, de chirurgie maatschap en de assistenten van het Ikazia ziekenhuis Rotterdam, hartelijk dank voor de belangstelling en klinische vorming die zo belangijk is om het fundamenteel onderzoek in de goede context te zien. Helaas overstemde het gegons van dit aanstormende werkje mijn chirurgische onderzoeks output.

Staf en assistenten urologie alsmede OK personeel in het AZR Dijkzigt speciale dank voor de medewerking bij het aanleveren van menselijk biopsie materiaal en het kunnen opbrengen van de nodige flexibiliteit met betrekking tot een promovendus in de afrondende fase; dit laatste geldt speciaal ook voor mijn opleider Dr J.M. Nijman, de staf en assistent kinderurologie in het Sophia kinderziekenhuis.

Els Forman, bedankt voor het handmatig oplossen van digitale incompatibiliteit.

Cees de Vries, tekenaar, hartelijk dank voor de illustratieve tekeningen die anders dan computer grafiek, zelfs als ze zijn ingescand, nog sfeer hebben en de hand van de meester tonen.

Hartelijk dank ook de heren van het varkensslachthuis (Spaanse polder, Rotterdam) voor het mij vaak letterlijk toewerpen van het zo noodzakelijke te onderzoeken weefsel.

De sponsors zoals die werden genoemd in het begin van dit proefschrift wil ik hartelijk danken voor de ondersteuning. De farmaceutische bedrijven, bedankt dat u het fundamenteel onderzoek een warm hart toedraagt.
De leden van de commissies zoals die zijn ingesteld ter beoordeling van dit proefschrift wil ik danken voor hun tijd en belangstelling.

Ir. E. de Valk MBA, Elwin, Bedankt, dat je ondanks de afstand toch contact hield en op de hoogte bleef van mijn onderzoeks activiteiten en dat je paranimf wilt zijn.

Mijn broer. Bram, jij hebt alles van heel nabij gevolgd, je bent paranimf en zelfs co-auteur van één van de artikelen. Bedankt voor je inzet, je ongezouten commentaar en vooral je vriendschap. Nu jij?

Melanie, bedankt dat we dankzij en ondanks je eigen promotie steun, begrip, tijd, hulp, geduld, gezelligheid, lach, en liefde konden delen. Er komen nóg betere tijden.

Curriculum Vitae

Gommert Abraham van Koeveringe was born on June 30, 1966 in 's-Gravenpolder, the Netherlands. He attended secondary school (gymnasium) at the "Christelijk Lyceum voor Zeeland" in Goes and passed the final examination in May 1984. In that same year, he commenced medical school at the Erasmus University Rotterdam. The first introduction to Urology started in 1986, when, during his studies, he was working in a student nursing team at the first Dutch kidney stone lythotrypter. Also in 1986, he started working as a junior research assistant at the Urodynamics division (project manager: Dr ir. R. van Mastrigt) of the department of Urology of the Erasmus University Rotterdam.

After obtaining his doctoral degree in 1989, he was rewarded a grant by the internationalization committee of the Erasmus University to take part in an exchange program with Johns Hopkins University in Baltimore, U.S.A. At the James Buchanan Brady Urological Institute, he conducted a consecutive urodynamic research project for 6 months (project manager: J. L. Mostwin, MD, PhD, associate professor of Urology). In 1990, an International Congress visit was combined with a clinical urological rotation at the urological institute (chief: Prof. dr P.C. Walsh) of Johns Hopkins Hospital. His medical degree was obtained in June 1991 at the Erasmus University.

From 1991 to 1993, he continued his research in a project supported by the Dutch kidney foundation at the Urodynamics division (project manager: Dr ir. R. van Mastrigt) of the department of Urology (head: Prof. dr F. H. Schröder). In 1994 he started two years of residency in General Surgery at the Ikazia Hospital, Rotterdam (head: Dr H.F. Veen), as a part of his training in Urology. In 1996, he started as a resident in the Urology department of the University Hospital Rotterdam "Dijkzigt" (head: Prof. dr F. H. Schröder). Currently, he is working in the department of pediatric Urology of the Sophia childrens Hospital Rotterdam (head: Dr J.M. Nijman).

List of Publications

Publications in journals and books:

1. **G.A.van Koeveringe**, R.van Mastrigt
   Discrimination of excitatory pathways in smooth muscle by phaseplot analysis.
   In : Dysfunction of the lower urinary tract: present achievement and future perspectives. Eds.: P.E.V.van Kerrebroeck, F.M.J. Debruyne, Medicom Europe, Bussum, 1990 pp. 14-19.
2. **G.A.van Koeveringe**, R.van Mastrigt
   Excitatory pathways in smooth muscle investigated by phase plot analysis of isometric force development.
   Am.J.Physiol. 261: R138-R144 (1991).
3. J.L. Mostwin, O.M. Karim, **G.A. van Koeveringe**, E. Brooks
   The Guinea pig as a model of gradual urethral obstruction.
   J.Urol. 145-4 : 854-858 (1991).
4. **G.A. van Koeveringe**, J.L. Mostwin, R. van Mastrigt, A.J. van Koeveringe
   Effect of partial urethral obstruction on force development of the guinea pig bladder.
   Neurourol.Urodyn. 12: 555-571 (1993)
5. J. Groen, E. van Asselt, R. van Mastrigt, R. Bosch, **G.A. van Koeveringe**
   Comparison of detrusor contractility of guinea pig bladders in situ and strips from these in vitro.
   J Urol. 150: 1002-1006 (1993).
6. J. Groen, E. van Asselt, R. van Mastrigt, **G.A. van Koeveringe**, R. Bosch
   Contractility parameters of guinea pig bladder in situ: Similarity to human bladder contractility.
   J. Urol. 151: 1405-1410 (1994)
7. J.L. Mostwin, O.M.A. Karim, **G. van Koeveringe**, N. Seki
   Guinea pig as an animal model for the study of urinary bladder function in the normal and obstructed state.
   Neurourol Urodyn. 13(2):137-45, 1994.
8. **G.A. van Koeveringe**, R. van Mastrigt
   Photolysis of caged calcium using a low cost flash unit and efficacy analysis with a calcium selective electrode.
   Cell Calcium 15:423-430 (1994)
9. J.L. Mostwin, O.M.A. Karim, **G. van Koeveringe**
   Electrical properties of obstructed guinea pig bladder. (Review)
   Adv Exp Med Biol. 385:21-8; discussion 75-9, 1995.
10. **G.A. van Koeveringe**, R. van Mastrigt
   Ultra-violet light induces calcium release from intracellular stores in urinary bladder smooth muscle.

Submitted, 1996.
11. **G.A. van Koeveringe**, R. van Mastrigt
Length dependency of the force-velocity relation in smooth muscle fibers of the urinary bladder.
Submitted, 1996.
12. **G.A. van Koeveringe**, R. van Mastrigt.
Time constants of isometric force development in smooth muscle fibers of the urinary bladder.
Submitted, 1997.
13. **G.A. van Koeveringe**, R. van Mastrigt.
The temperature dependence of the force-velocity relation determined in biopsy material of the human detrusor.
Submitted, 1997.

Abstracts:

1. **G.A.van Koeveringe**, R.van Mastrigt
Excitation-contraction coupling in the smooth muscle of the urinary bladder of the pig.   Abstract: Symposium on smooth muscle, London, April 1988.   *J.Muscle Res. Cell Mot.* 9-5 : 467 (1988)
2. O.M. Karim, **G.A. van Koeveringe**, J.L. Mostwin
Development of abnormal voiding patterns following partial obstruction of the Guinea pig urethra.
Abstract: # 666 A.U.A. meeting 1990, New Orleans
J.Urol. 143-4 : 355A (1990).
3. **G.A. van Koeveringe**, J.L. Mostwin, R. van Mastrigt, A.J. van Koeveringe
Effect of obstruction on force development in guinea pig bladder muscle.
Abstract: # 667 A.U.A. meeting 1990, New Orleans
J.Urol. 143-4 : 355A (1990).
4. **G.A. van Koeveringe**, R van Mastrigt
Excitatory pathways and time constants in smooth muscle contraction
Abstract: D5 XIXth European Conference on Muscle Contraction and Cell Motility, Brussels, 1990.   *J.M.Res.Cell Mot.* 12: 94 (1991).
5. **G.A. van Koeveringe**, J.L. Mostwin, R. van Mastrigt, A.J. van Koeveringe
Functional change in guinea pig urinary bladder smooth muscle after partial urethral obstruction.
Abstract: XXth European Conference on Muscle Contraction and Cell Motility, Oxford, 1991.   *J.M.Res.Cell Mot.* 13: 259(A) (1992).
6. J. Groen, E. van Asselt, R. van Mastrigt, R. Bosch, **G.A. van Koeveringe**
Detrusor contractility in guinea pig bladder wall and bladder wall strips.
Abstract: ICS meeting Halifax, 1992
Neurourol.Urodyn. 11-4 : 324-325 (1992).
7. **G.A. van Koeveringe**, R. van Mastrigt

Measurement of free calcium using an ion selective electrode after flash
photolysis of caged calcium with a low cost flash unit.
Abstract: XXIth European Conference on Muscle Contraction and Cell
Motility, Bielefeld, 1992. *J.Muscle Res. Cell Mot.* 14 : 266 (1993)

8. **G.A. van Koeveringe**, R. van Mastrigt
Contractile responses to flash photolysis of intracellularly loaded caged
calcium in intact bladder muscle strips.
Abstract: XXIth European Conference on Muscle Contraction and Cell
Motility, Bielefeld, 1992. *J.Muscle. Res. Cell Mot.* 14 : 266 (1993)

9. J. Groen, R. van Mastrigt, E. van Asselt, **G.A. van Koeveringe**, R. van
Mastrigt
Contractility parameters of the Guinea pig bladder measured in situ and
in vitro.   Abstract: Abstract: I.C.S. meeting 1993, Rome, I
Neurourol. Urodyn. 12: 316 (1993).

10. **G.A. van Koeveringe**, R. van Mastrigt
Contractile responses of bladder strips to flash photolysis of intracellular
caged calcium.   Abstract: A.U.A. meeting 1993, San Antonio
J.Urol. 149-4 : 341A (1993).

11. **G.A. van Koeveringe**, R. van Mastrigt
An ultraviolet light flash evokes contractions in pig urinary bladder
smooth muscle.   Abstract: I.C.S. meeting 1993, Rome, I
Neurourol. Urodyn. 12: 403-405 (1993).

12. **G.A. van Koeveringe**, R. van Mastrigt.
Ultraviolet licht veroorzaakt calcium afgifte uit intracellulaire calcium
voorraden in glad spierweefsel van de urineblaas. (Dutch)
Abstract: NVU meeting, 1,2 November 1996, Hengelo, the Netherlands
Urograaf: 4: p21, 1996

13. **G.A. van Koeveringe**, R. van Mastrigt.
The force-velocity relation, determined in transurethral biopsies of the
human detrusor, is temperature dependent.
Abstract: submitted for presentation on the ICS meeting 1997,
Yokohama, Japan.

Videotape

1. P.C. Walsh, F.H. Schröder, **G.A. van Koeveringe**, W. Kirkels
VIDEOTAPE: Radical prostatectomy, simultaneous demonstration by
Patrick.C. Walsh MD and Fritz.H. Schröder, MD.
Symposium 7 October 1992.
Distributor: Roussel BV, Hoevelaken, NL